

Machine Learning for Fluid Mechanics

Regression problems of 2nd kind



Bernd Noack

HIT, China & TU Berlin

TU Berlin, Germany, 2020-03-02

Preview course

- A) Features $\mathbf{u} \mapsto \boldsymbol{\gamma}$ ($\dim(\boldsymbol{\gamma}) = 2, 3$)
and reduced-order representations
 $\mathbf{u} \mapsto \mathbf{a} \mapsto \hat{\mathbf{u}} \approx \mathbf{u}$ where $\dim(\mathbf{a}) \ll \dim(\mathbf{u}, \hat{\mathbf{u}})$
- B) Principles of machine learning
- C) Regression problem of first type
 $(\mathbf{a}^m, b^m), m = 1, \dots, M \Rightarrow b = K(a)$
- D) Regression problem of second type + MLC
 $K^* = \operatorname{argmin}_K J(K), \quad b = K(a)$
- E) Reduced-order modeling
Model-based control

Material covered so far / today

Regression problem: Find a function $a \mapsto b = f(a)$ which minimizes $J(f) = \min$ based on data $a^m, b^m, m = 1, \dots, M$ (1st kind) or based on testing $J(f)$ (2nd kind).

Meta	Autoencoder 	Learning from data
Regr. probl. of 1st kind Fitting	Interpolation 	Extrapolation
Regr. probl. of 2nd kind Variational	Exploitation 	Exploration

Overview

1. Introduction

..... *Control as model-free regression problem*

2. Exploitation

..... *Downhill simplex algorithm*

3. Exploration

..... *Latin hypercube + Monte Carlo*

4. Genetic algorithm

..... *Evolving in a high-dimensional parameter space*

5. Genetic programming

..... *From parameter to function optimization*

Overview

1. Introduction

..... *Control as model-free regression problem*

2. Exploitation

..... *Downhill simplex algorithm*

3. Exploration

..... *Latin hypercube + Monte Carlo*

4. Genetic algorithm

..... *Evolving in a high-dimensional parameter space*

5. Genetic programming

..... *From parameter to function optimization*

Models for turbulence control

≡ Brunton & Noack 2015 AMR, ≡ Noack, Morzynski & Tadmor 2011 Springer

Linear model

$$\frac{d}{dt} \mathbf{a} = \mathbf{A}\mathbf{a} + \mathbf{B}\mathbf{b}$$

$$\mathbf{s} = \mathbf{C}\mathbf{a} + \mathbf{D}\mathbf{b}$$

$$\mathbf{b} = \mathbf{K}\mathbf{s}$$

≡ Rowley & Williams 2006 ARFM

≡ Sipp et al. 2010 ARM

Weakly non-linear model

$$\mathbf{a} = \mathbf{a}_B + \mathbf{a}_\omega$$

$$\mathbf{a}_B = c \|\mathbf{a}_\omega\|^2$$

$$\frac{d}{dt} \mathbf{a}_\omega = \mathbf{A}\mathbf{a}_\omega + \mathbf{B}\mathbf{b}$$

$$\mathbf{A} = \mathbf{A}_s + a_\omega \mathbf{A}_\omega$$

$$\mathbf{B} = \mathbf{B}_s + a_\omega \mathbf{B}_\omega$$

Moderately nonlinear model

$$\mathbf{a} = \mathbf{a}_B + \mathbf{a}_{\omega 1} + \mathbf{a}_{\omega 2}$$

$$\mathbf{a}_B = c_1 \|\mathbf{a}_{\omega 1}\|^2 + c_2 \|\mathbf{a}_{\omega 2}\|^2$$

$$\frac{d}{dt} \mathbf{a}_{\omega 1} = \mathbf{A}_1 \mathbf{a}_{\omega 1}$$

$$\frac{d}{dt} \mathbf{a}_{\omega 2} = \mathbf{A}_2 \mathbf{a}_{\omega 2} + \mathbf{B}_2 \mathbf{b}$$

$$\mathbf{A}, \mathbf{B}_{1,2} = \mathbf{A}, \mathbf{B}_{1,2}(\mathbf{a}_B), \dots$$

Strongly non-linear model

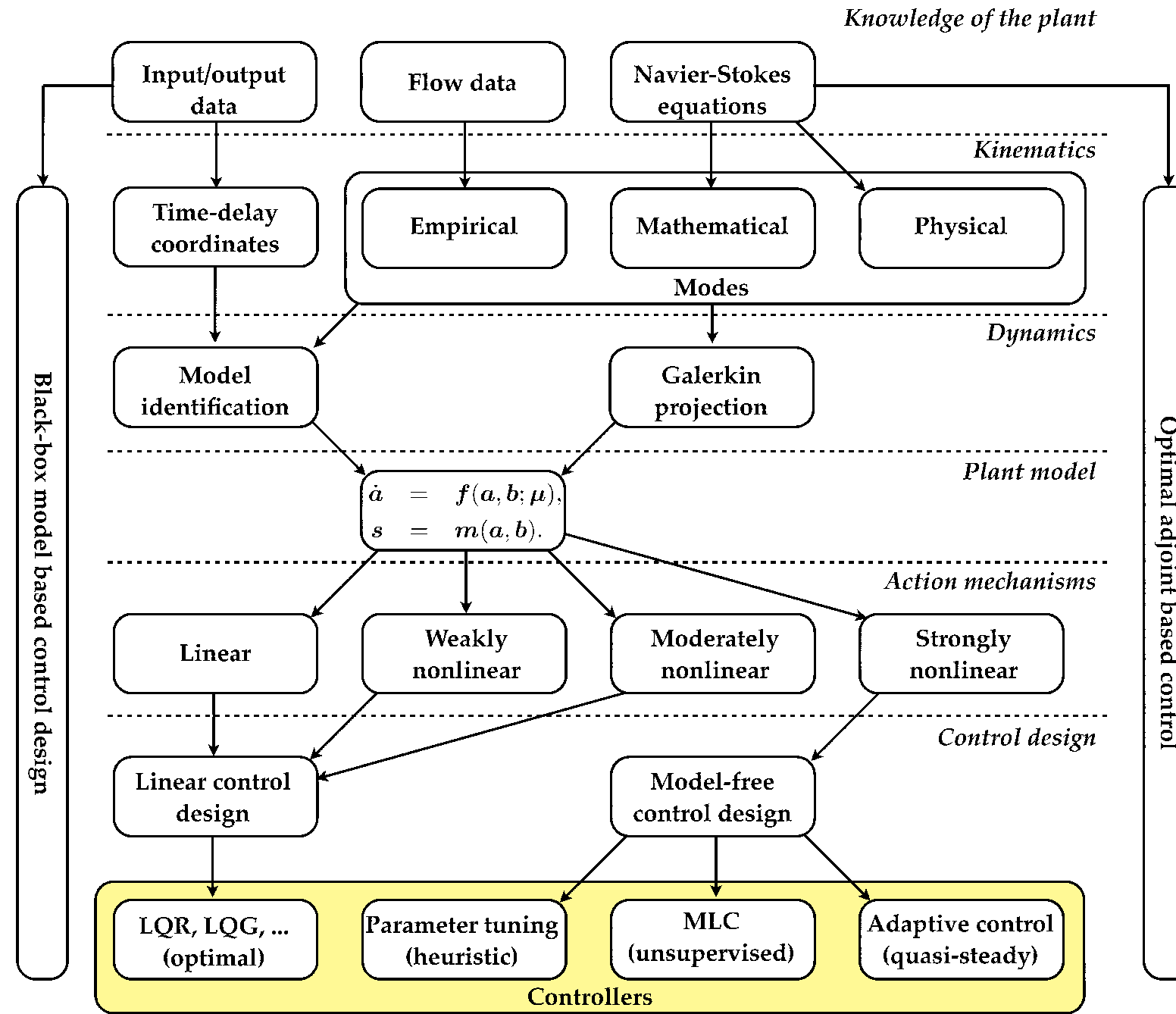
$$\frac{d}{dt} \mathbf{a} = \mathbf{A}\mathbf{a} + \mathbf{B}\mathbf{b}$$

$$\mathbf{A} = \mathbf{A}_0 + \sum a_i \mathbf{A}_i, \dots$$

- 'Chaos'
- Triadic frequency cross talk
- Turbulent energy cascade

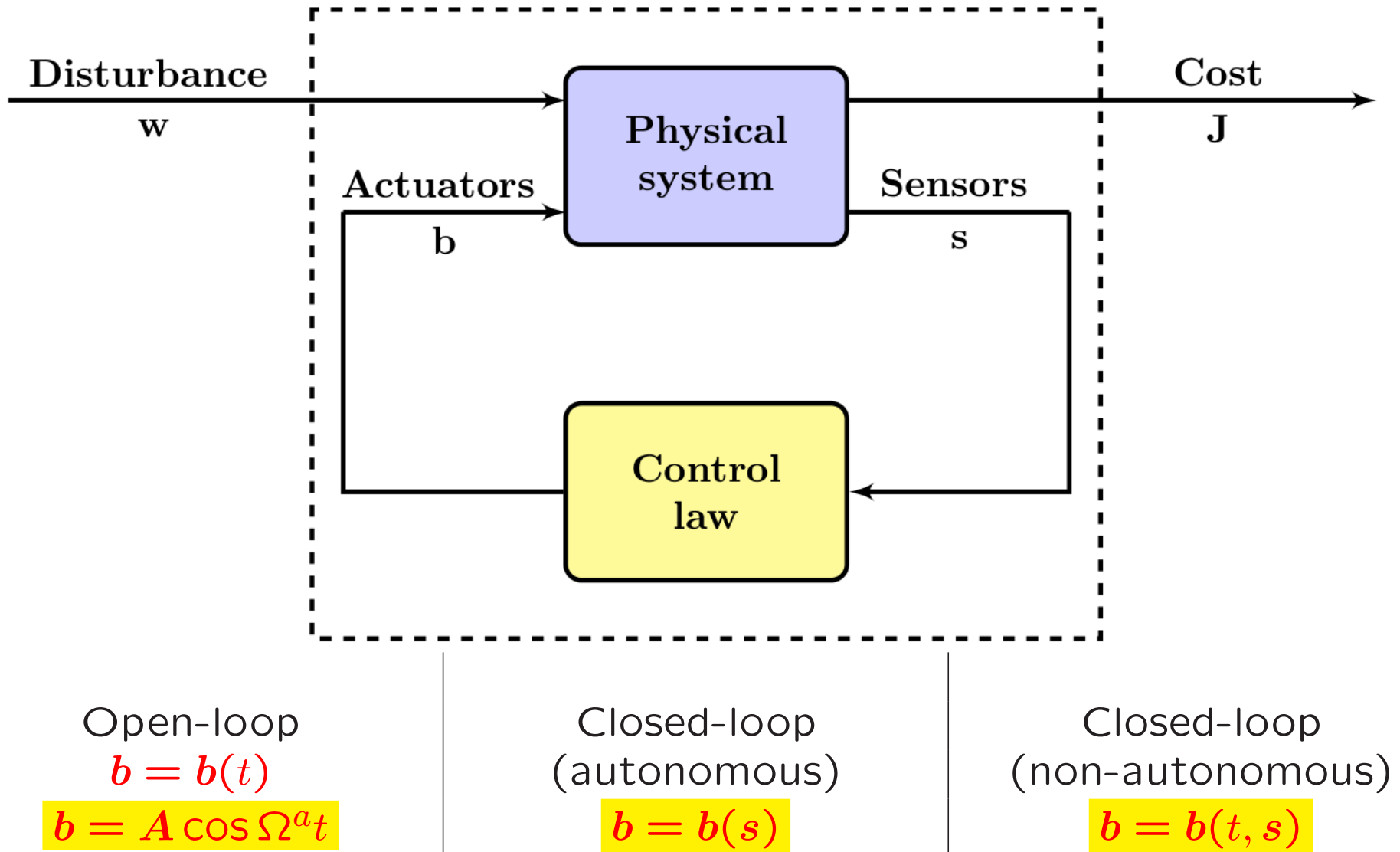
Not included: quasi-steady actuation, rare event manipulation,
convection-dominated phenomena

Turbulence control → modelling options



Control design

Brunton & Noack 2015 AMR



Why modeling for control?

☰ Brunton & Noack 2015 AMR

Humans should think of control as a *regression problem* and apply *evolutionary algorithms*

Ingo Rechenberg
1963 Diplomarbeit
HFI/ISTA, TU Berlin



Control problem:

$$\begin{aligned}\frac{da}{dt} &= F(a, b) \\ s &= G(a, b) \\ b &= K(s) \\ J &= \overline{j(a, b)}\end{aligned}$$



$$K_{opt}(s) = \arg \min J [K(s)]$$

Overview

1. Introduction

..... *Control as model-free regression problem*

2. Exploitation

..... *Downhill simplex algorithm*

3. Exploration

..... *Latin hypercube + Monte Carlo*

4. Genetic algorithm

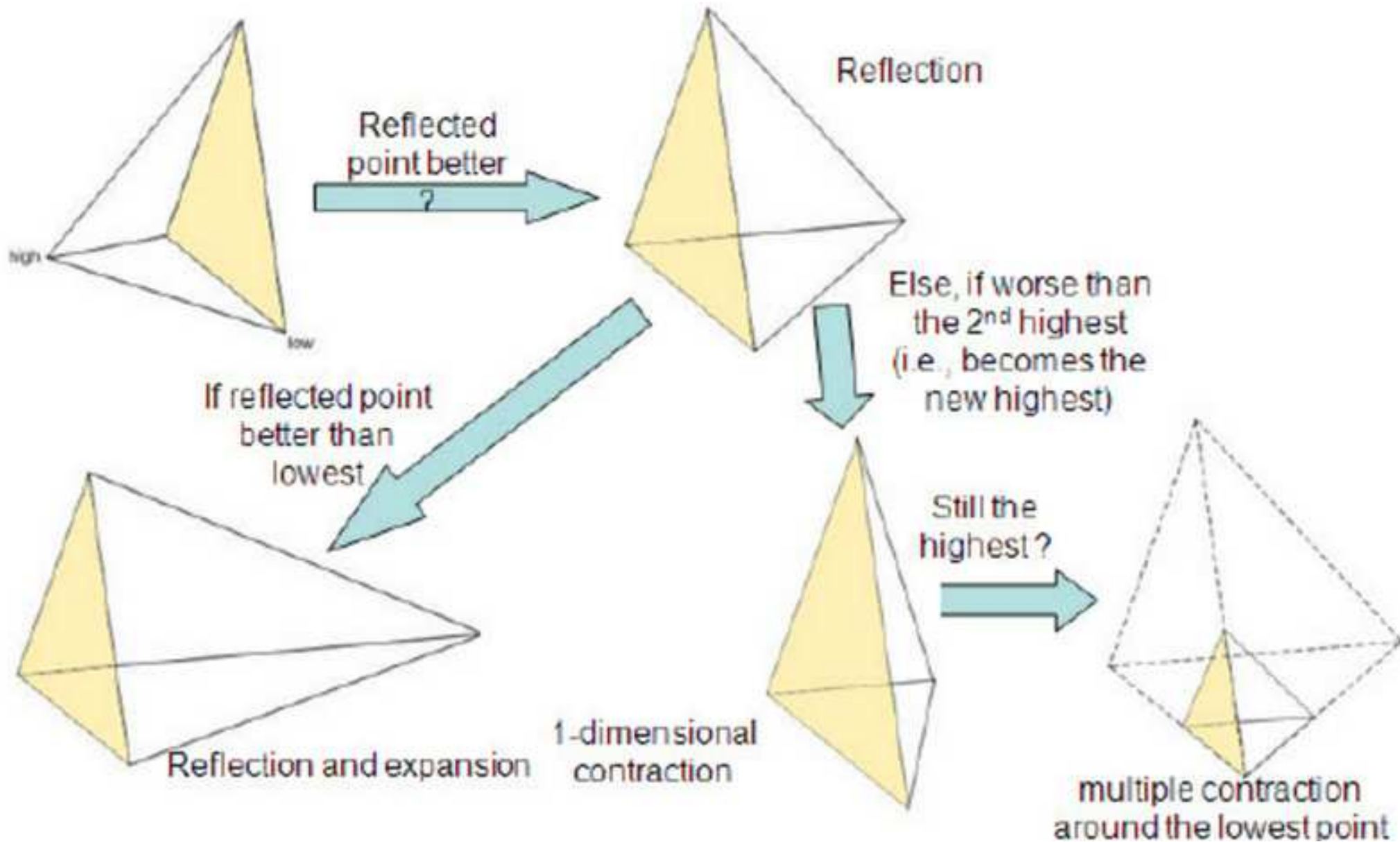
..... *Evolving in a high-dimensional parameter space*

5. Genetic programming

..... *From parameter to function optimization*

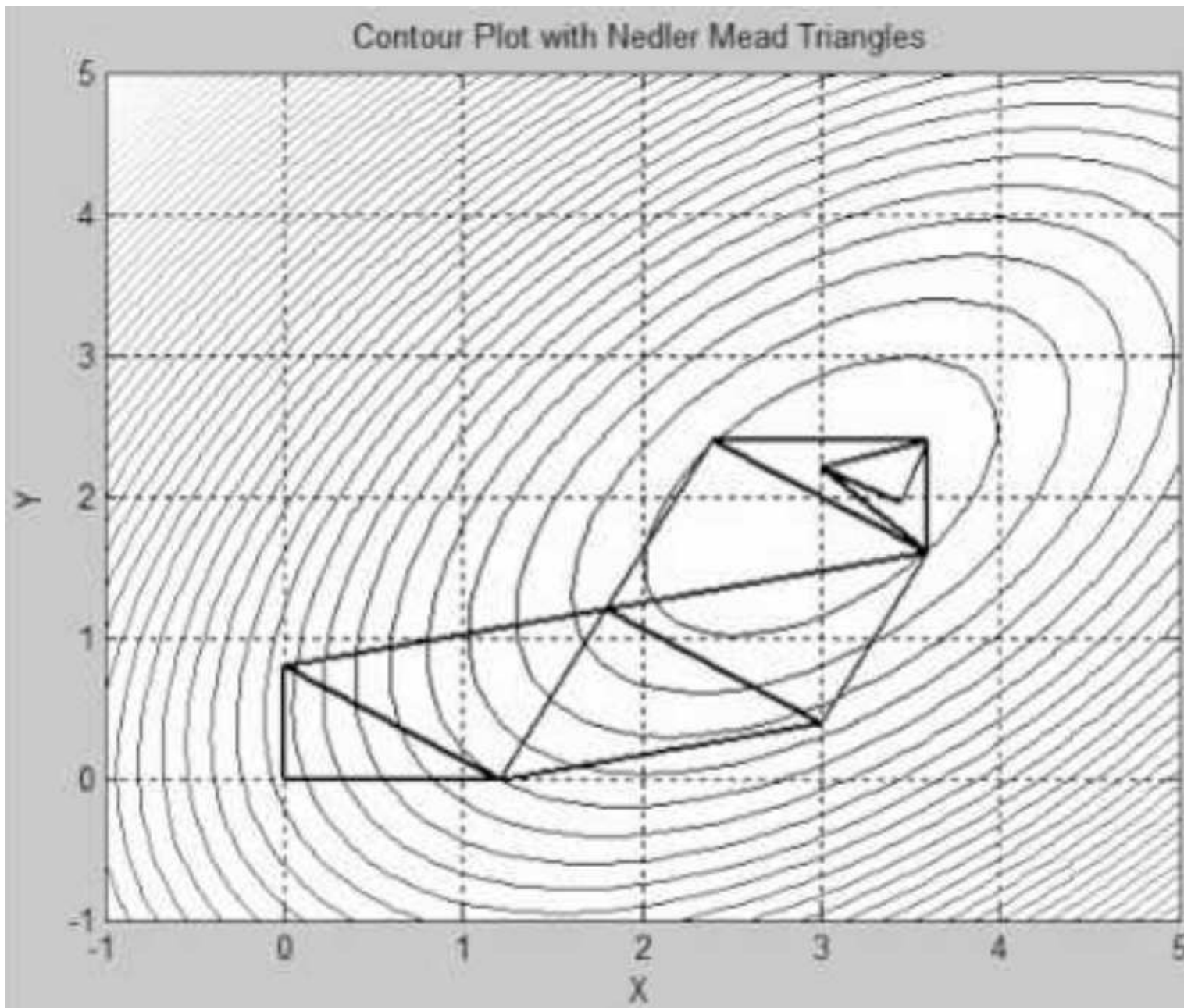
Downhill simplex method I

≡ Numerical recipes



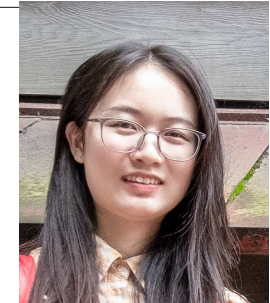
Downhill simplex method II

 Numerical recipes

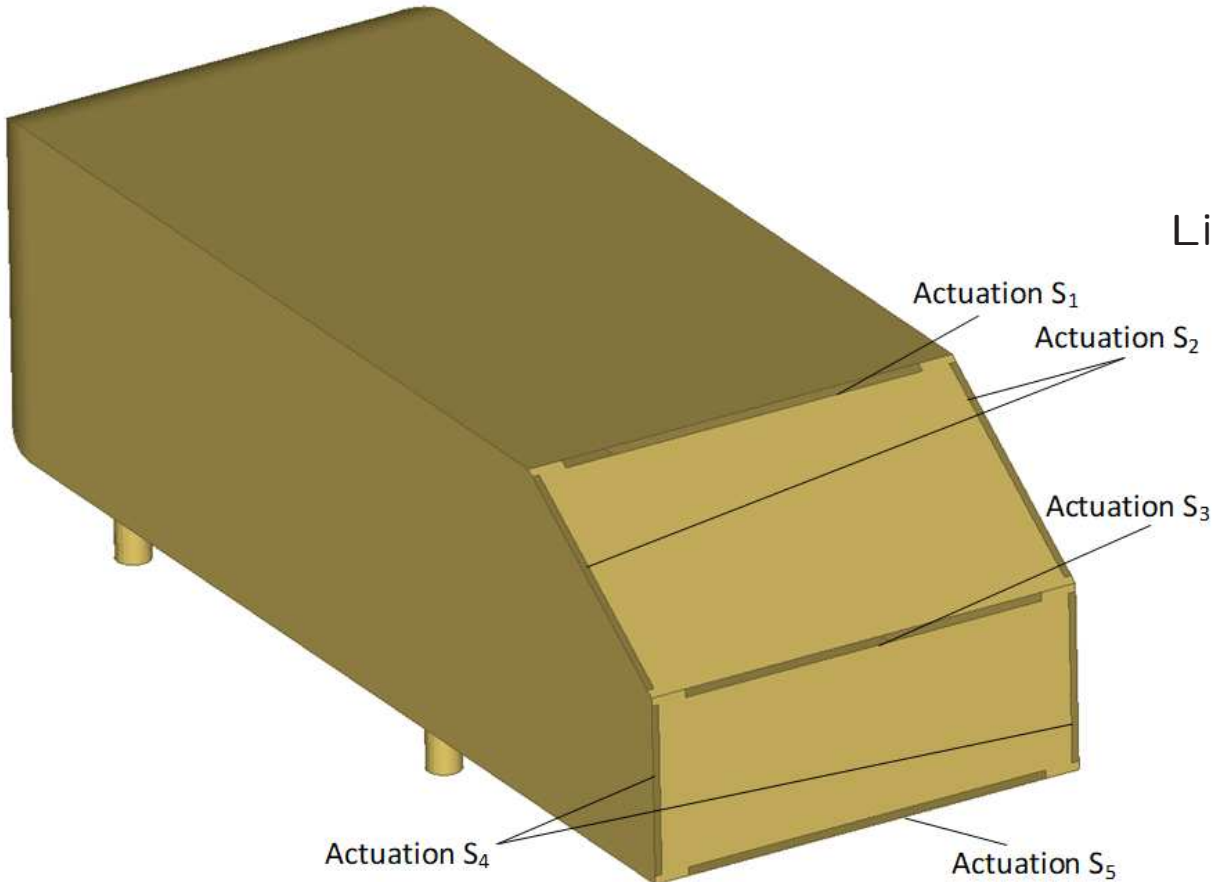


Drag reduction of simplified car model

Li, Li, Yang & Noack 2020 JCP (in preparation)



Li (Anne) Yiqing

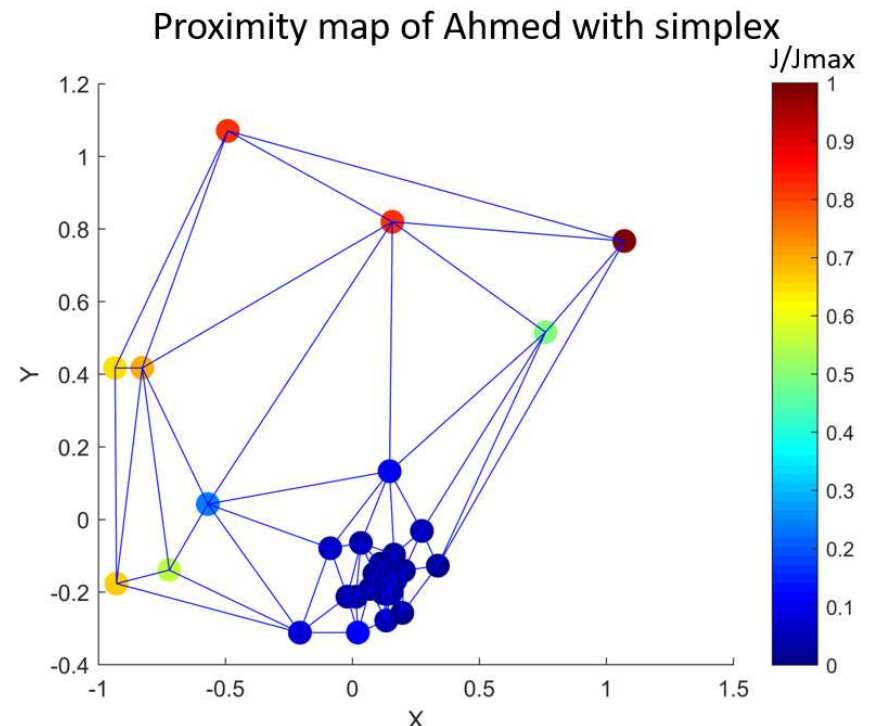
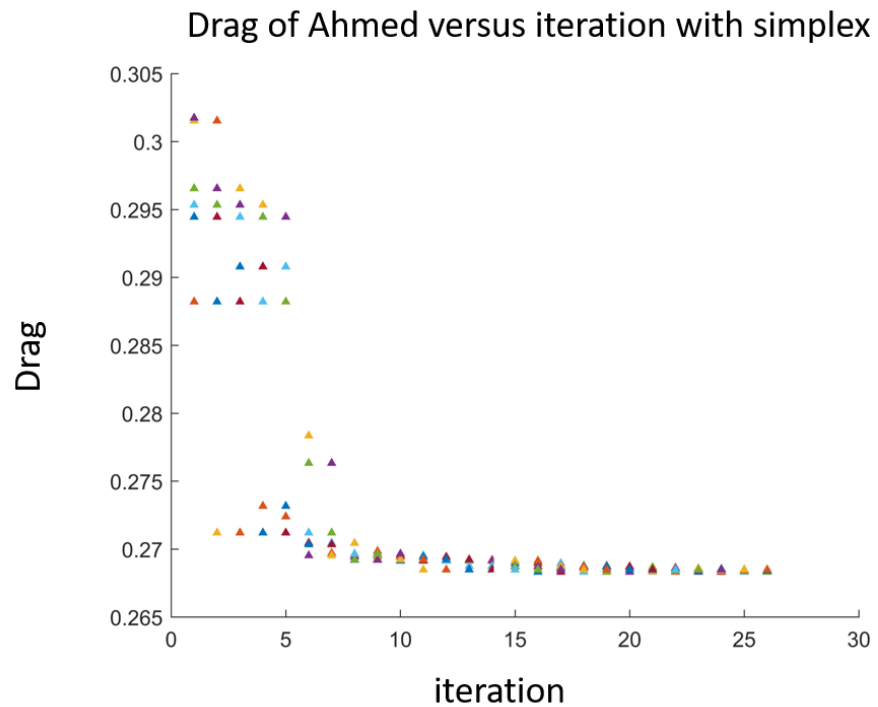
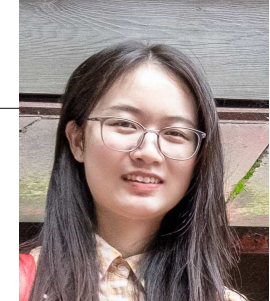


RANS Simulation with 5 independent actuator groups

—Constant blowing in streamwise direction b_1, b_2, b_3, b_4, b_5

Drag reduction of simplified car model

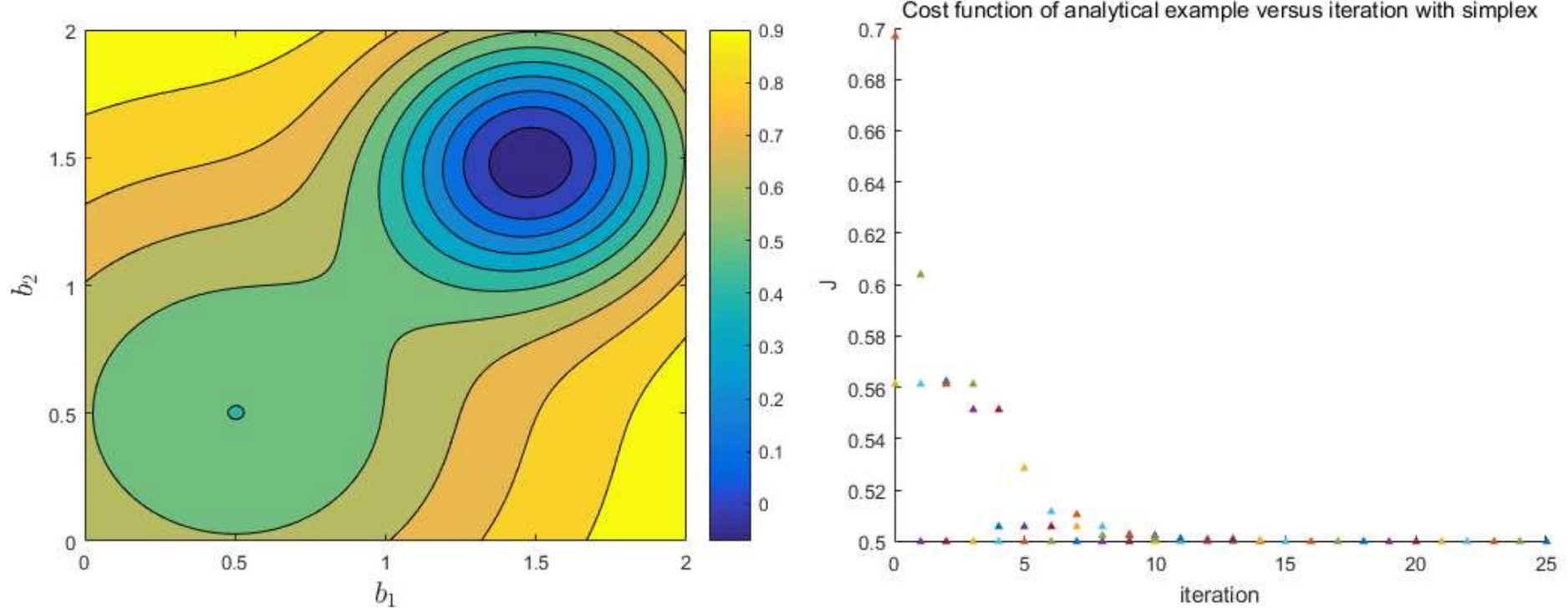
Li, Li, Yang & Noack 2020 JCP (in preparation)



RANS Simulation with 5 independent actuator groups

$U_\infty = 20 \text{ m/s},$	$b_1 = 24 \text{ m/s},$	$b_2 = 9 \text{ m/s},$
$b_3 = 3 \text{ m/s},$	$b_4 = 11 \text{ m/s},$	$b_5 = 14 \text{ m/s}$

Analytical example for downhill simplex



Downhill simplex method gets trapped in local minimum

$b_1 \approx 0.5, b_2 \approx 0.5$; Initial amoeba: $(0, 0), (0, 0.5), (0.5, 0)$

Overview

1. Introduction

..... *Control as model-free regression problem*

2. Exploitation

..... *Downhill simplex algorithm*

3. Exploration

..... *Latin hypercube + Monte Carlo*

4. Genetic algorithm

..... *Evolving in a high-dimensional parameter space*

5. Genetic programming

..... *From parameter to function optimization*

Latin hypercube sampling (LHS)

Step 1 **Initialize parameter**—Example

$$b_1 = 0, b \in \mathcal{B} := [0, 2] \times [0, 2] \times \dots \times [0, 2]$$

Step 2 **Compute new parameter** b_2

$$b_2 = \operatorname{argmax}_{b \in \mathcal{B}} \|b - b_1\|$$

—Furthest away from b_1

Step 3 **Compute new parameter** b_3

$$b_3 = \operatorname{argmax}_{b \in \mathcal{B}} \min \{\|b - b_1\|, \|b - b_2\|\}$$

—Furthest away from b_1 and b_2

:

Step M **Continue until M parameters**

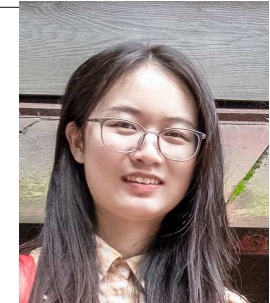
$$b_i, i = 1, \dots, M$$

Blackboard-Example 1: $[0, 2]$

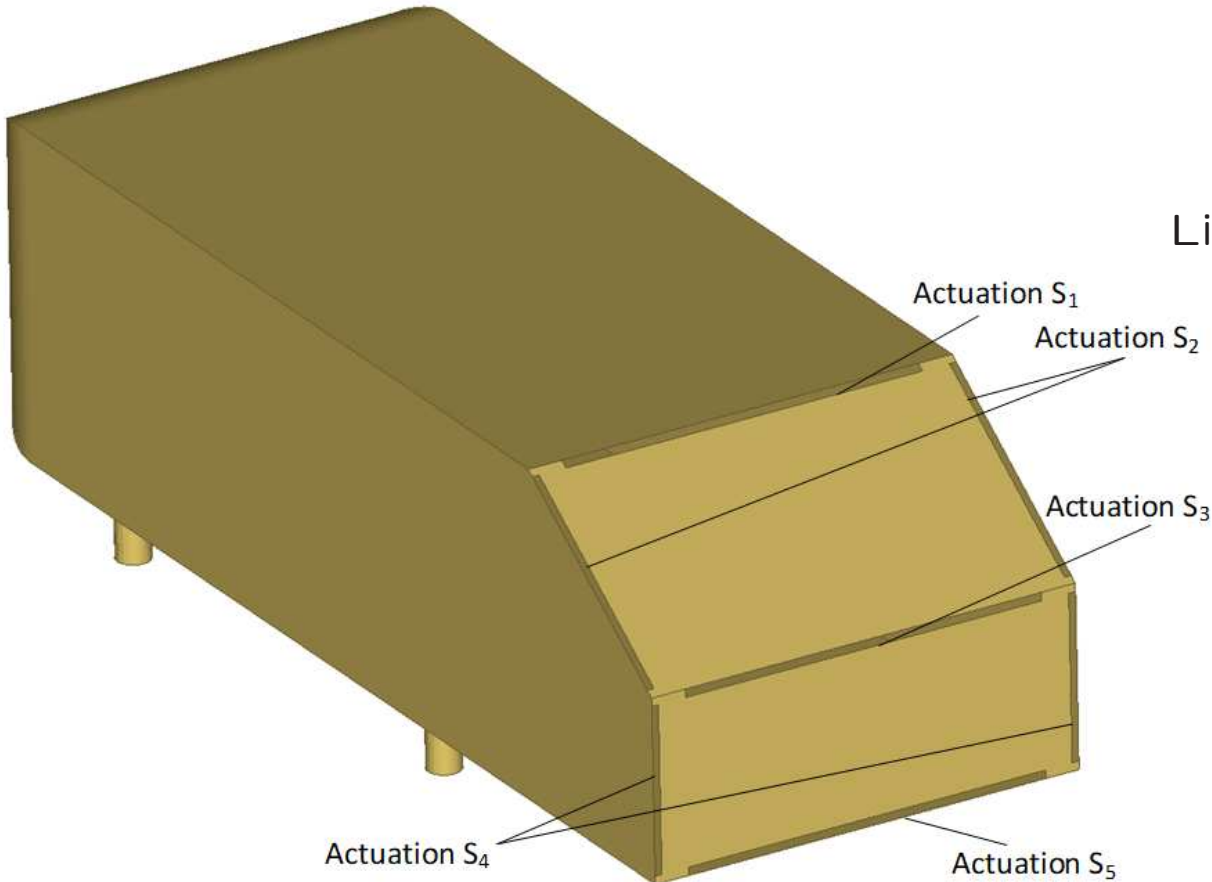
Blackboard-Example 2: $[0, 2] \times [0, 2]$

Drag reduction of simplified car model

Li, Li, Yang & Noack 2020 JCP (in preparation)



Li (Anne) Yiqing

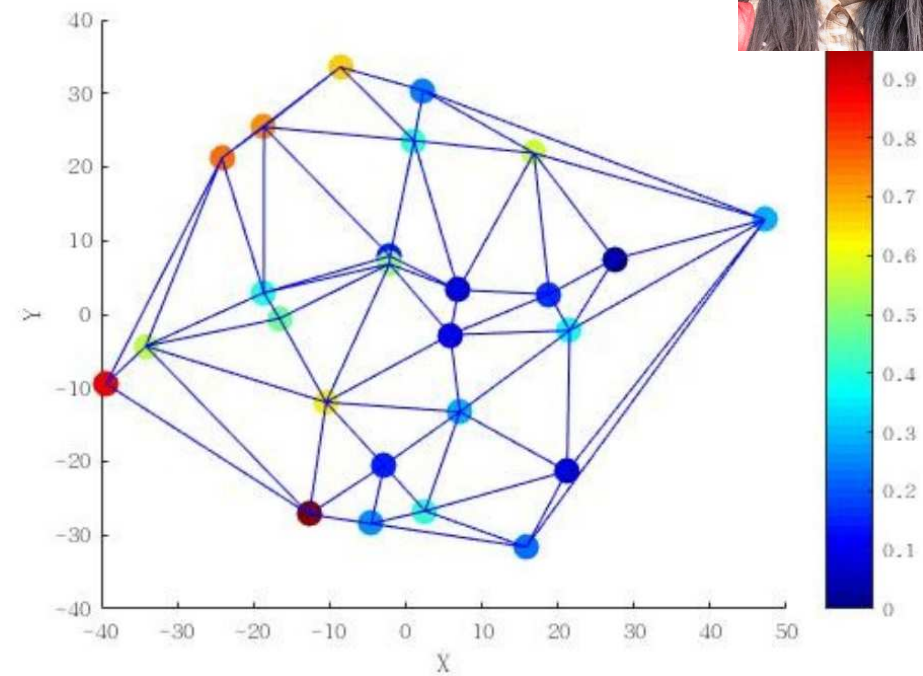
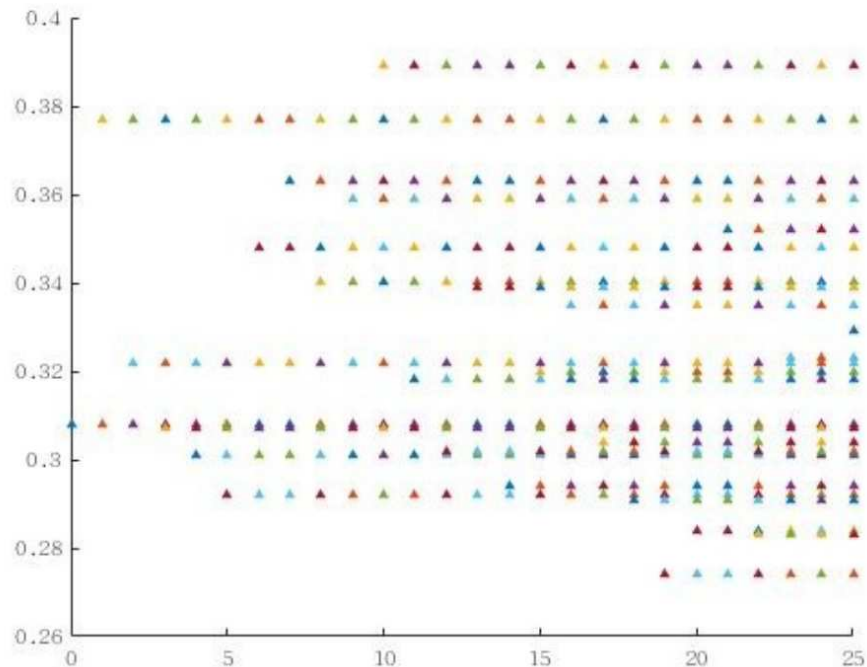
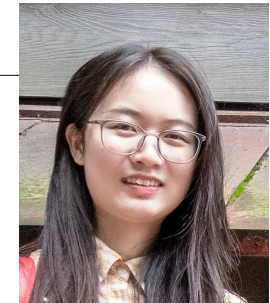


RANS Simulation with 5 independent actuator groups

—Constant blowing in streamwise direction b_1, b_2, b_3, b_4, b_5

Drag reduction of simplified car model

Li, Li, Yang & Noack 2020 JCP (in preparation)



RANS Simulation with 5 independent actuator groups

Latin hypercube sampling — 25 simulations

$U_\infty = 20 \text{ m/s}$,	$b_1 = 24 \text{ m/s}$,	$b_2 = 9 \text{ m/s}$,
$b_3 = 3 \text{ m/s}$,	$b_4 = 11 \text{ m/s}$,	$b_5 = 14 \text{ m/s}$

Overview

1. Introduction

..... *Control as model-free regression problem*

2. Exploitation

..... *Downhill simplex algorithm*

3. Exploration

..... *Latin hypercube + Monte Carlo*

4. Genetic algorithm

..... *Evolving in a high-dimensional parameter space*

5. Genetic programming

..... *From parameter to function optimization*

Machine learning control II

☰ Wahde 2008 WIT

Step 1: 1st generation with random control laws

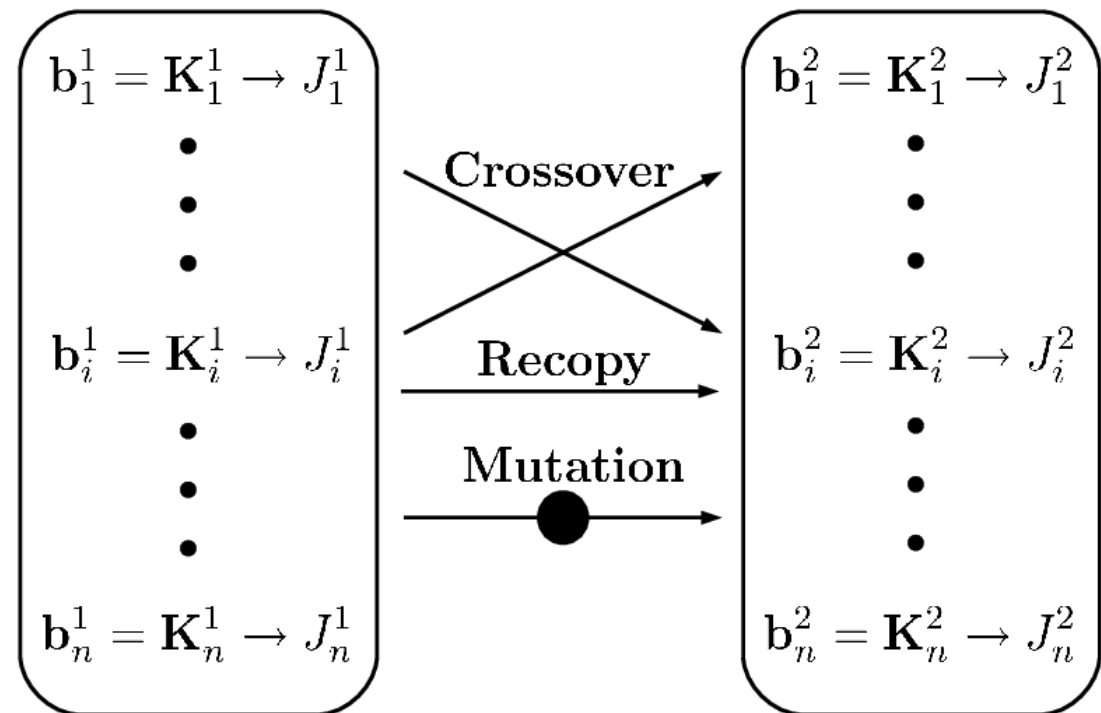
$$b_m^1 = K_m^1(s), m = 1, \dots, 100$$

Step 2–50:

Biologically inspired optimization of the control laws based on the 'fitness grades'

$$J [b = K(s)]$$

Optimization process

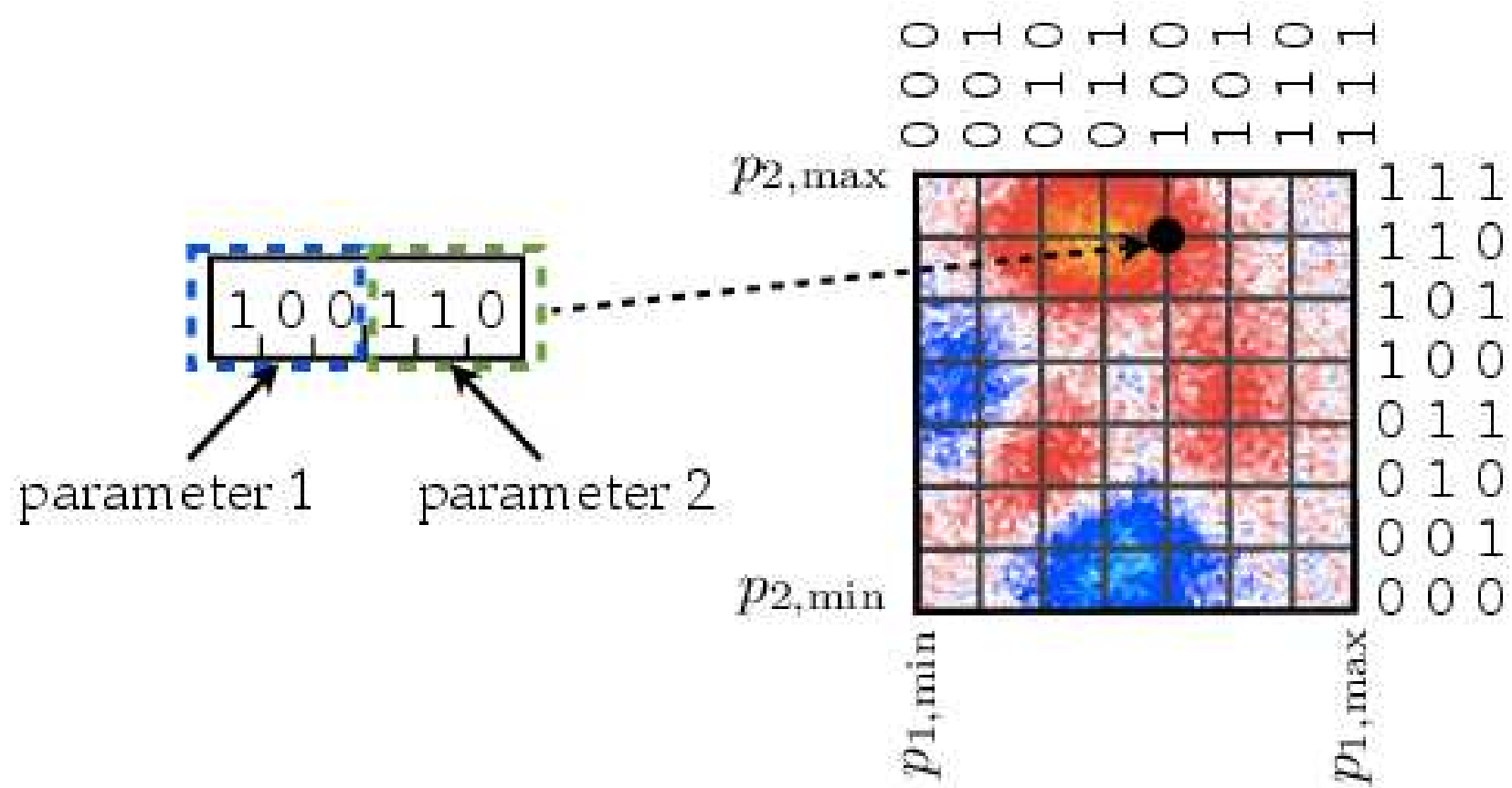


☰ H. P. Schwefel 1965 & I. Rechenberg 1973

Genetic algorithm based control I

Linear feedback law $b = p_1 s_1 + p_2 s_2$

Example of genome representation

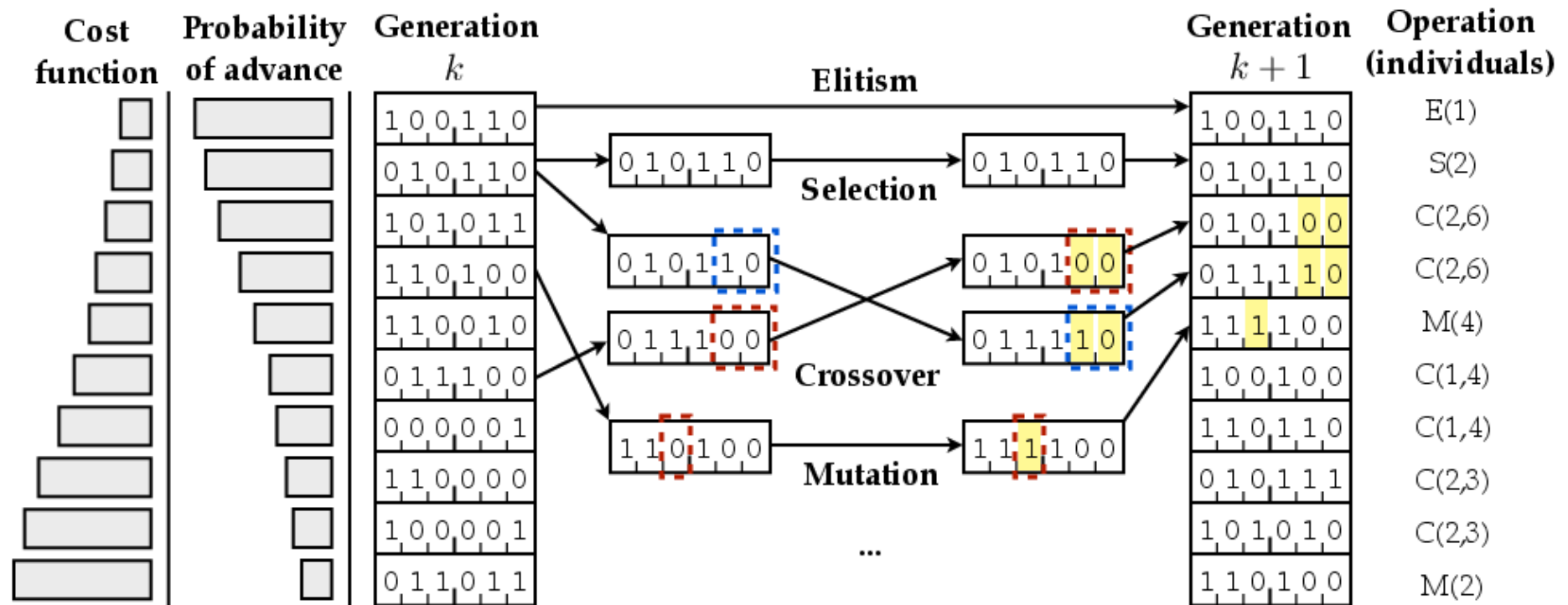


Genetic algorithm based control *II*

(1) **First generation:** with random feedback laws.

— Sort feedback laws according to cost functional J

(2) **Build next generation** with genetic operations.



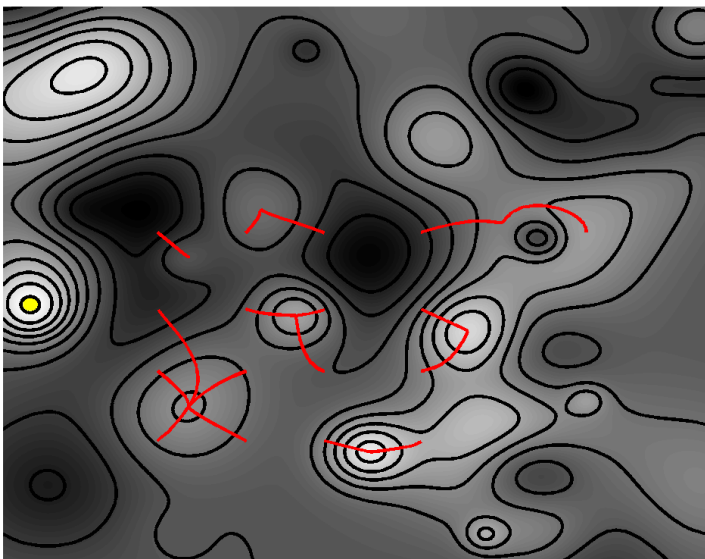
(3) **Repeat (2)** until convergence criterion is reached.

Machine learning control III

☰ Duriez, Brunton & Noack 2016 Springer, ☳ Gautier et al. 2015 JFM

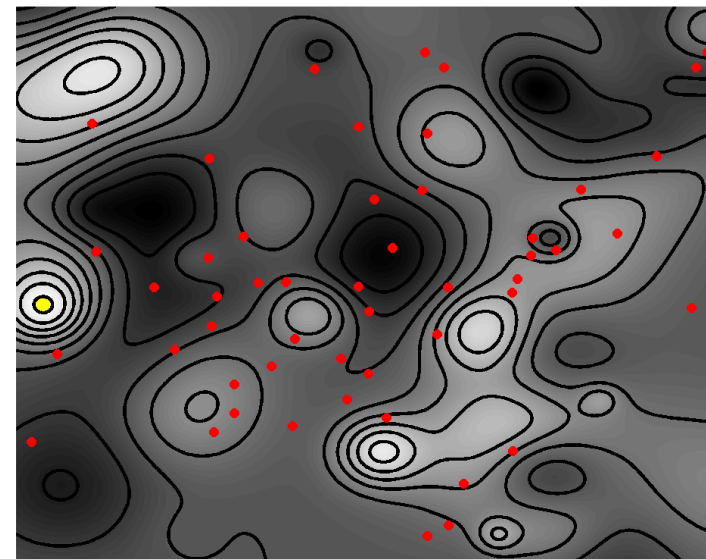
Gradient search

requires structure identification
of the control law and yields pa-
rameter identification
(local minimization)



Genetic algorithm/programming

= evolutionary algorithm for regres-
sion with parameter/structure identi-
fication of the control law
(global minimization)

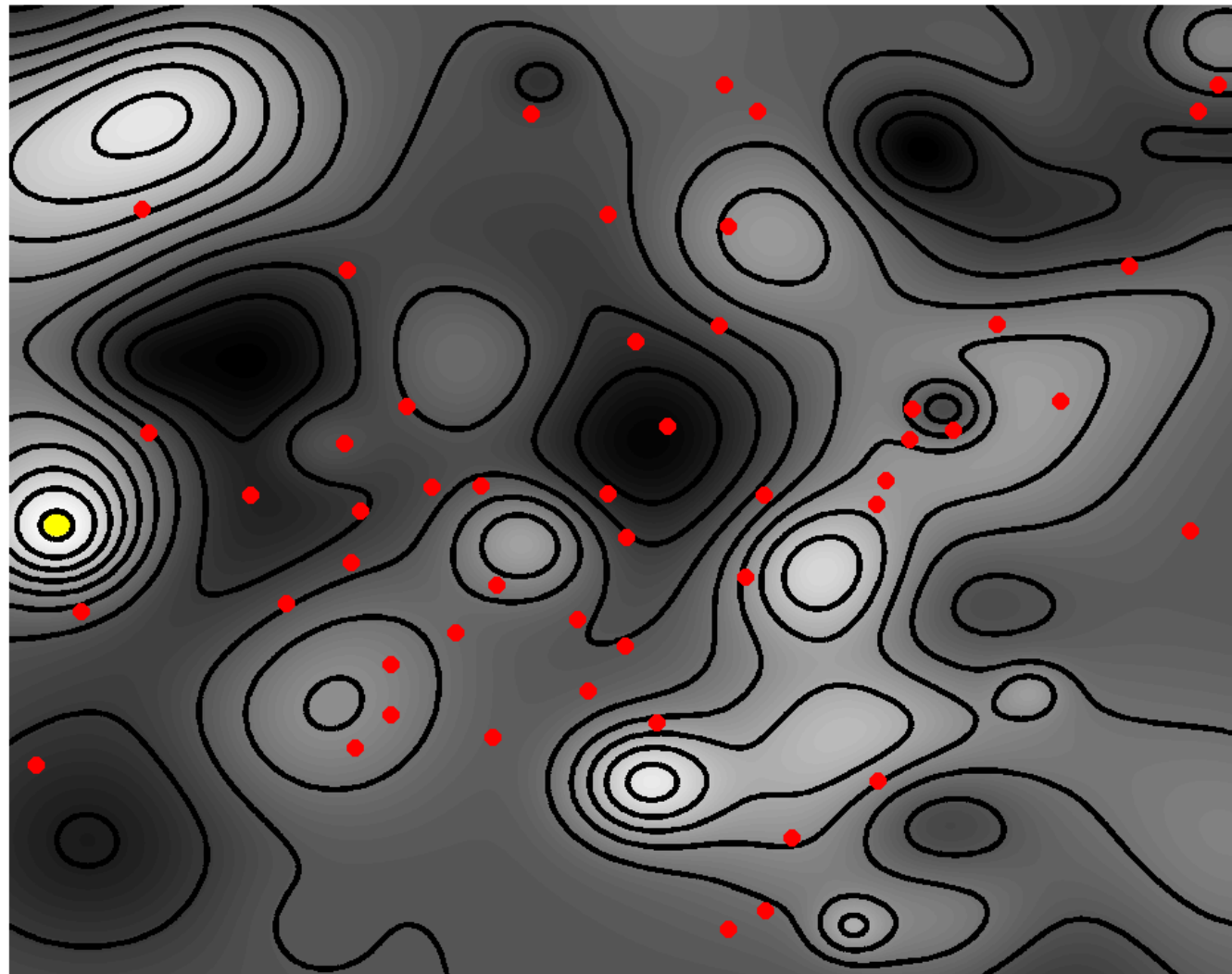


Example of an evolutionary minimization

Machine learning control III

☰ Duriez, Brunton & Noack 2016 Springer, ☰ Gautier et al. 2015 JFM

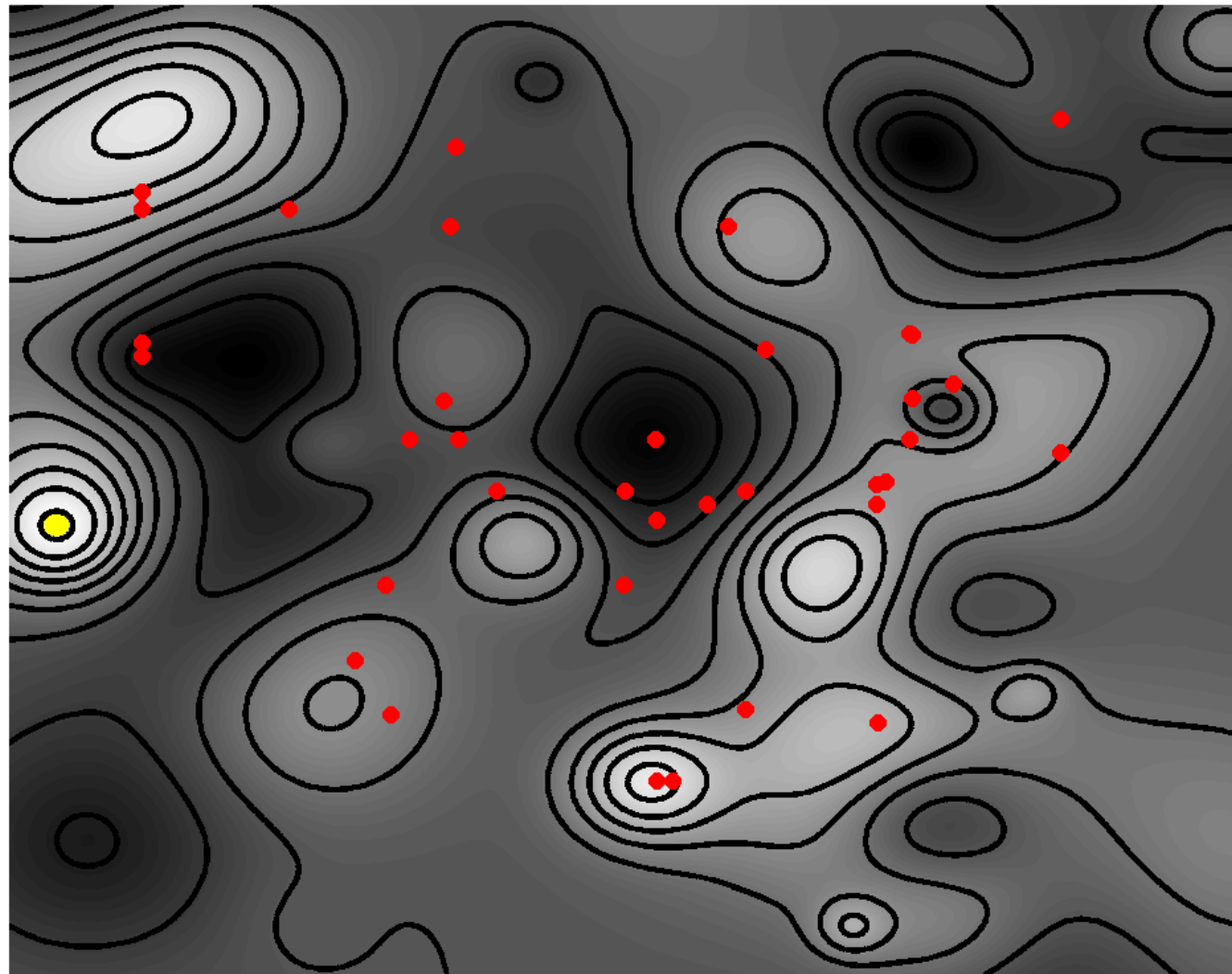
$n = 1$



Machine learning control III

☰ Duriez, Brunton & Noack 2016 Springer, ☰ Gautier et al. 2015 JFM

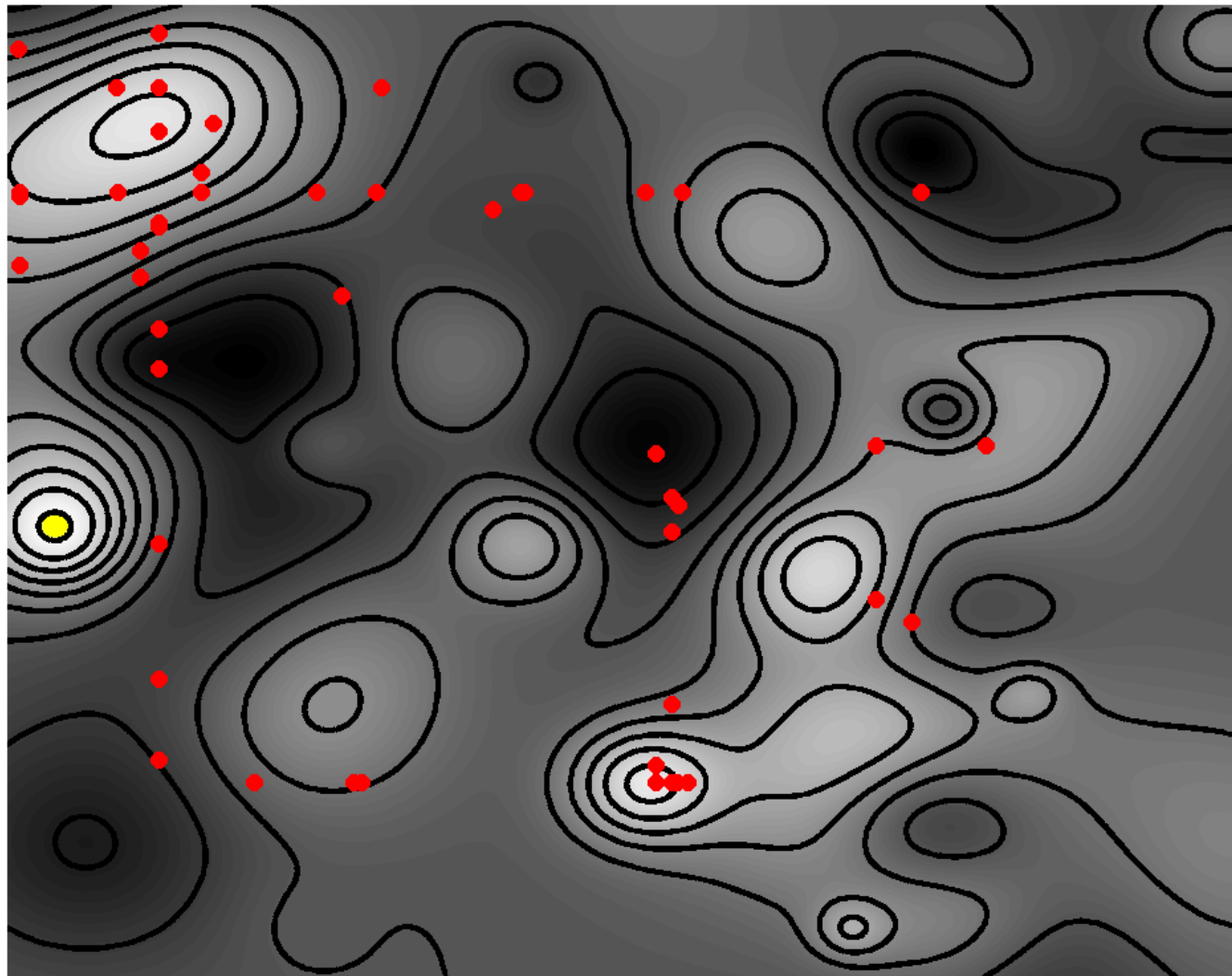
$n = 2$



Machine learning control III

☰ Duriez, Brunton & Noack 2016 Springer, ☰ Gautier et al. 2015 JFM

$n = 3$



Machine learning control III

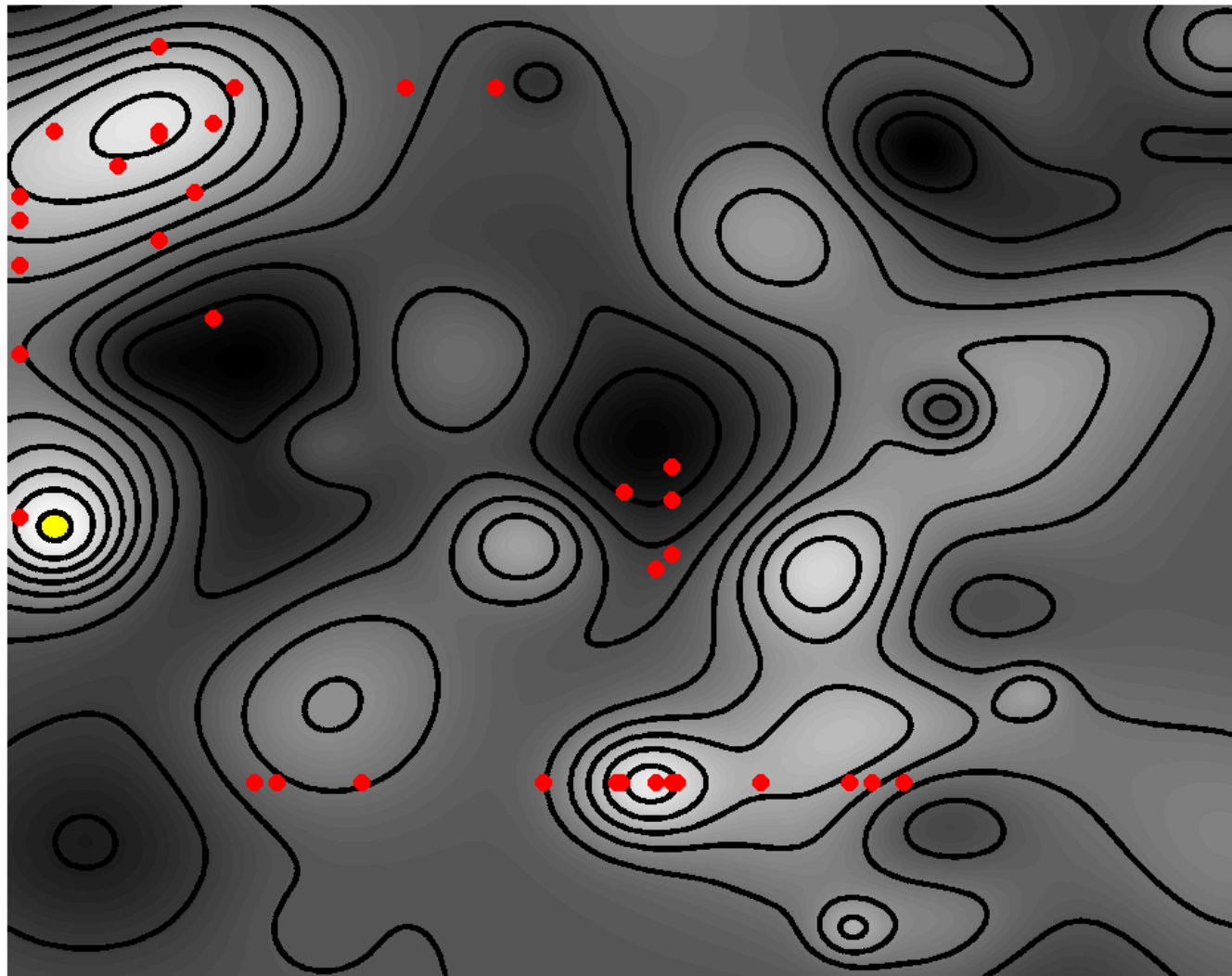


Duriez, Brunton & Noack 2016 Springer,



Gautier et al. 2015 JFM

$n = 4$



Machine learning control III

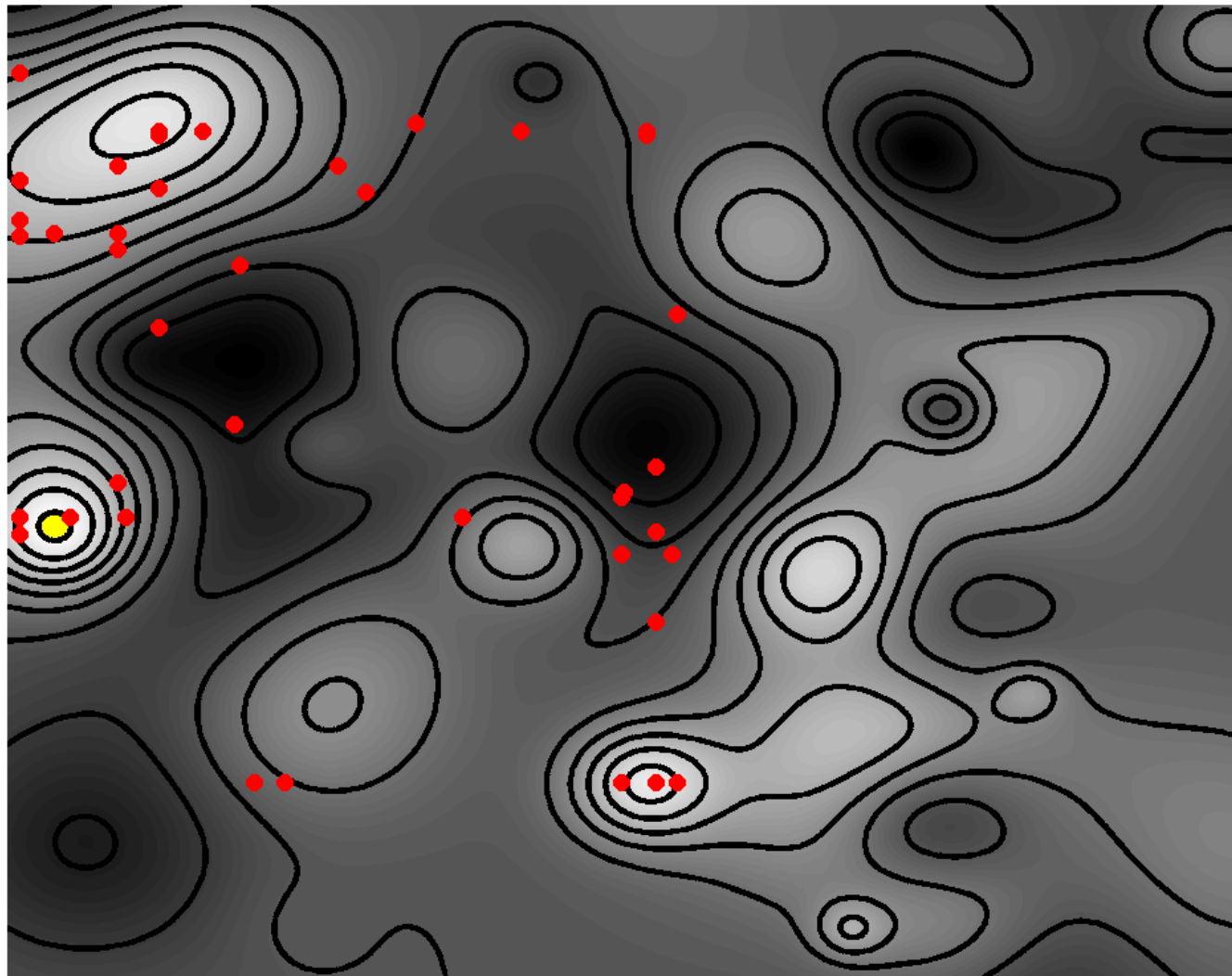


Duriez, Brunton & Noack 2016 Springer,



Gautier et al. 2015 JFM

$n = 5$



Machine learning control III

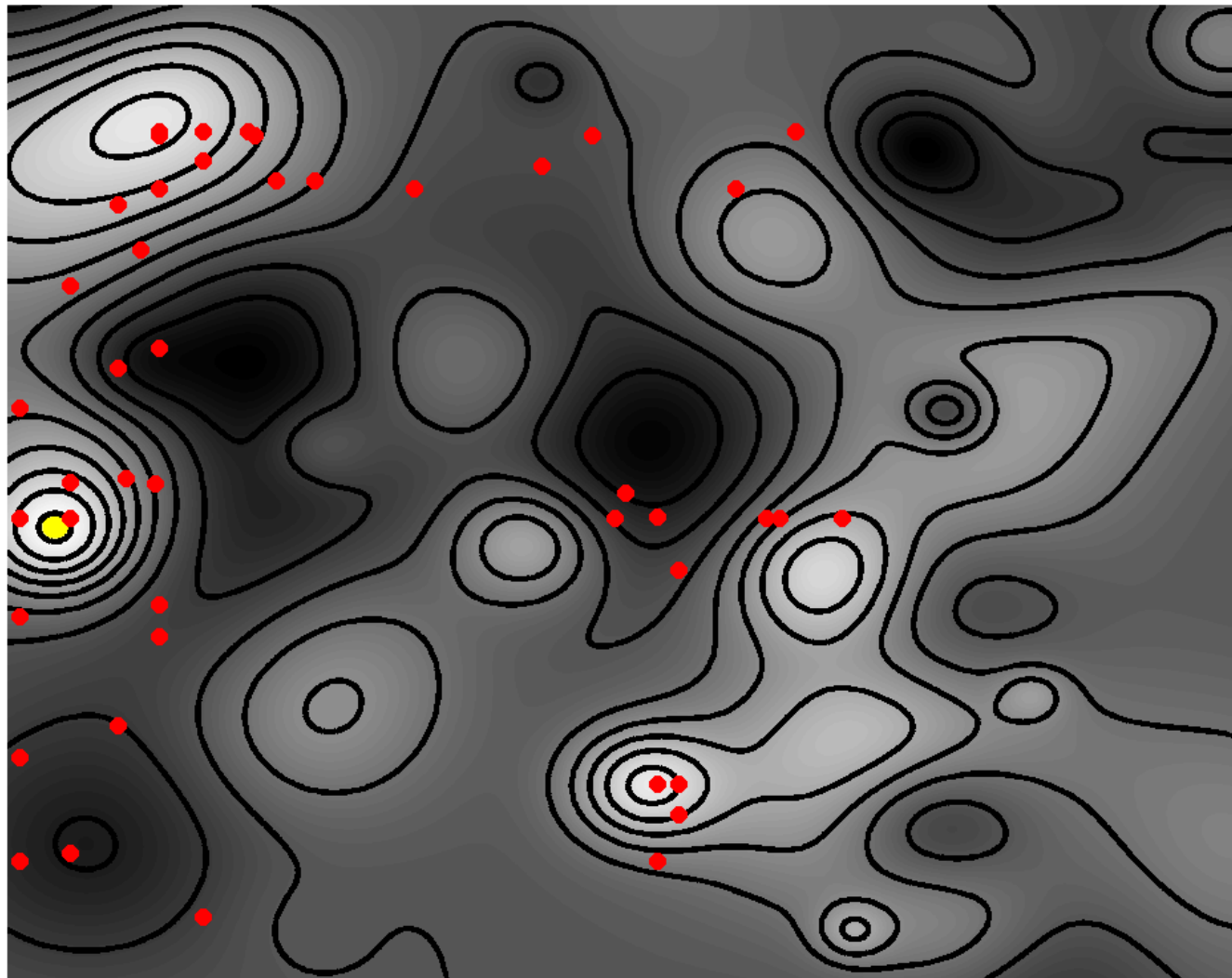


Duriez, Brunton & Noack 2016 Springer,



Gautier et al. 2015 JFM

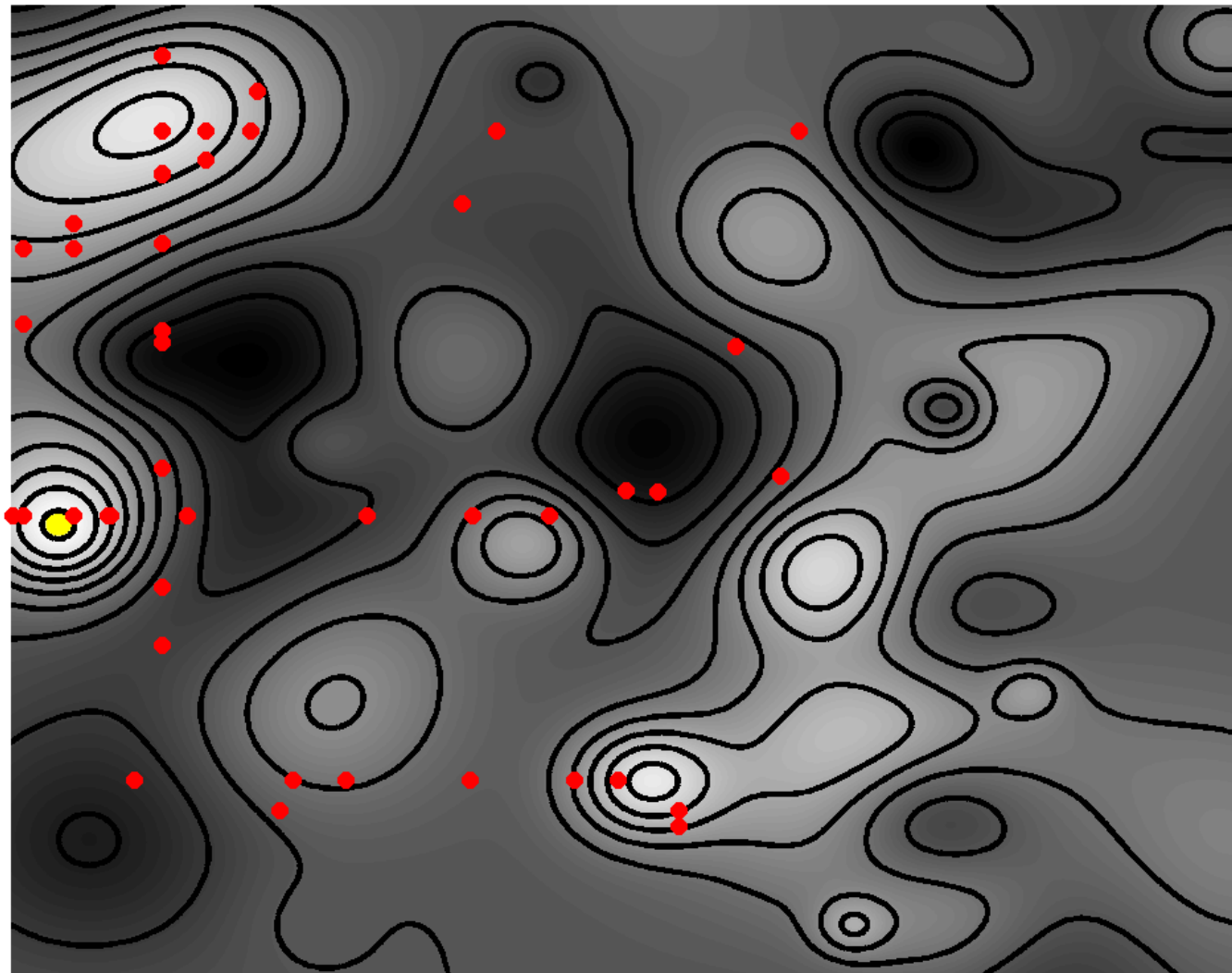
$n = 6$



Machine learning control III

☰ Duriez, Brunton & Noack 2016 Springer, ☰ Gautier et al. 2015 JFM

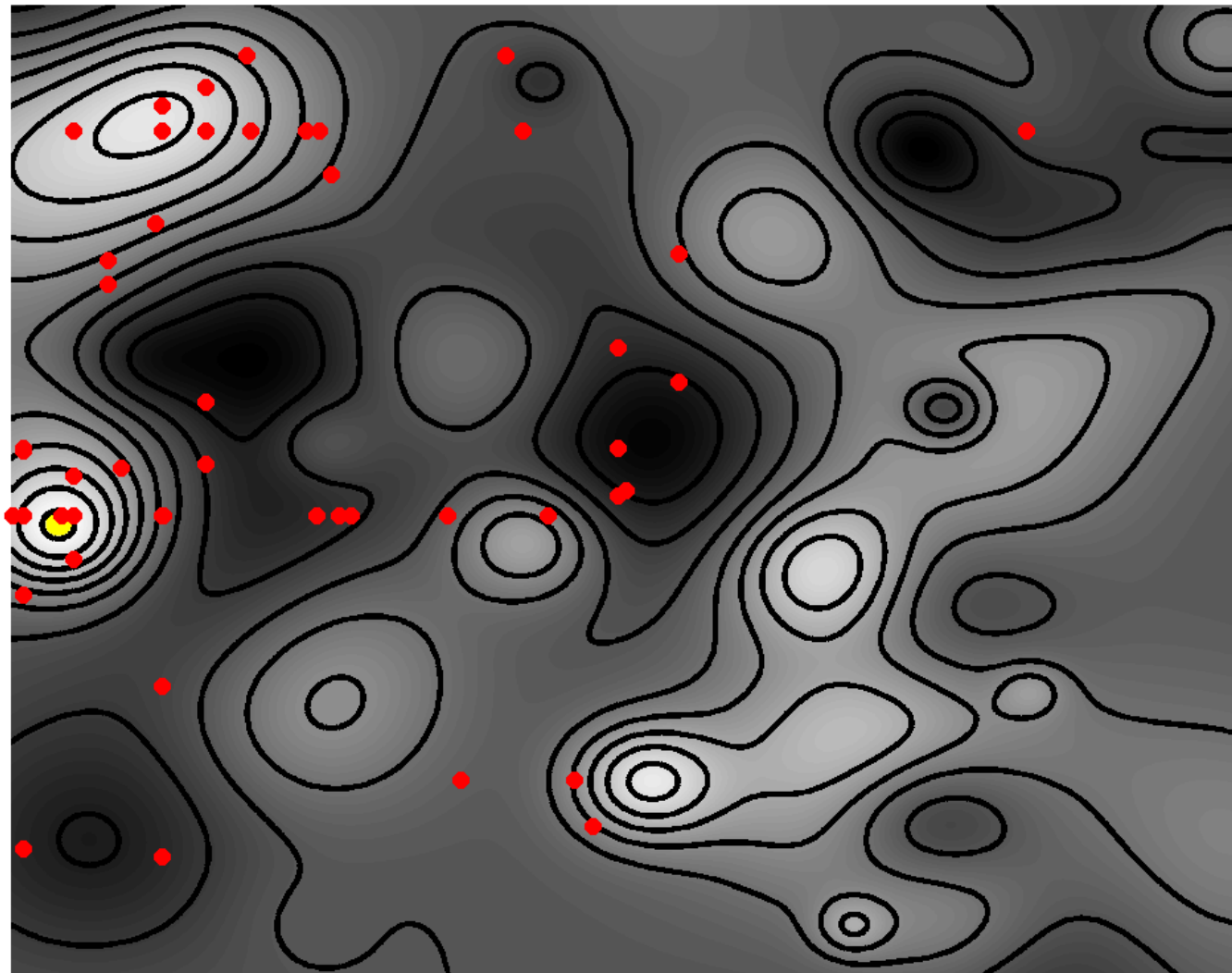
$n = 7$



Machine learning control III

☰ Duriez, Brunton & Noack 2016 Springer, ☳ Gautier et al. 2015 JFM

$n = 8$



Machine learning control III

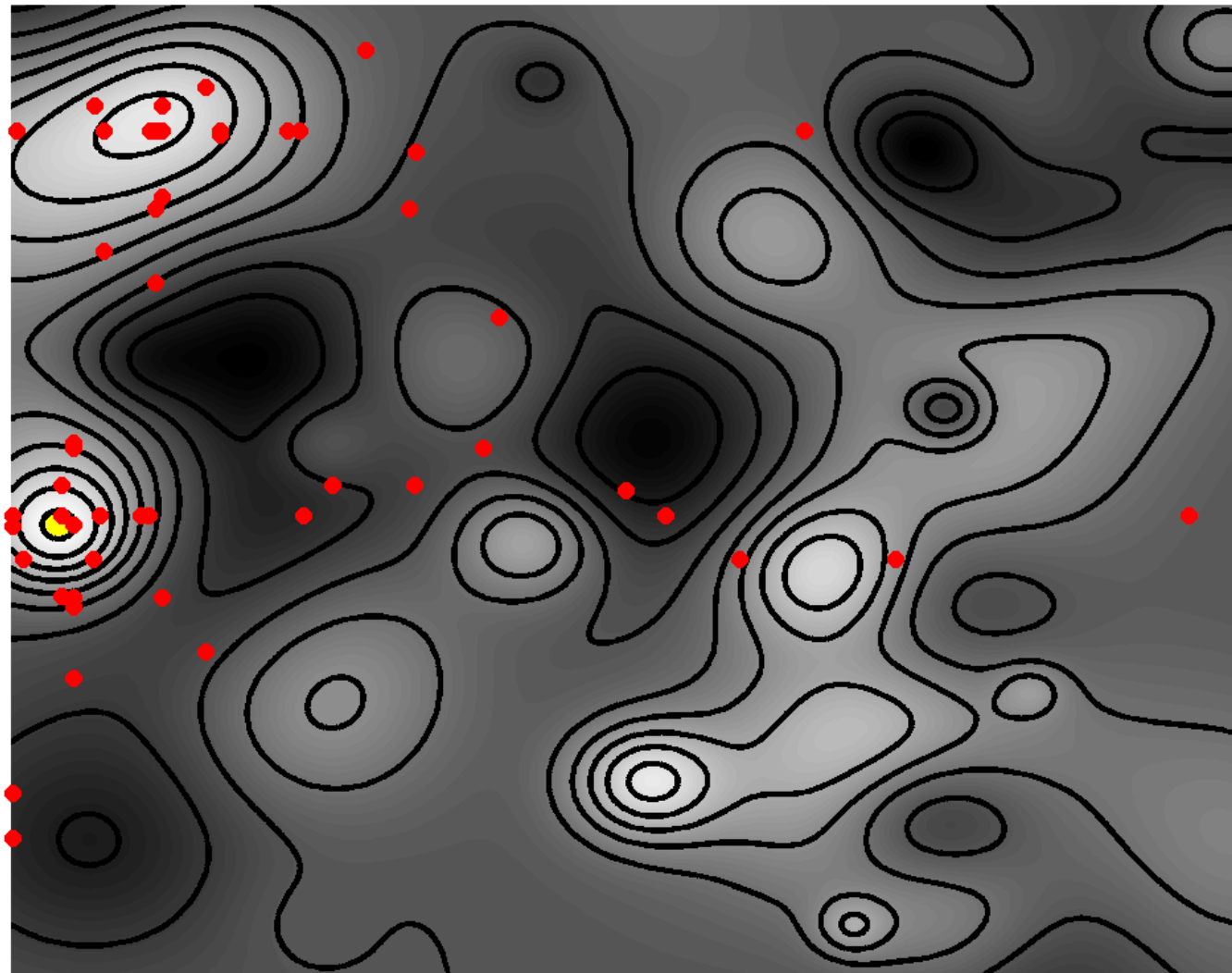


Duriez, Brunton & Noack 2016 Springer,



Gautier et al. 2015 JFM

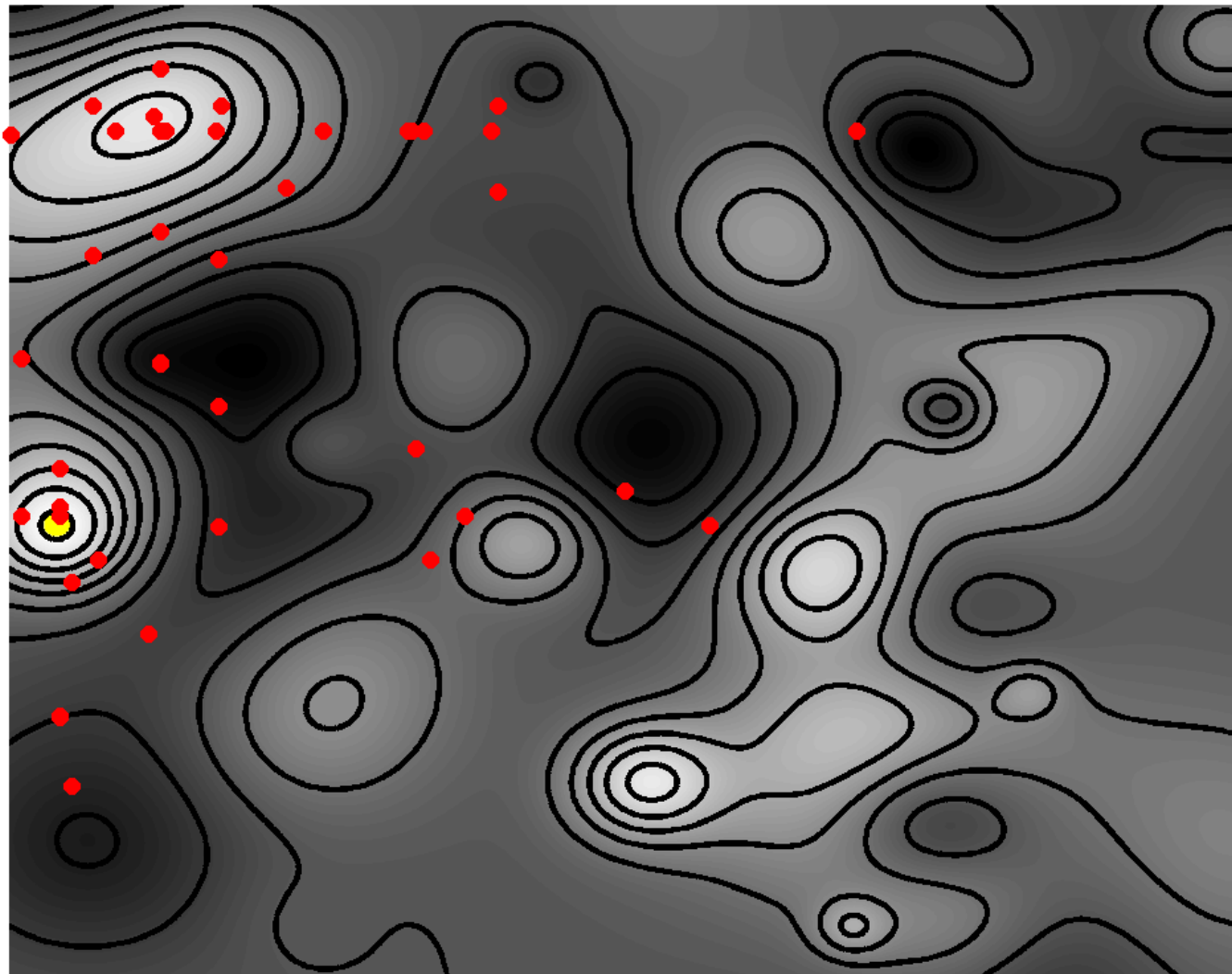
$n = 9$



Machine learning control III

☰ Duriez, Brunton & Noack 2016 Springer, ☰ Gautier et al. 2015 JFM

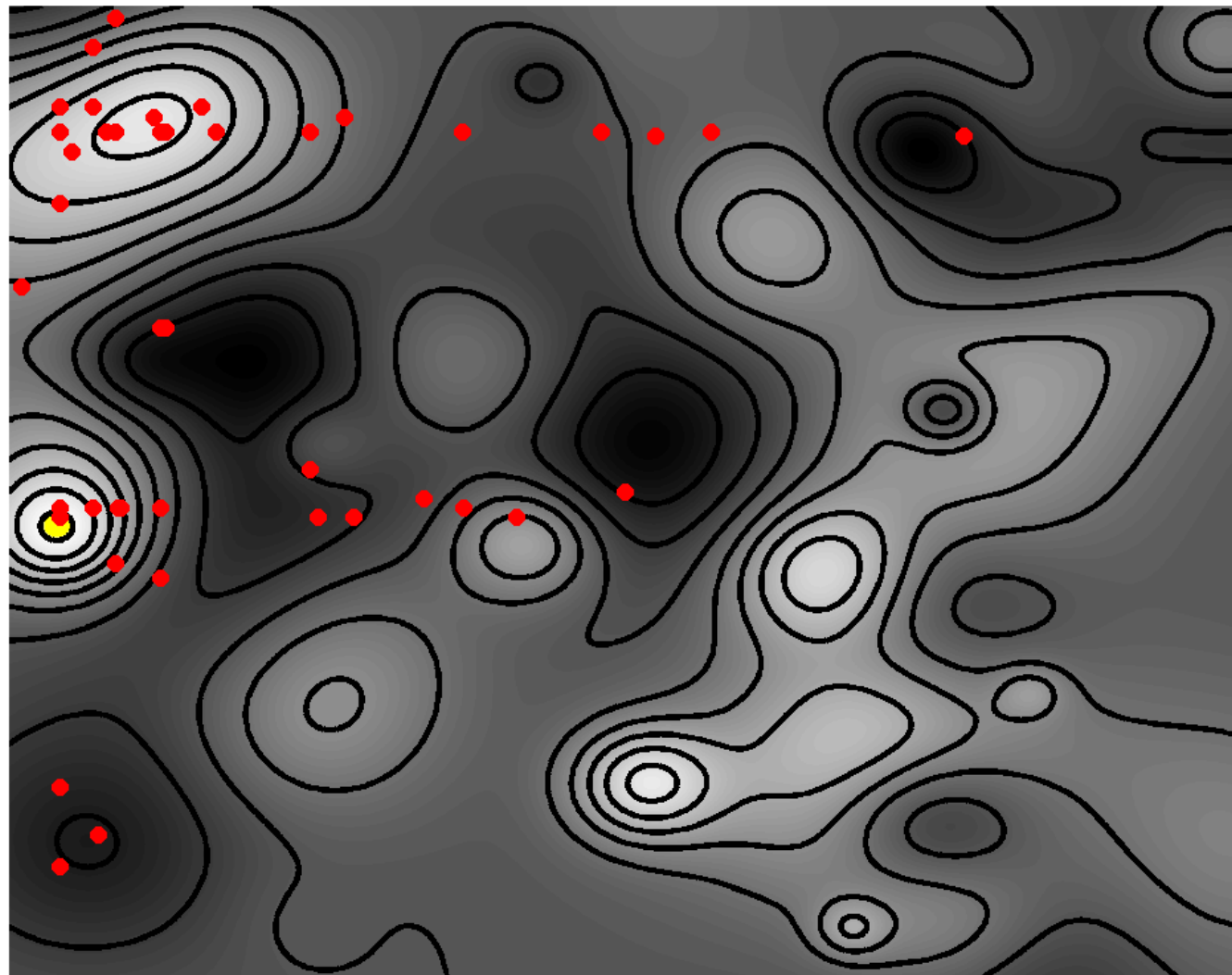
$n = 10$



Machine learning control III

☰ Duriez, Brunton & Noack 2016 Springer, ☰ Gautier et al. 2015 JFM

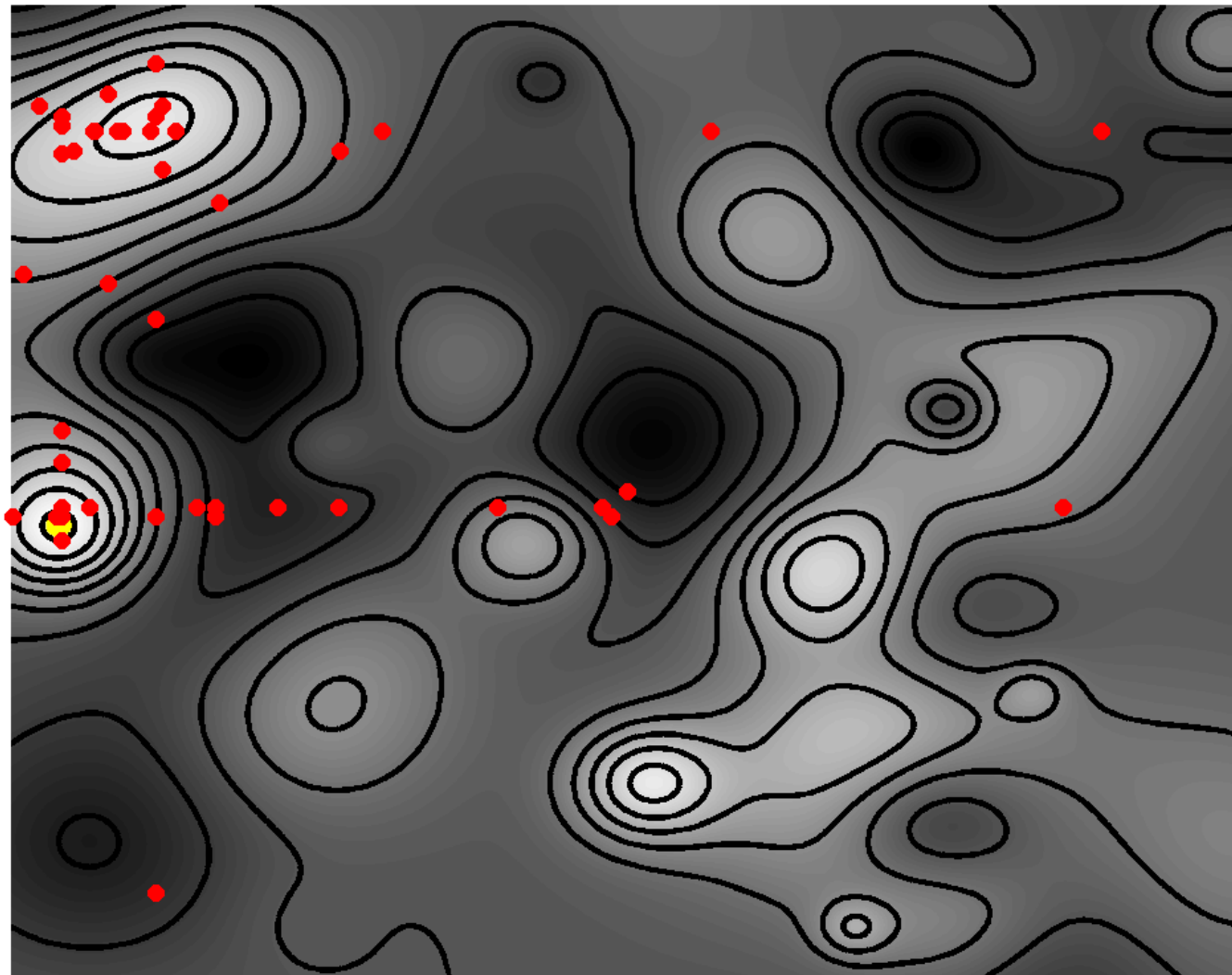
$n = 11$



Machine learning control III

☰ Duriez, Brunton & Noack 2016 Springer, ☳ Gautier et al. 2015 JFM

$n = 12$



Machine learning control III

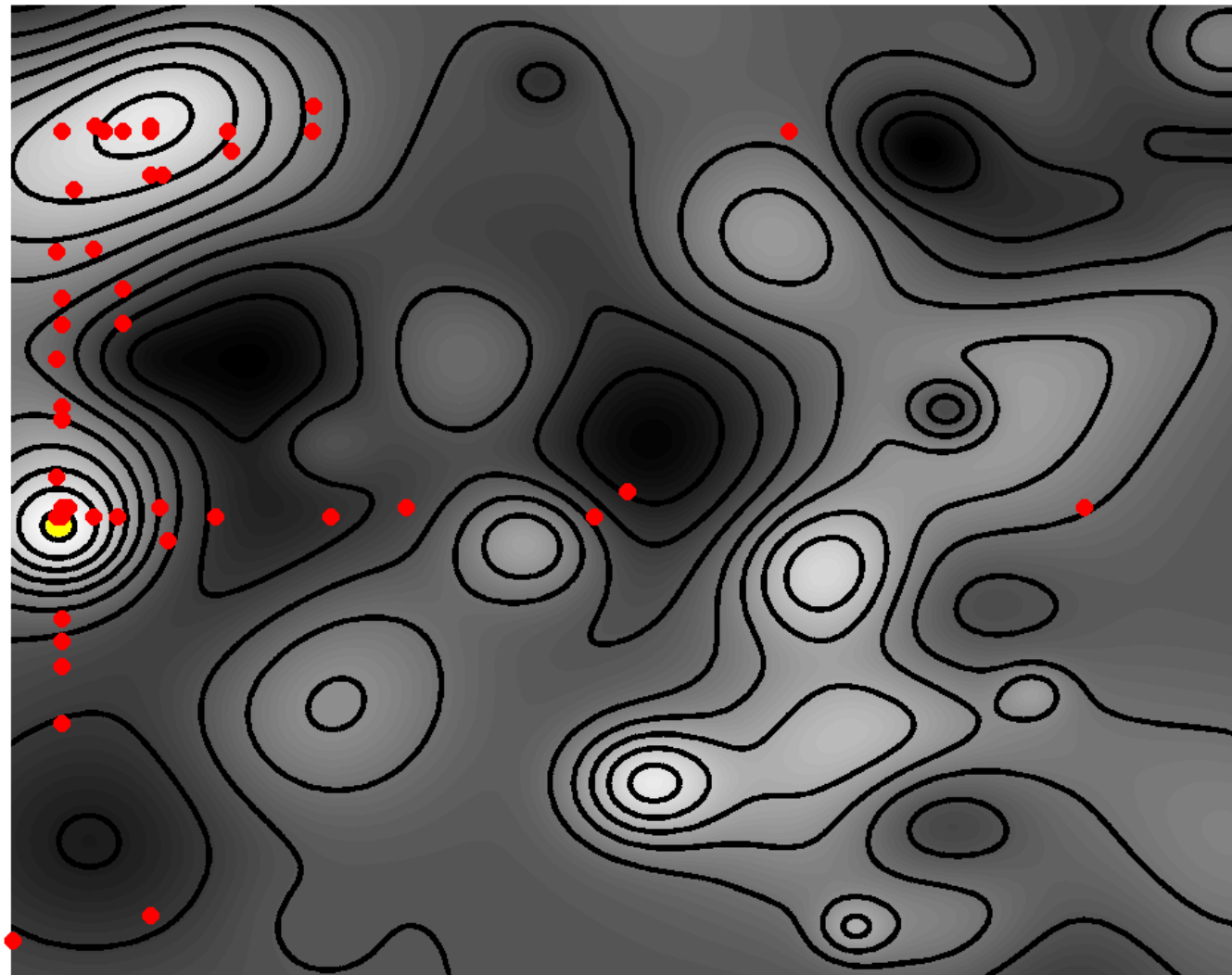


Duriez, Brunton & Noack 2016 Springer,



Gautier et al. 2015 JFM

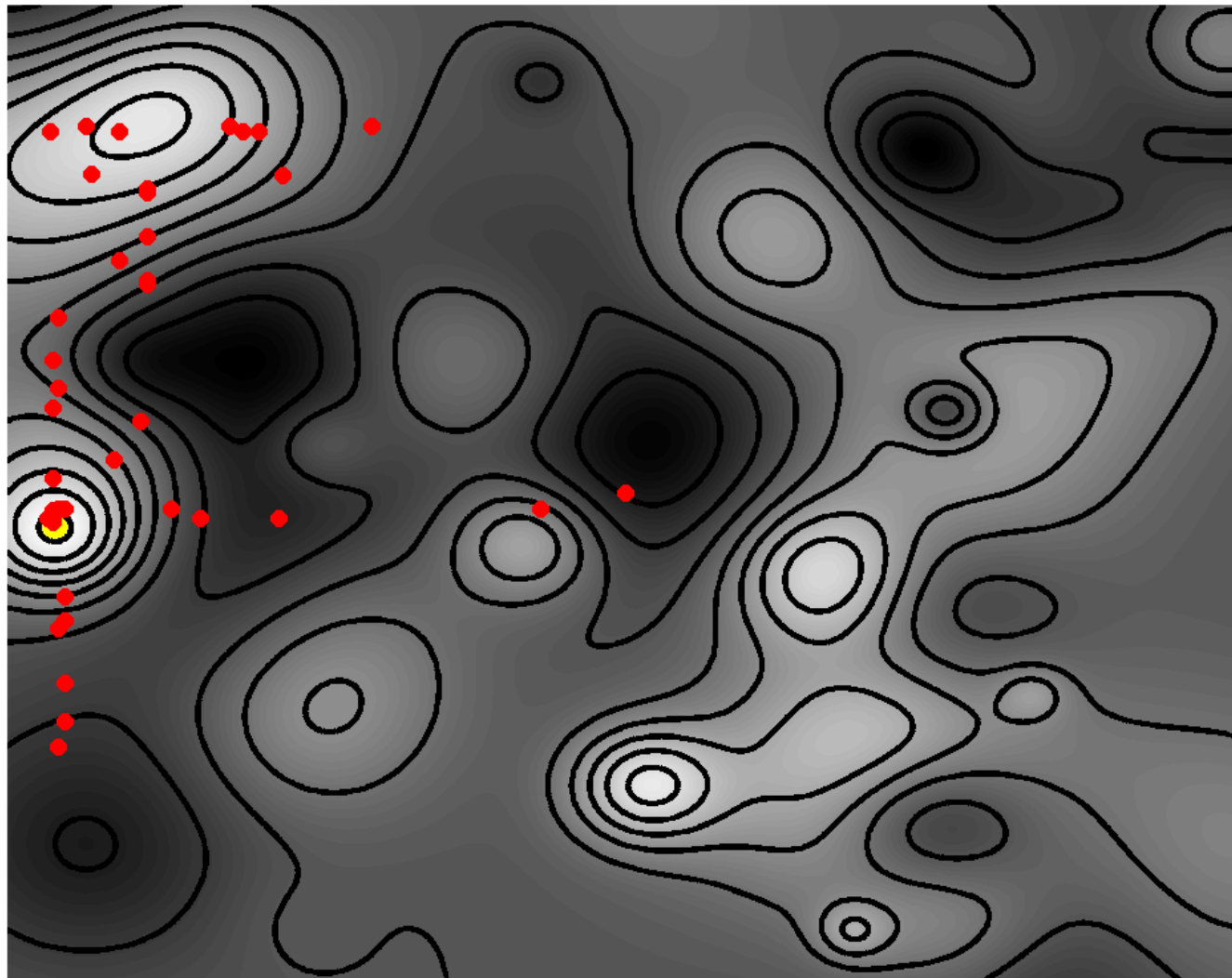
$n = 13$



Machine learning control III

☰ Duriez, Brunton & Noack 2016 Springer, ☰ Gautier et al. 2015 JFM

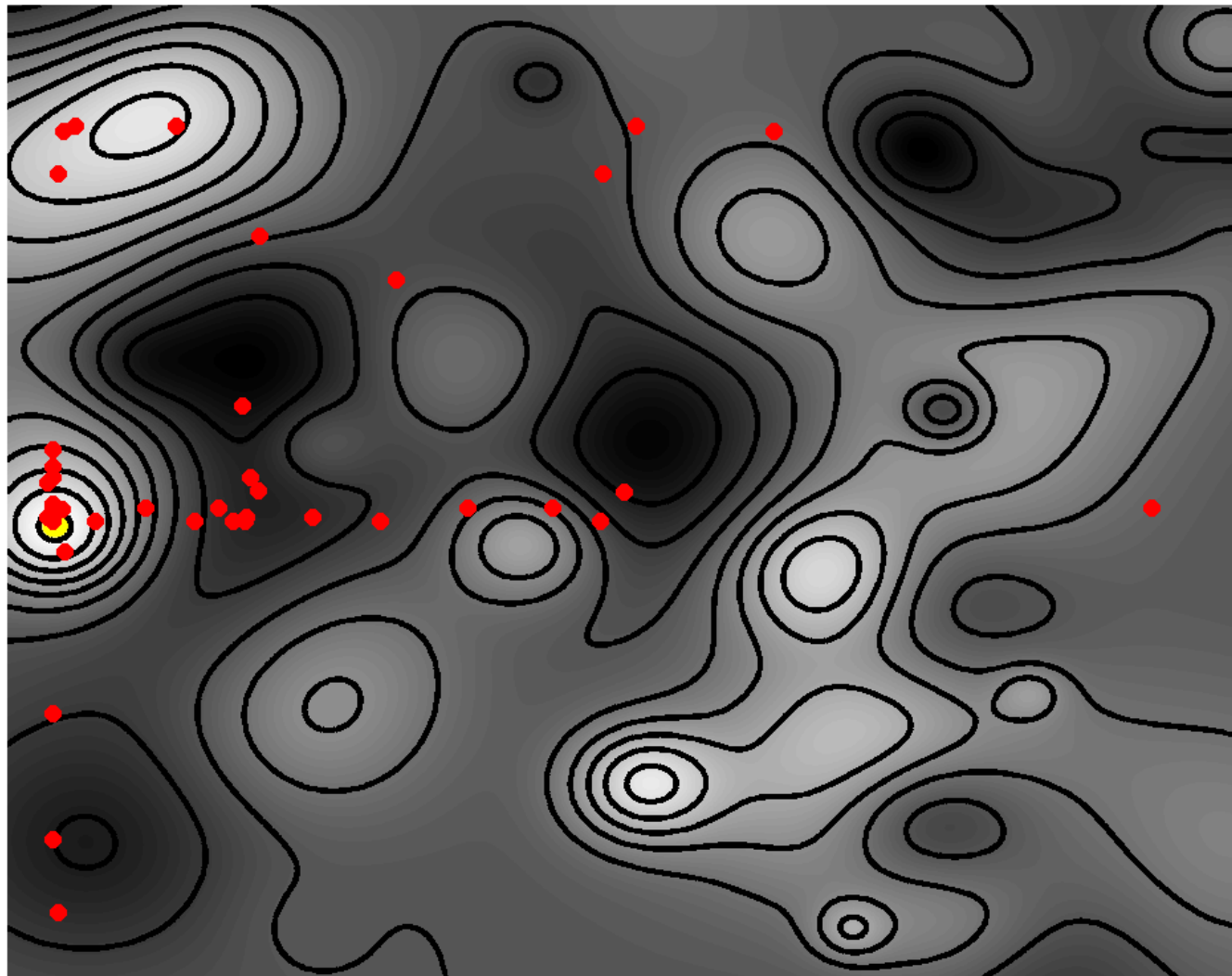
$n = 14$



Machine learning control III

☰ Duriez, Brunton & Noack 2016 Springer, ☰ Gautier et al. 2015 JFM

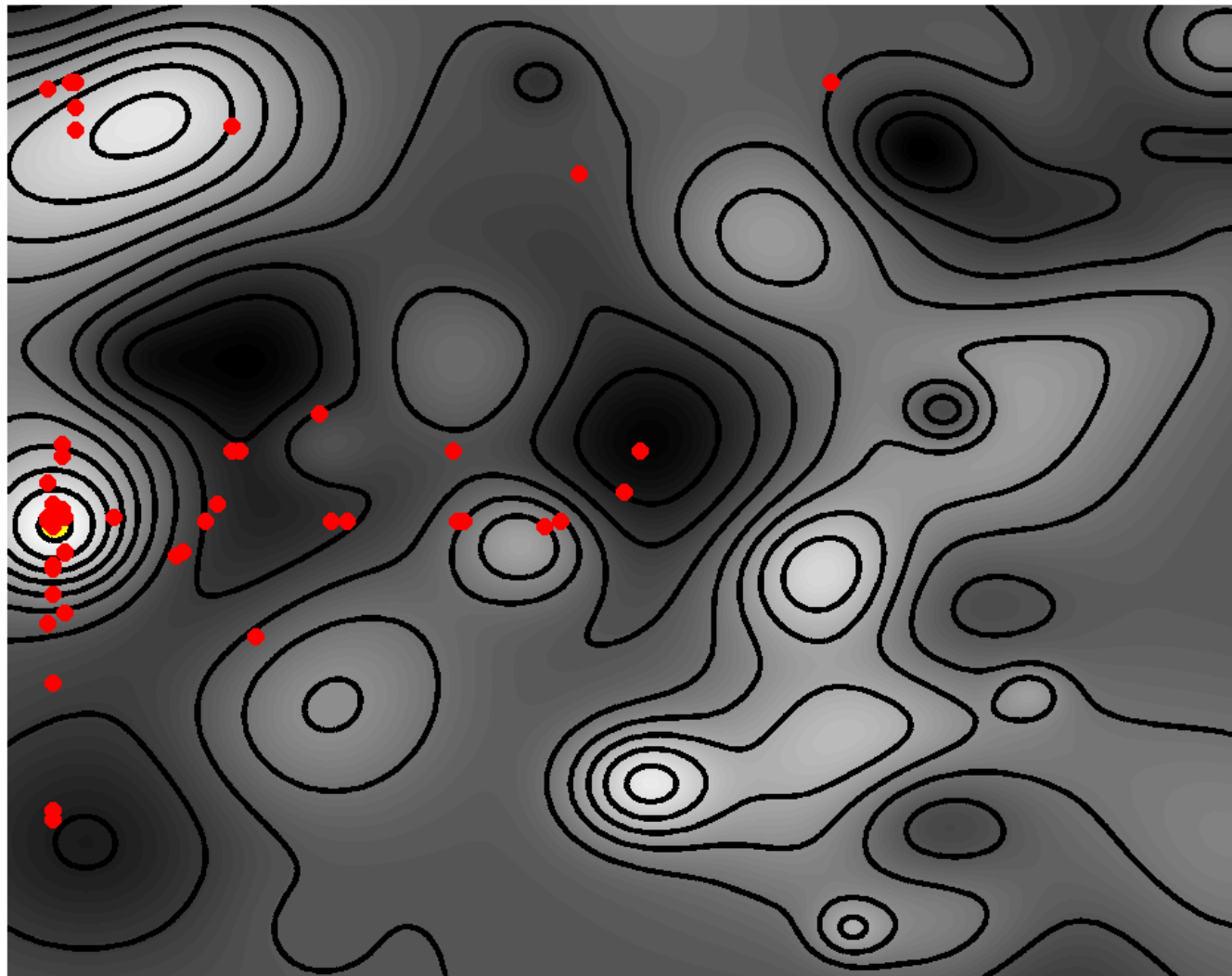
$n = 15$



Machine learning control III

☰ Duriez, Brunton & Noack 2016 Springer, ☰ Gautier et al. 2015 JFM

$n = 16$



Machine learning control III

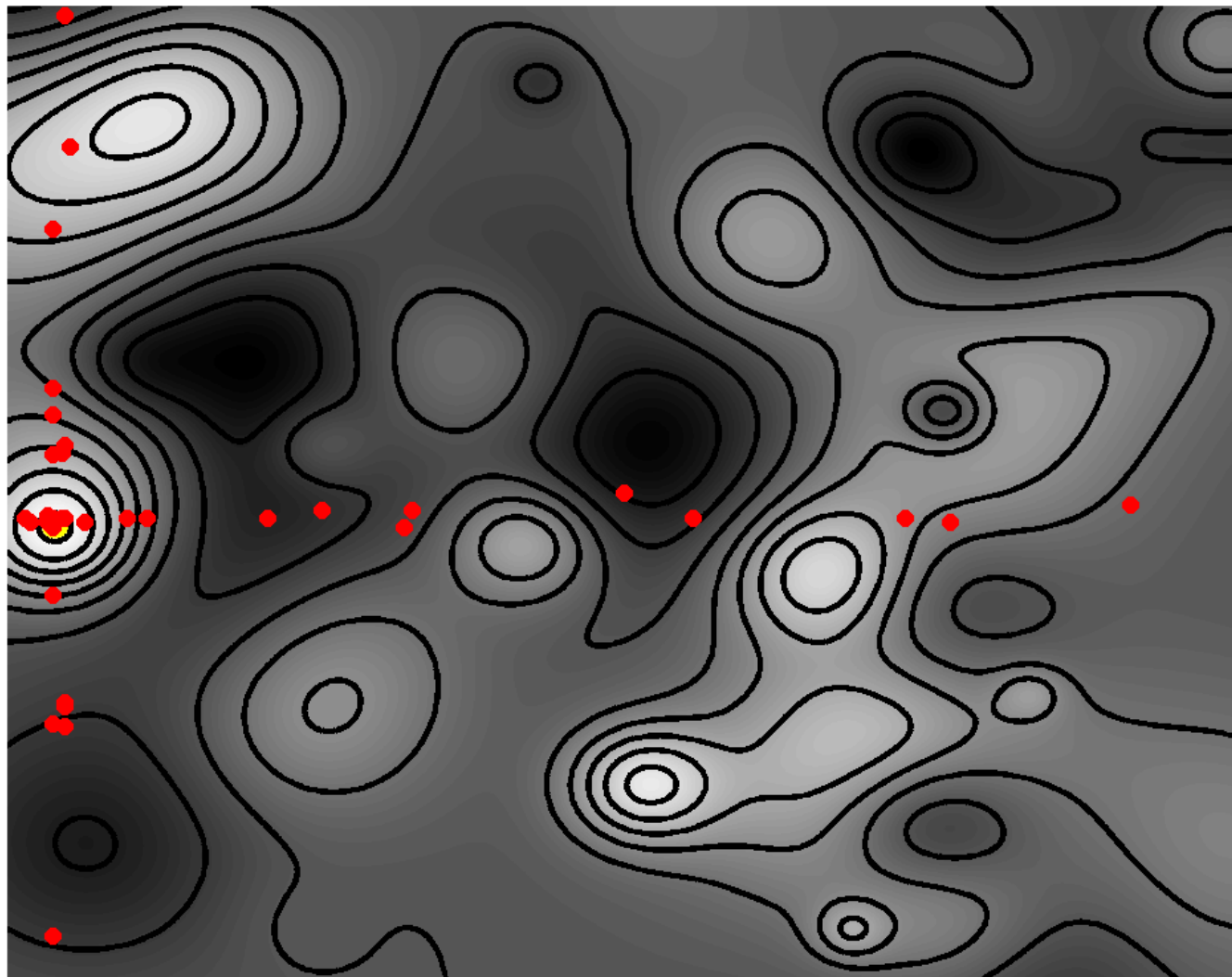


Duriez, Brunton & Noack 2016 Springer,



Gautier et al. 2015 JFM

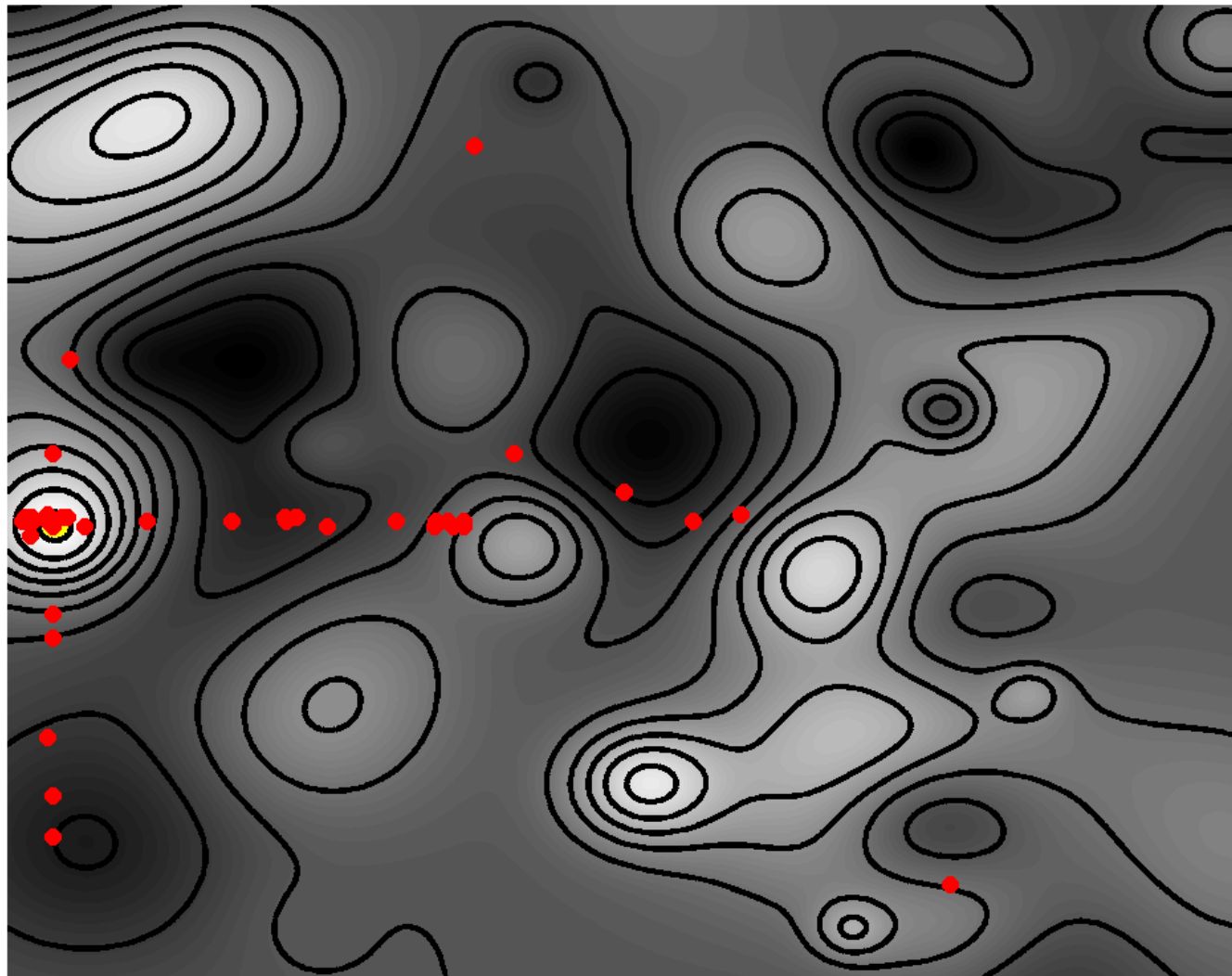
$n = 17$



Machine learning control III

☰ Duriez, Brunton & Noack 2016 Springer, ☰ Gautier et al. 2015 JFM

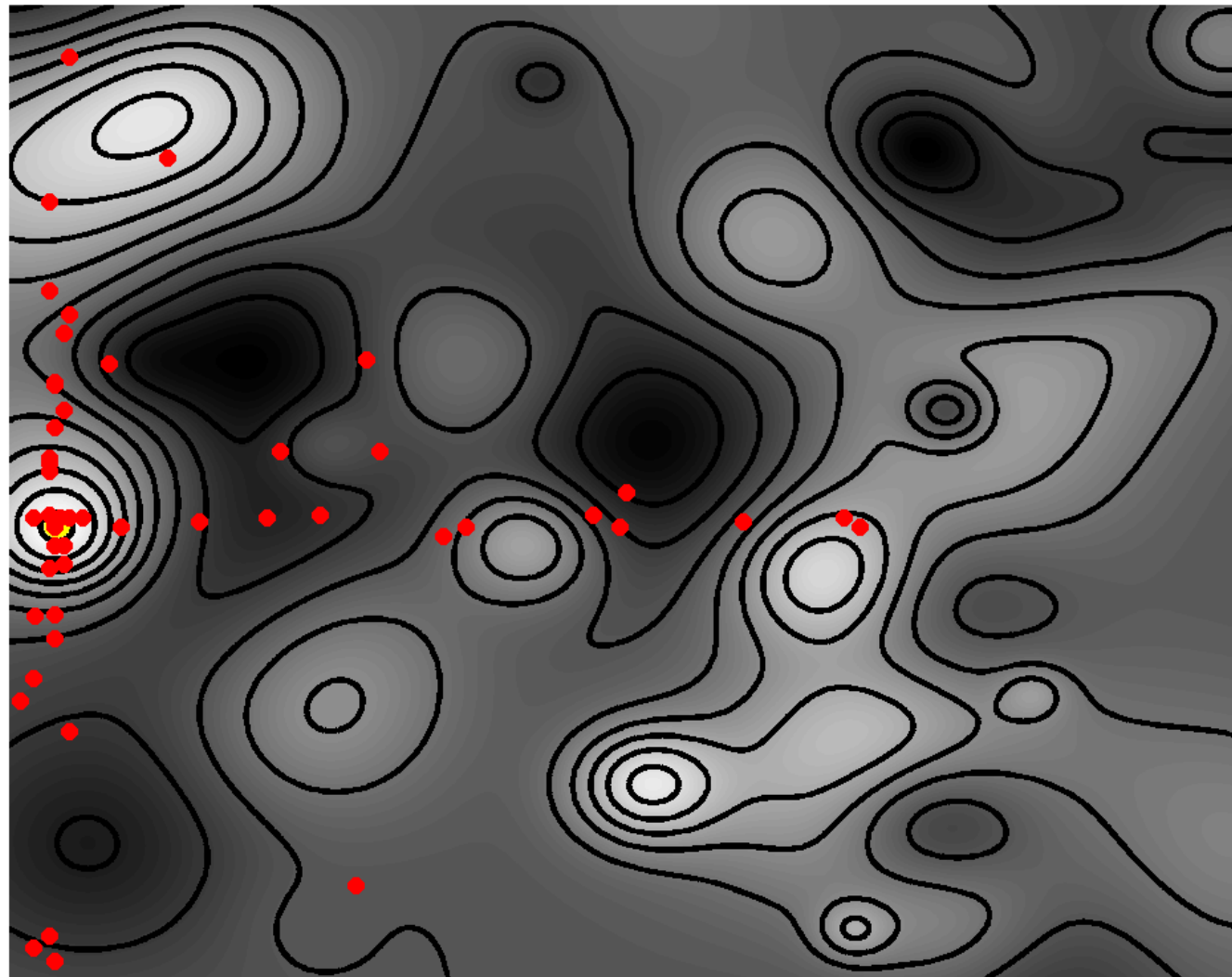
$n = 18$



Machine learning control III

☰ Duriez, Brunton & Noack 2016 Springer, ☰ Gautier et al. 2015 JFM

$n = 19$



Machine learning control III

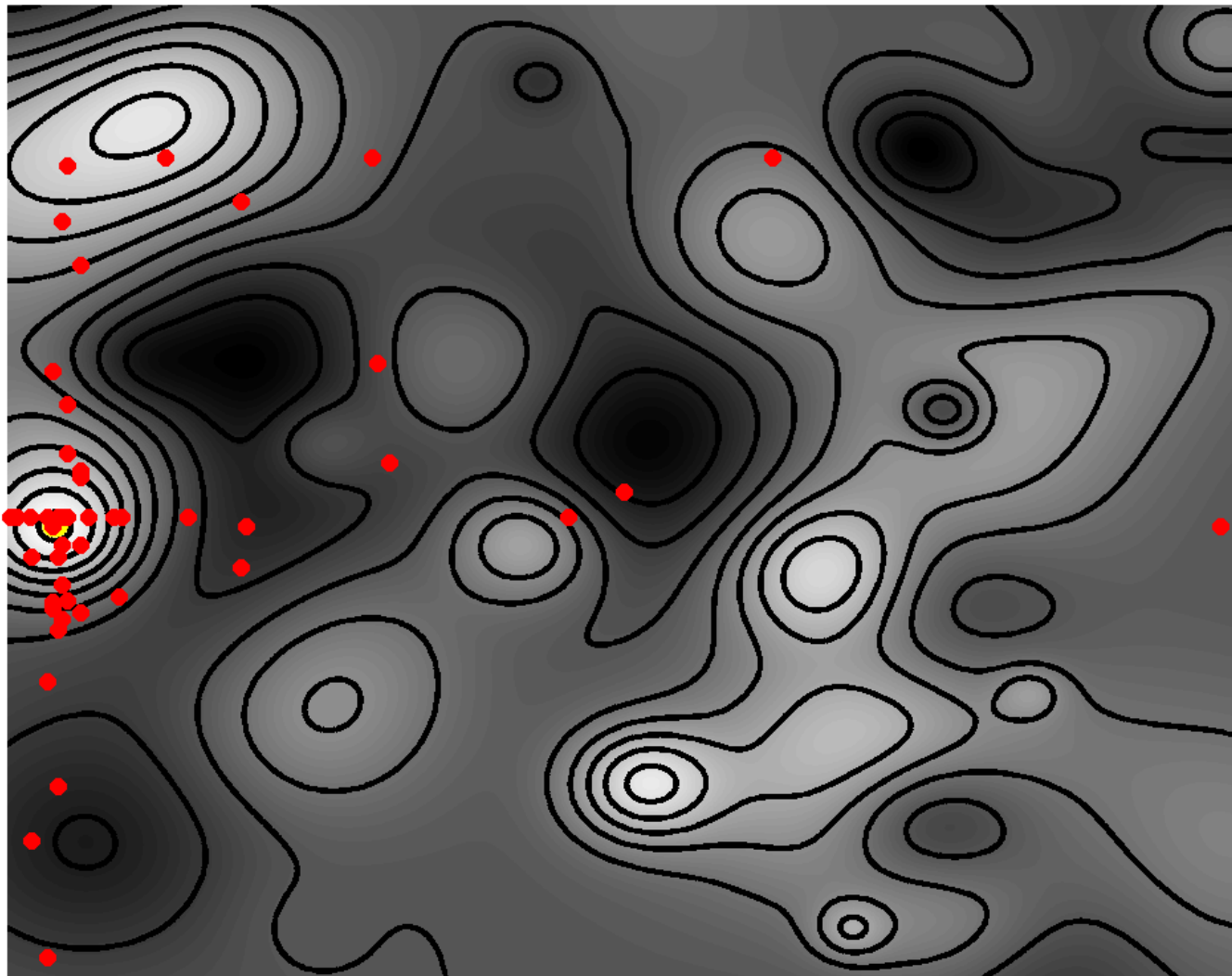


Duriez, Brunton & Noack 2016 Springer,



Gautier et al. 2015 JFM

$n = 20$



Overview

1. Introduction

..... *Control as model-free regression problem*

2. Exploitation

..... *Downhill simplex algorithm*

3. Exploration

..... *Latin hypercube + Monte Carlo*

4. Genetic algorithm

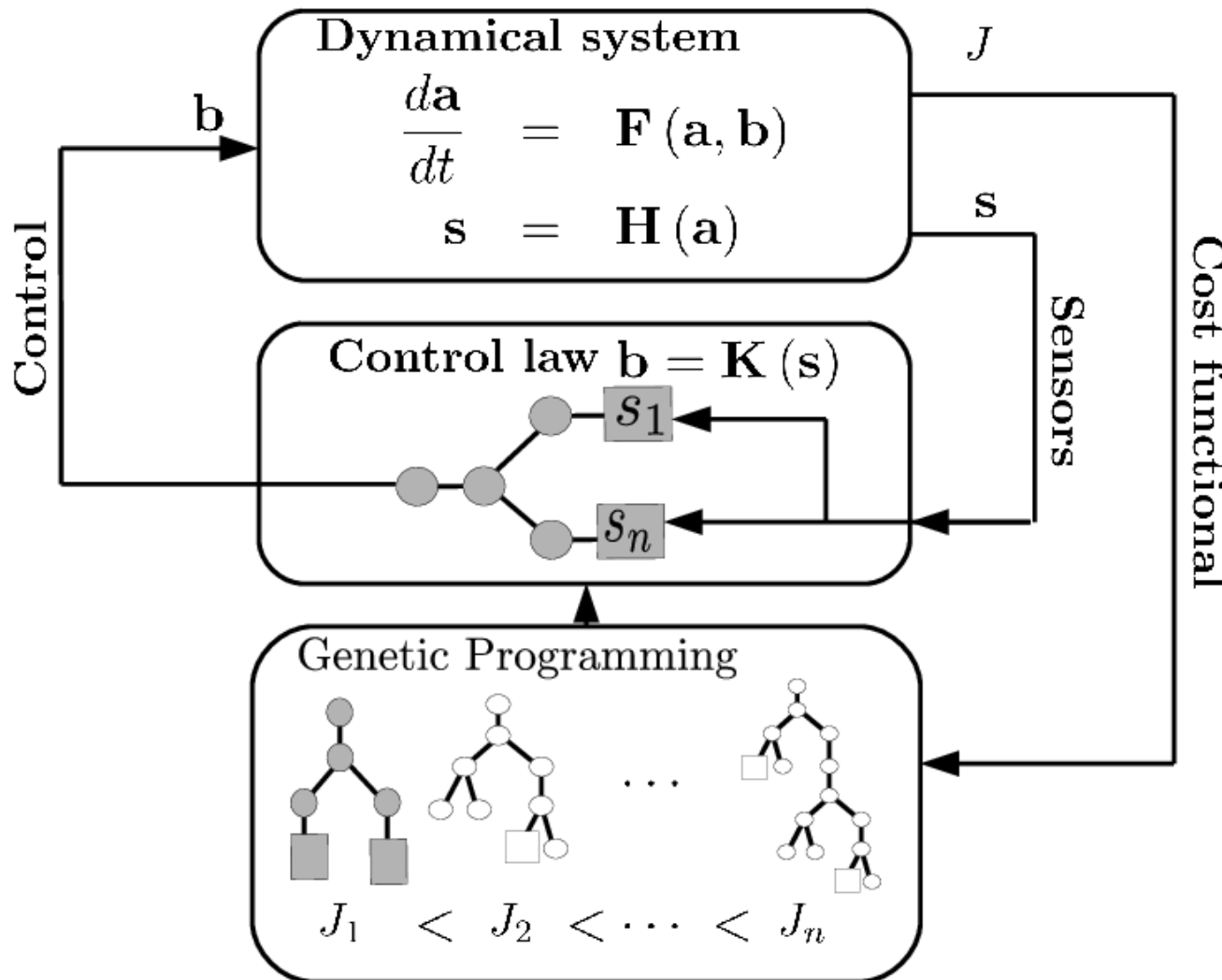
..... *Evolving in a high-dimensional parameter space*

5. Genetic programming

..... *From parameter to function optimization*

Machine learning control

Duriez, Brunton & Noack 2016 Springer, Wahde 2008



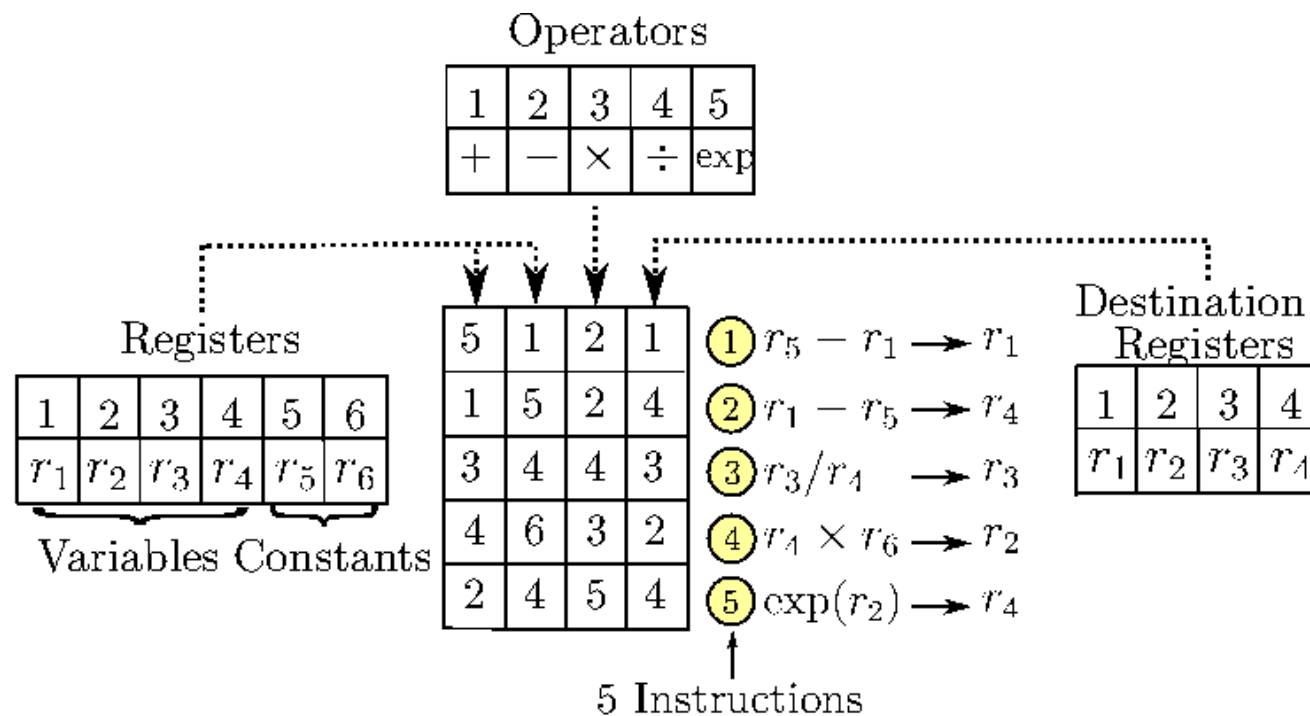
Regression problem: Find $\mathbf{b} = \mathbf{K}(\mathbf{s})$ so that $J = \min$

Regression method = Genetic programming

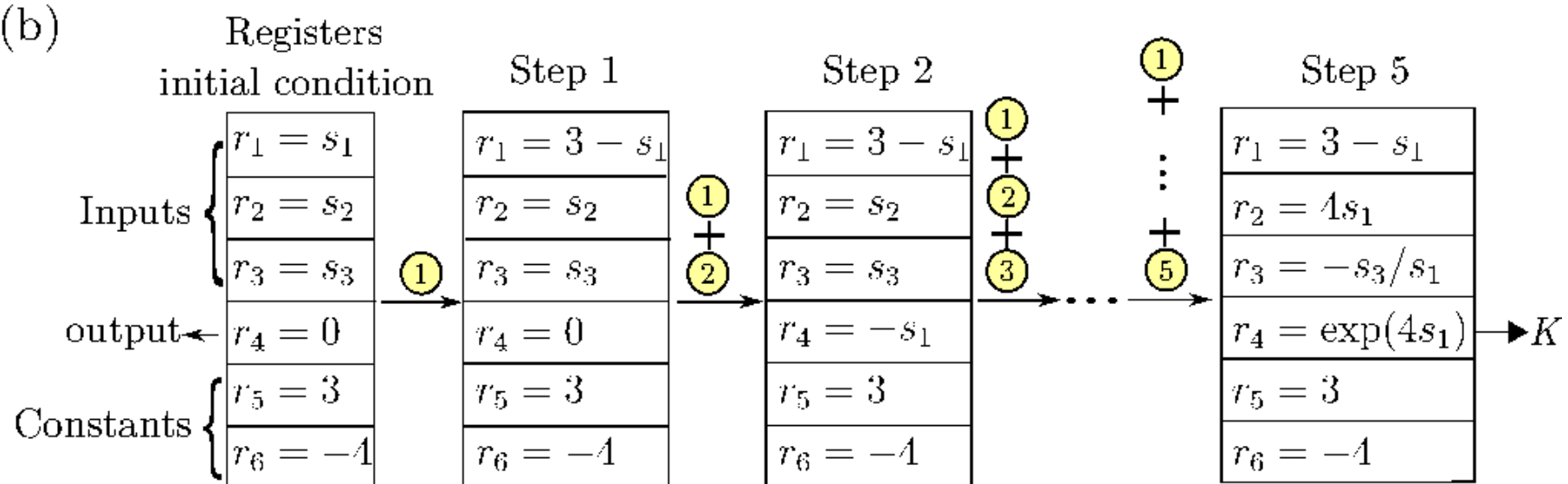
Linear genetic programming – Ansatz

☰ Wahde 2008: Biologically Inspired Optimization

(a)

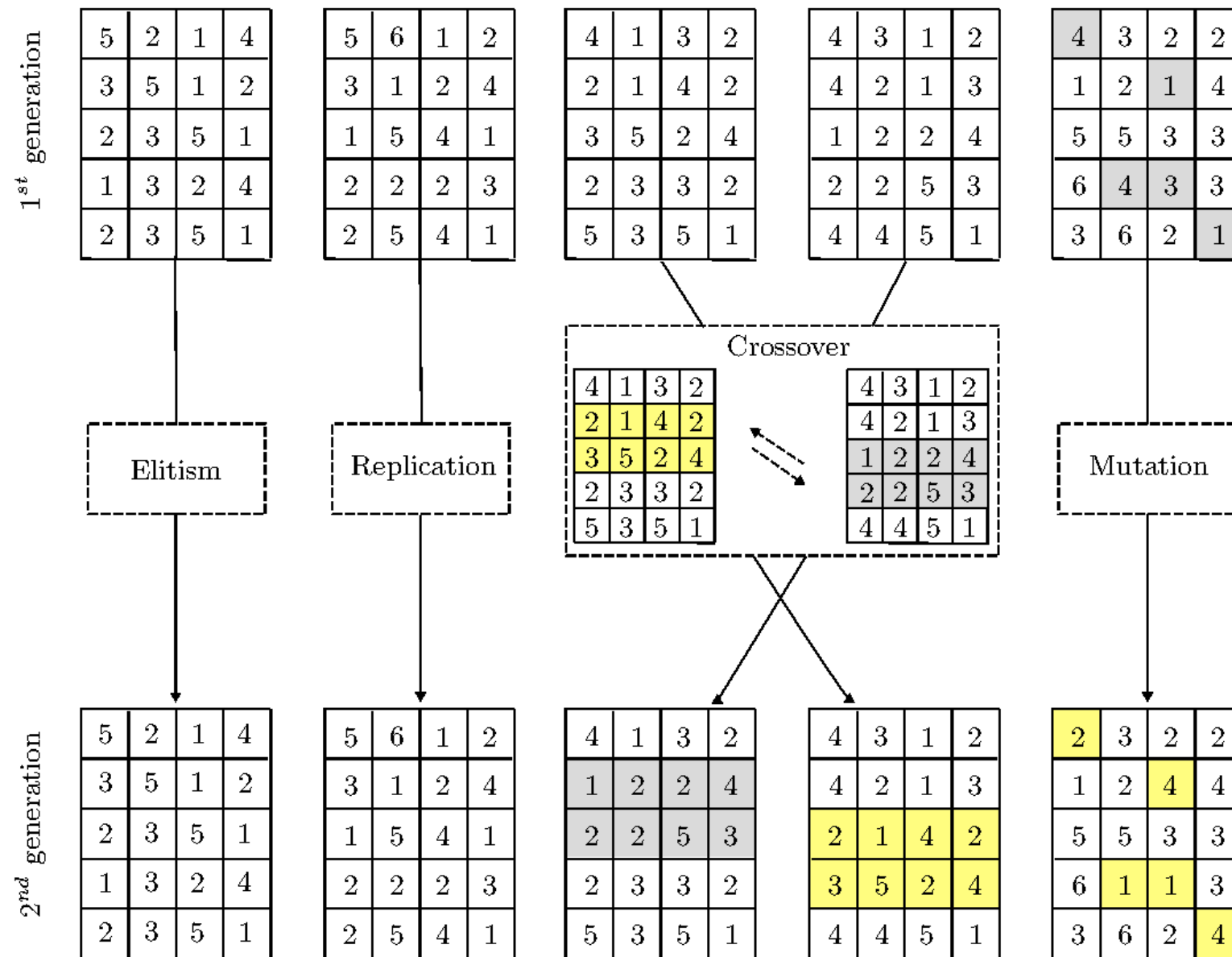


(b)



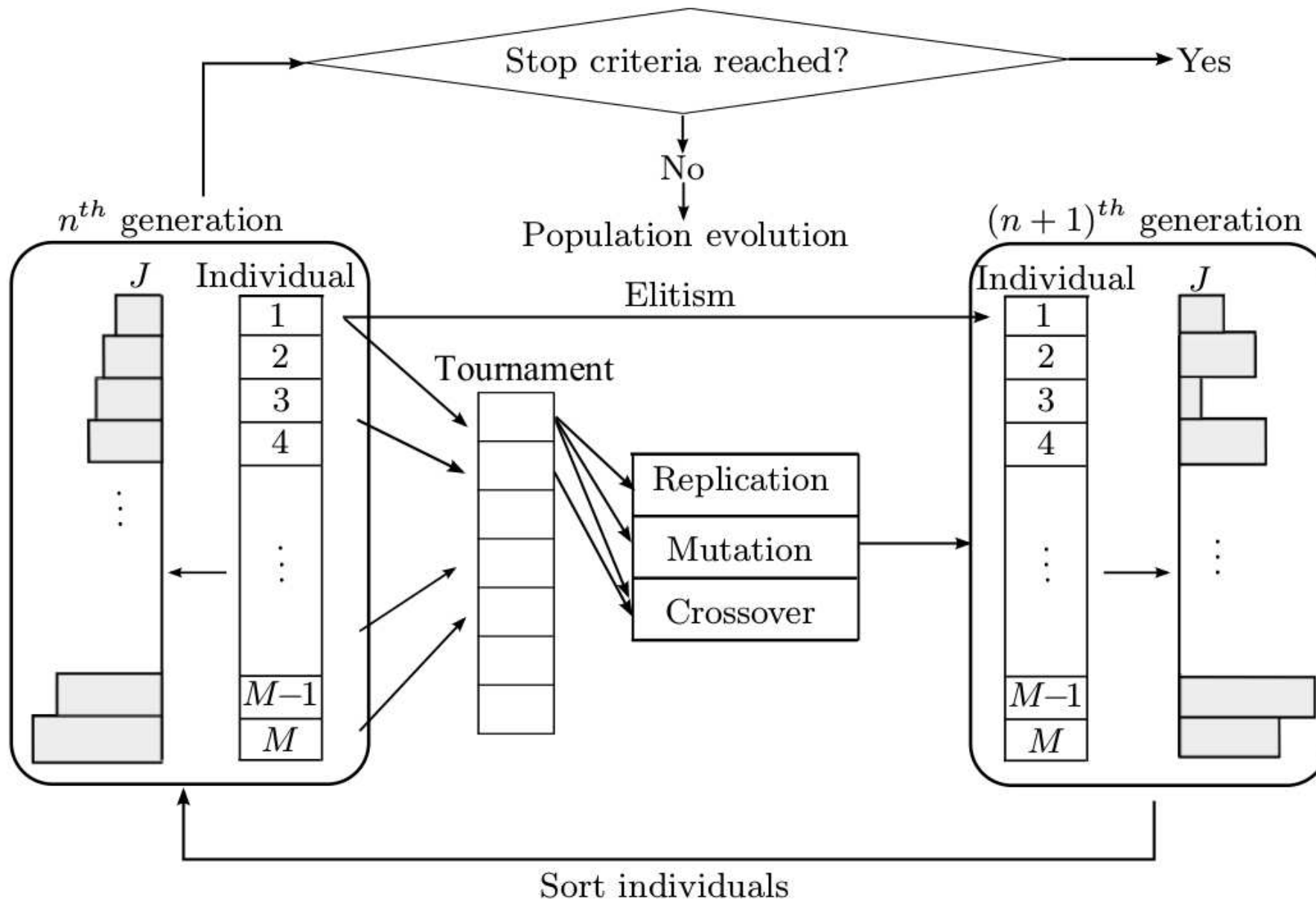
Linear genetic programming – Operations

☰ Wahde 2008: *Biologically Inspired Optimization*



Linear genetic programming — Algorithm

≡ Wahde 2008: *Biologically Inspired Optimization*



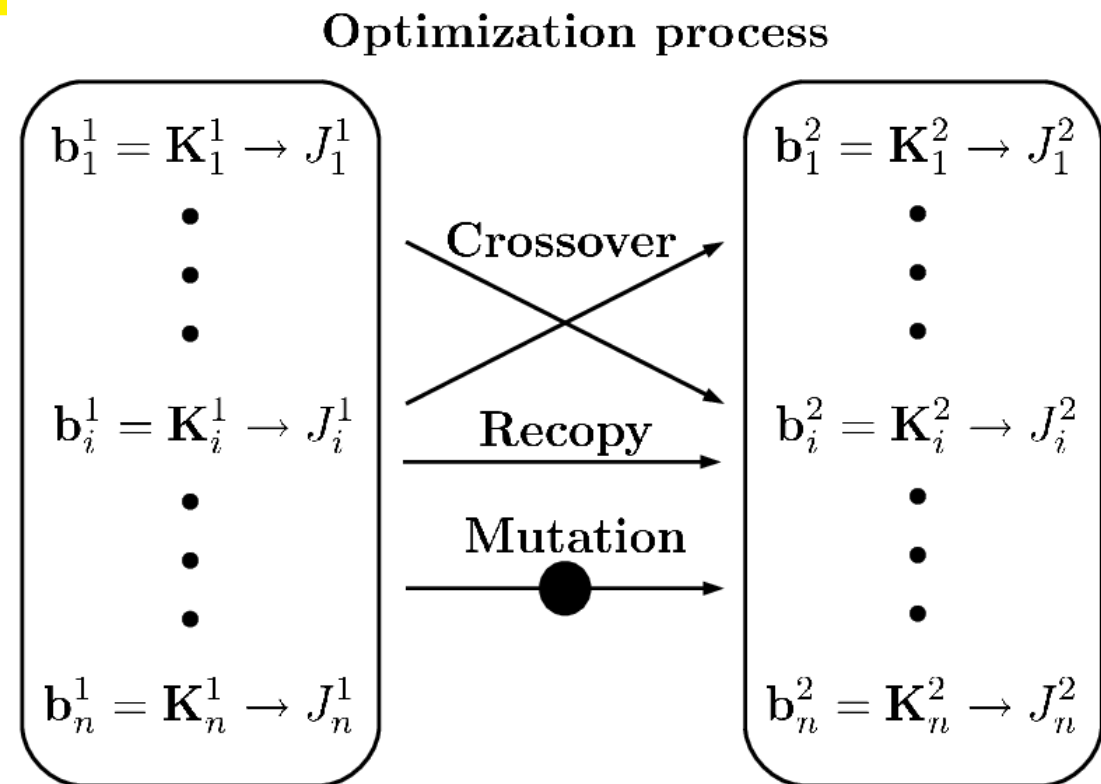
Step 1: 1st generation with random nonlinear control laws

$$b_m^1 = K_m^1(s), m = 1, \dots, 100$$

Step 2~10:

Biologically inspired optimization of the control laws based on the 'fitness grades'

$$J [b = K(s)]$$



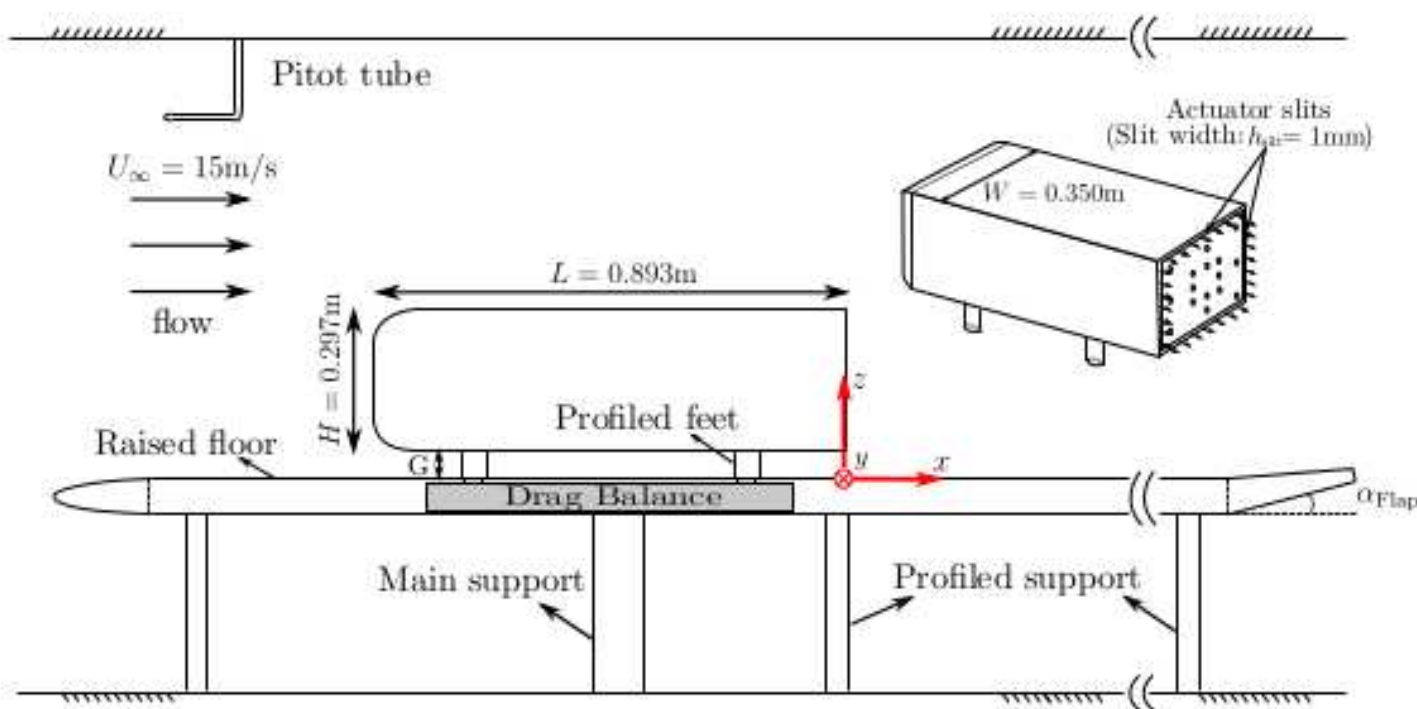
☰ J.R. Koza 1992 *Genetic Programming, The MIT Press*

Detailed description

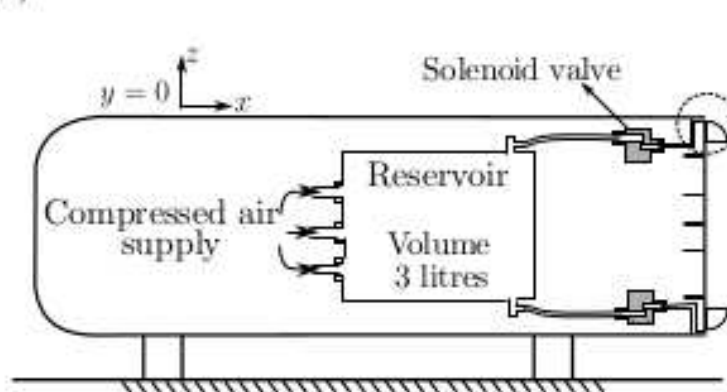
Drag reduction of simplified car model

≡ Barros, et al. 2016 JFM & ≡ Östh et al. 2014 JFM

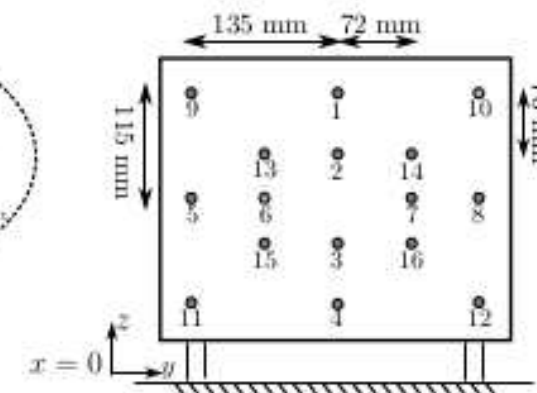
(a)



(b)

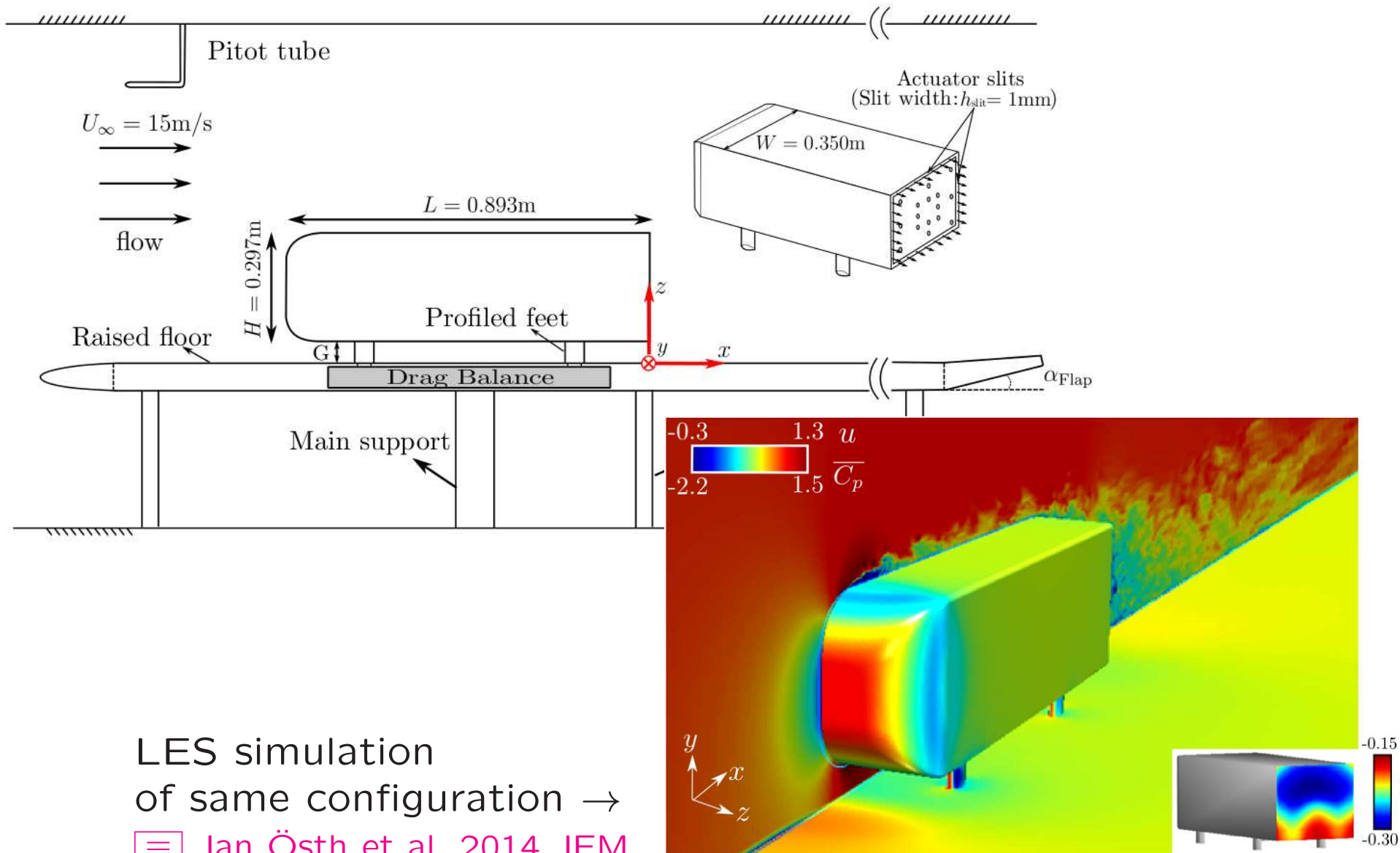


(c)



Drag reduction of simplified car model

≡ Barros, et al. 2016 JFM & ≡ Östh et al. 2014 JFM



MLC-based drag reduction

☰ Li+ 2017 EF & ☰ Barros+ 2016 JFM



Experiment: $Re = 3 \times 10^5$

MIMO control problem:

Ansatz $\mathbf{b} = K(s)$

Drag reduction: 22%

Energy investment: 3%

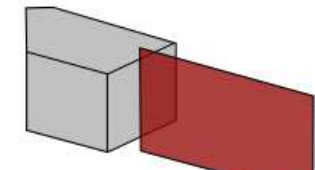
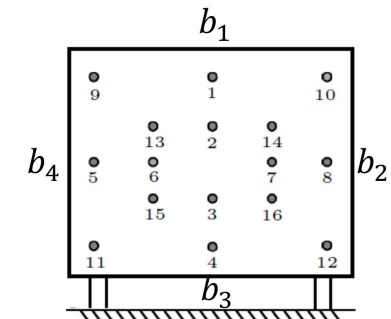
MLC application

Testing time < 1 hour

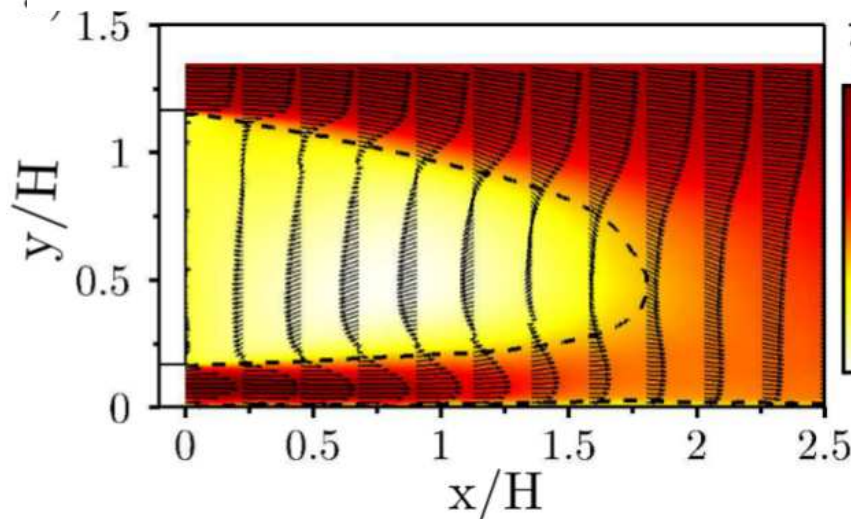
MLC law:

$$b_1 = b_2 = b_3 = b_4 = b$$

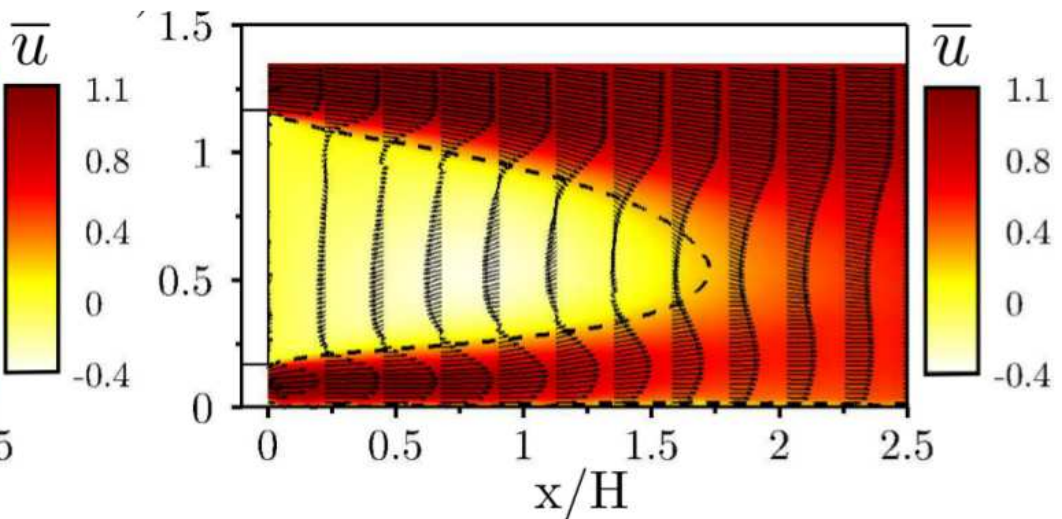
$$b = H [\tanh \tanh(s'_4 - 0.1)]$$



Unforced



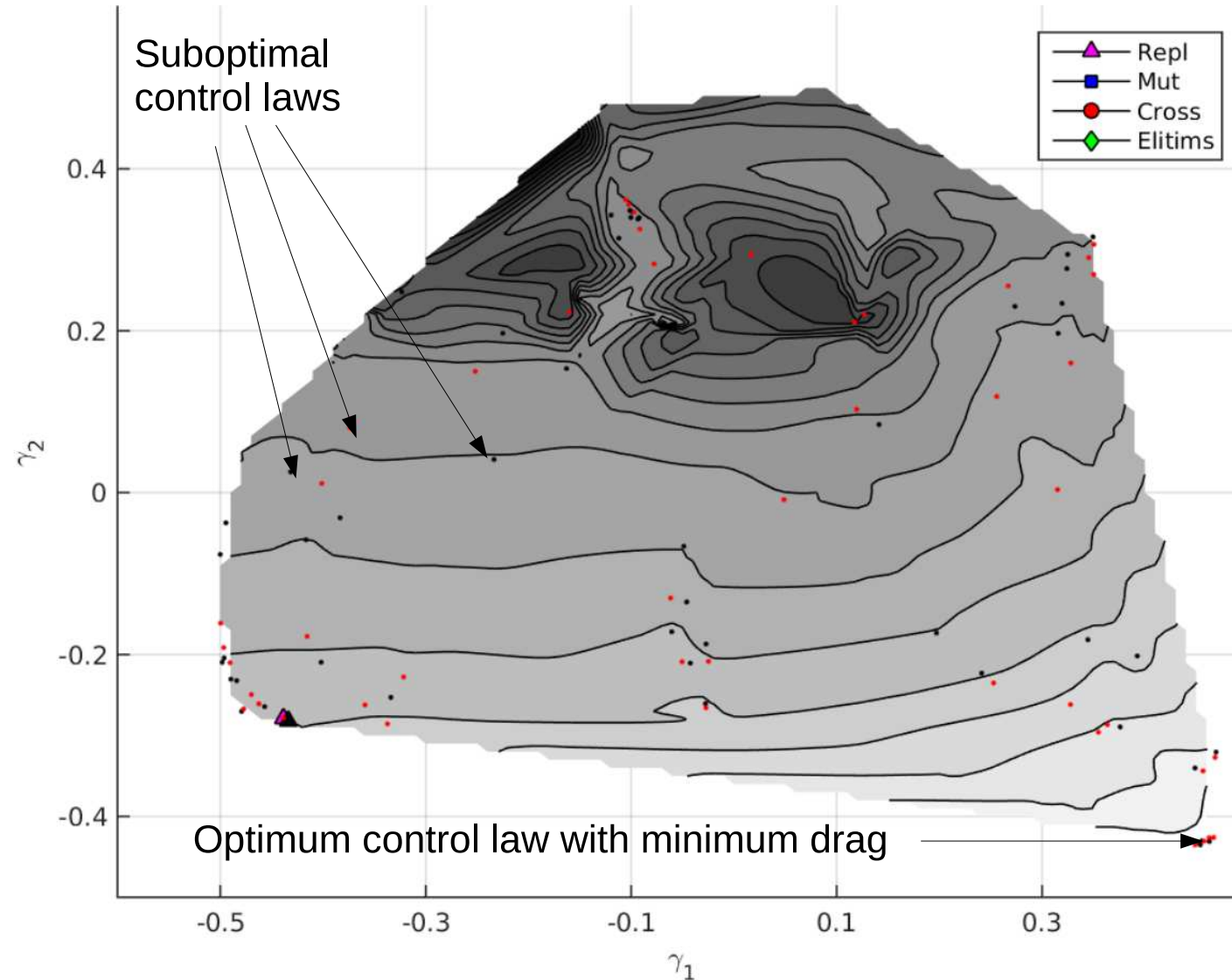
MLC controlled





Proximity plot for MLC of car model

☰ 2017 Kaiser+ FSSIC ☰ 2016 Kaiser+ TCFD



MLC with 5 generations with 50 control laws each.

[More](#)

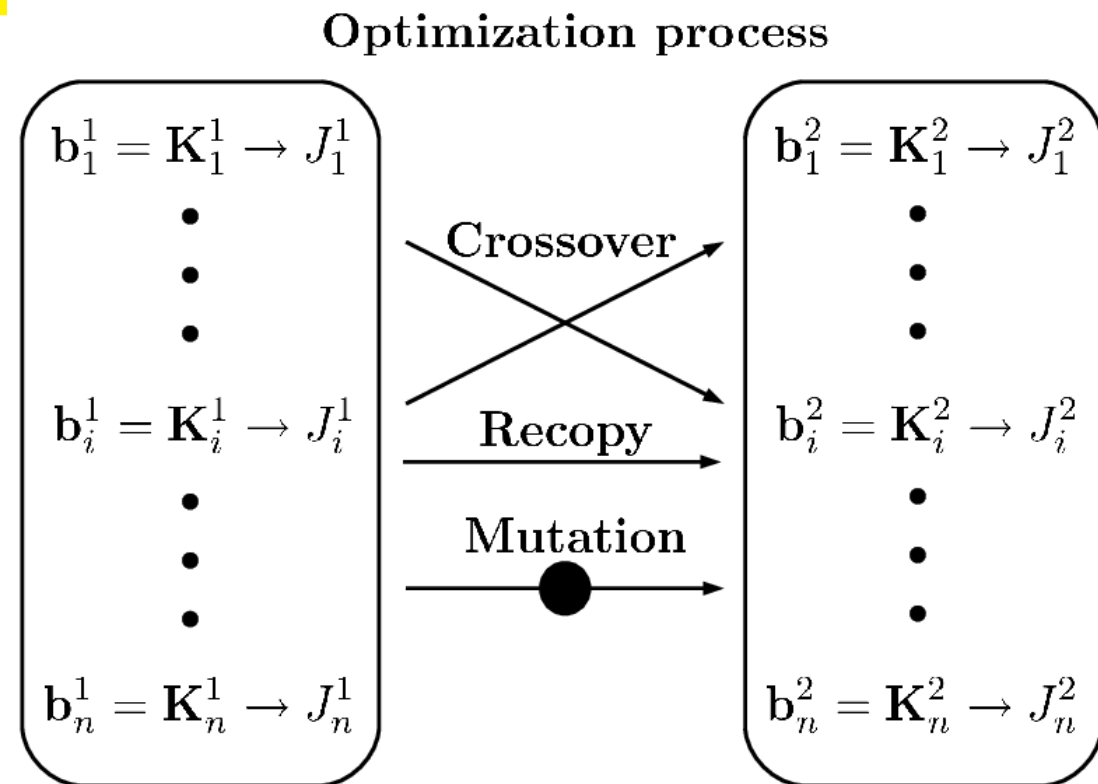
Step 1: 1st generation with random nonlinear control laws

$$b_m^1 = K_m^1(s), m = 1, \dots, 100$$

Step 2~10:

Biologically inspired optimization of the control laws based on the 'fitness grades'

$$J [b = K(s)]$$



☰ J.R. Koza 1992 *Genetic Programming, The MIT Press*

Detailed description

Machine Learning for Fluid Mechanics

Examples of Turbulence Control



Bernd Noack

HIT, China & TU Berlin

TU Berlin, Germany, 2020-03-03

Overview

A. Turbulence control by evolution [D. Fan++]

..... *More success stories of MLC*

B. Turbulence control by exploitation [A. Nair+]

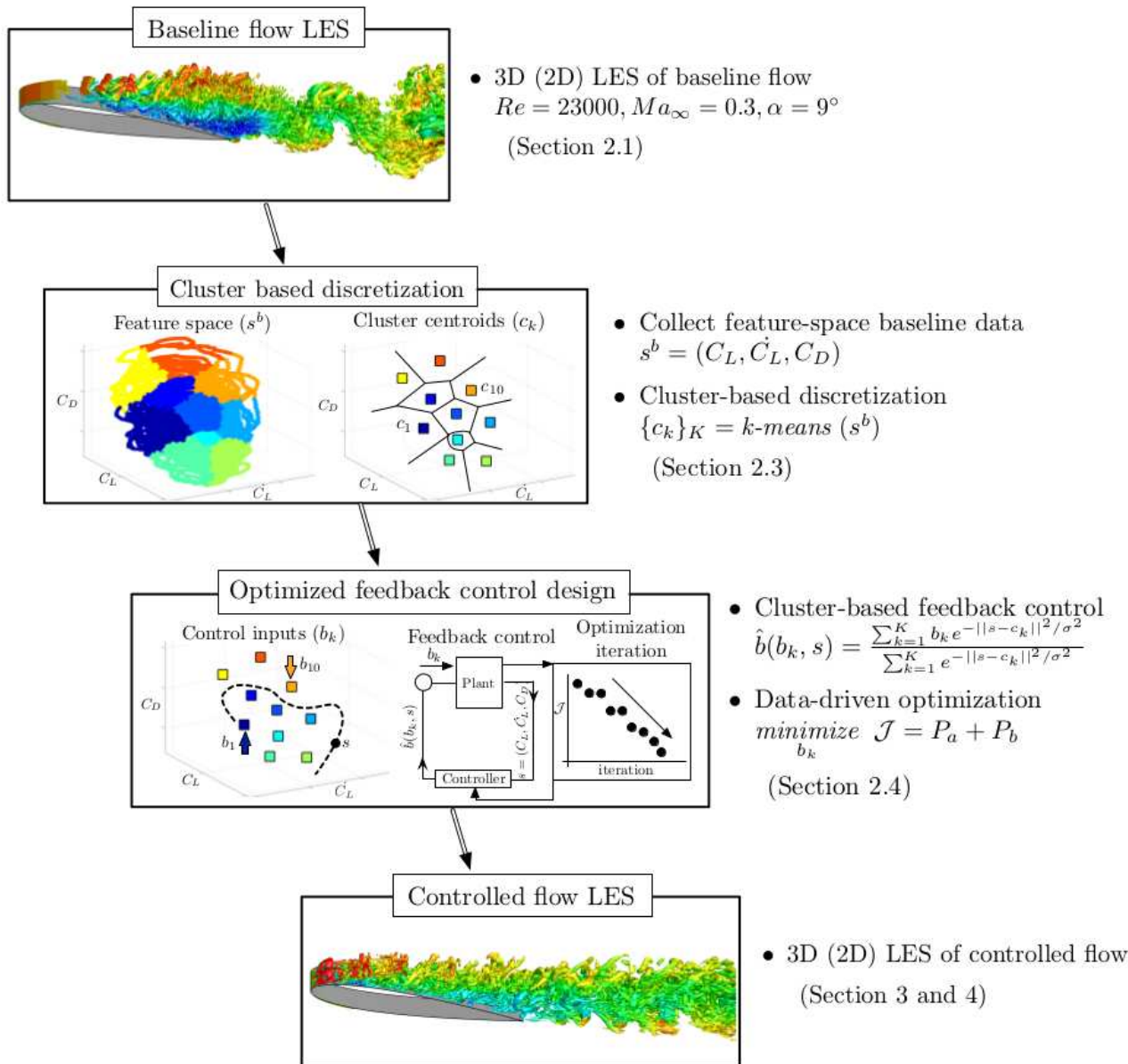
..... *Cluster-based control for airfoil separation*

C. Turbulence control by exploration [E. Kaiser+]

..... *Cluster-based control for ramp separation*

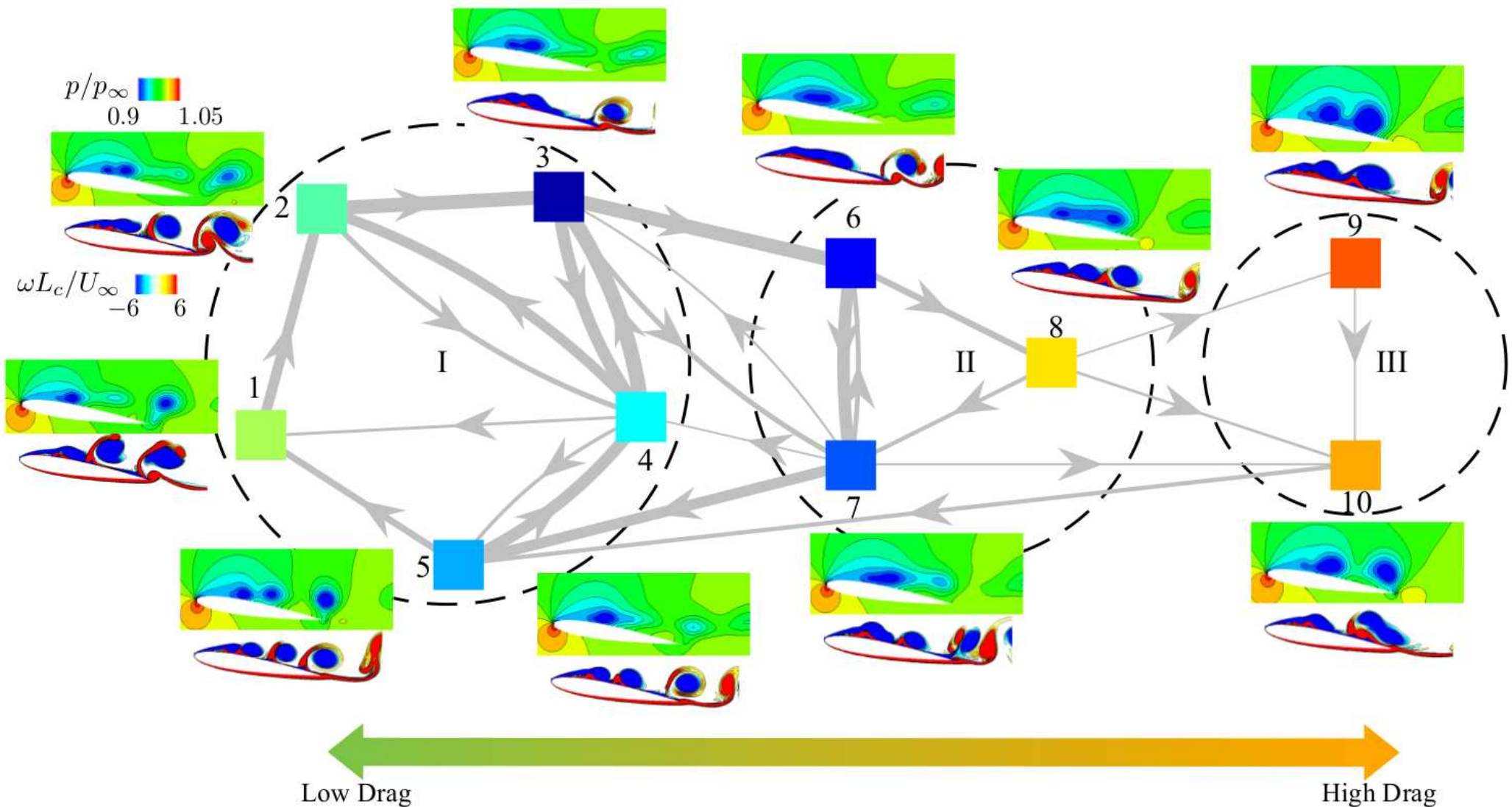
Cluster-based feedback control

☰ A.G. Nair, C.-A. Yeh, E. Kaiser, B.R. Noack, S.L. Brunton & K. Taira 2019 JFM



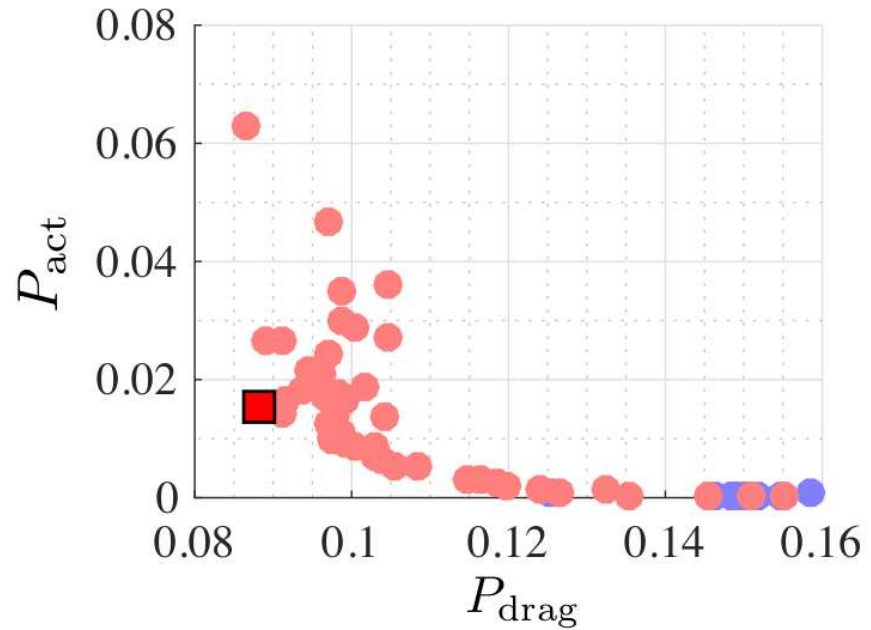
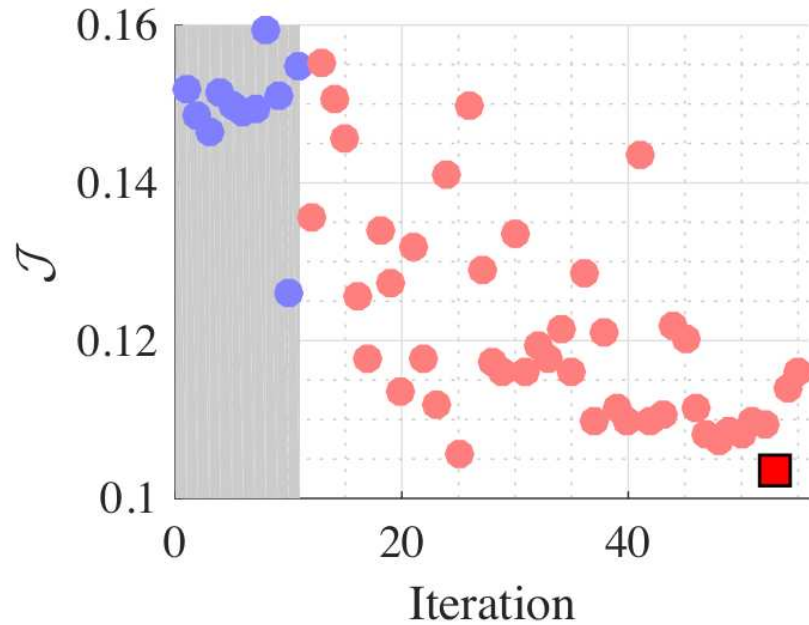
Cluster-based feedback control

☰ A.G. Nair, C.-A. Yeh, E. Kaiser, B.R. Noack, S.L. Brunton & K. Taira 2019 JFM



Cluster-based feedback control

A.G. Nair, C.-A. Yeh, E. Kaiser, B.R. Noack, S.L. Brunton & K. Taira 2019 JFM



Cost function $J = J_{\text{drag}} + J_{\text{act}}$ where

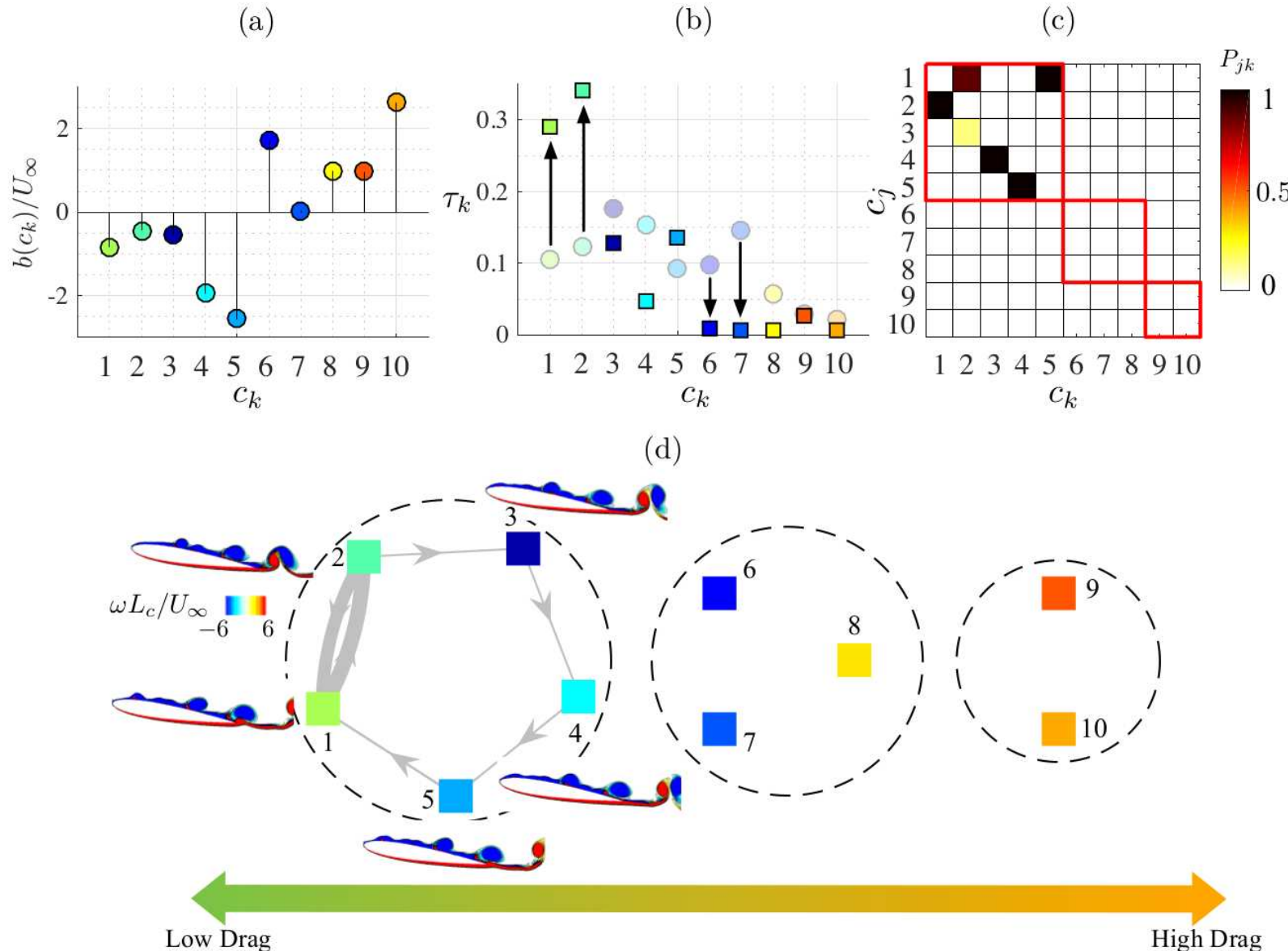
$J_{\text{drag}} = c_D^a (c_L/c_L^a)^{3/2}$ (flight endurance); $J_{\text{act}} = \text{act. power}$

Simplex optimization of cluster-based control law:

Lift preserved, drag reduced by 41 %

Cluster-based feedback control

A.G. Nair, C.-A. Yeh, E. Kaiser, B.R. Noack, S.L. Brunton & K. Taira 2019 JFM



Overview

A. Turbulence control by evolution [D. Fan++]

..... *More success stories of MLC*

B. Turbulence control by exploitation [A. Nair+]

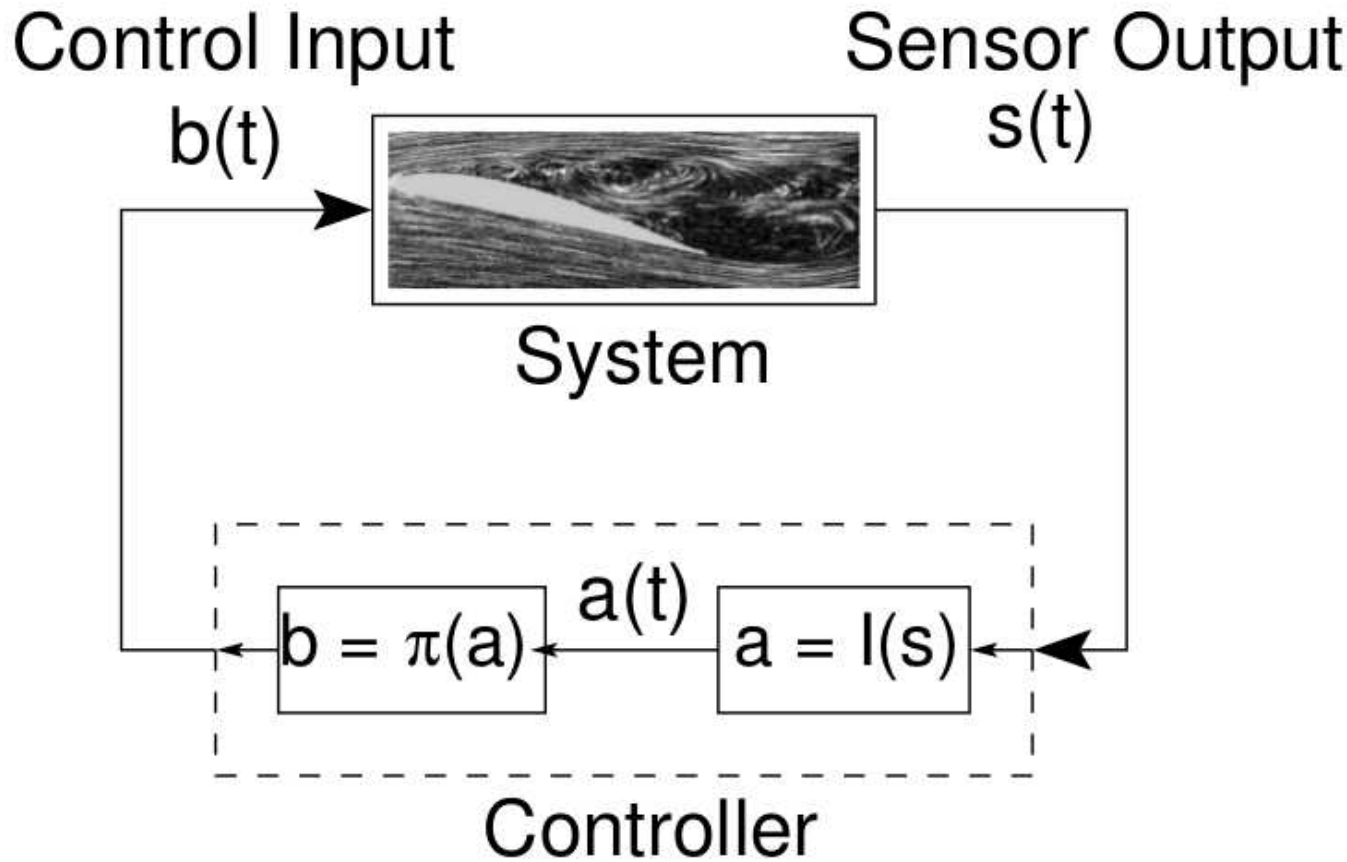
..... *Cluster-based control for airfoil separation*

C. Turbulence control by exploration [E. Kaiser+]

..... *Cluster-based control for ramp separation*

Cluster-based feedback control

☰ Kaiser+ 2014 JFM, Kaiser+ 2017 TCFD

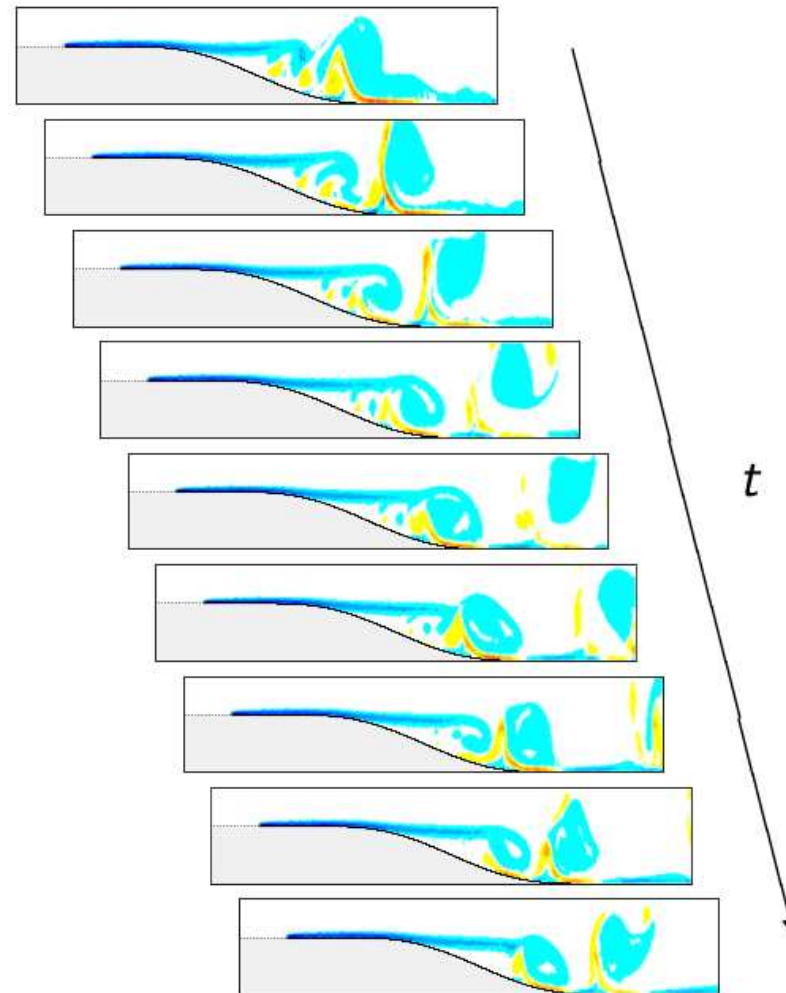
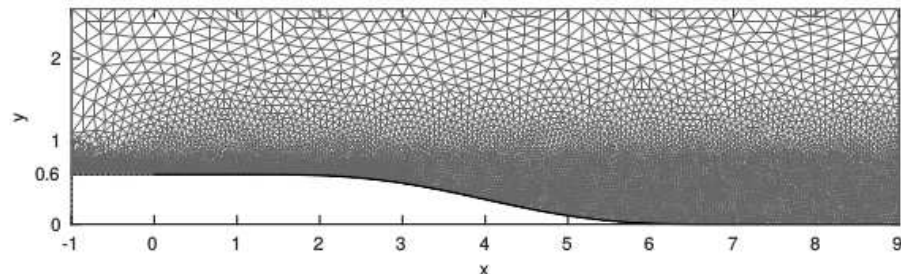


- ▶ Cluster affiliation function: $a = I(s)$ with $a = k$ if $s \in \mathcal{C}_k$.
- ▶ Cluster-dependent control law: $b = \pi(a)$.

Flow separation over a smooth ramp

☰ Kaiser+ 2014 JFM, Kaiser+ 2017 TCFD

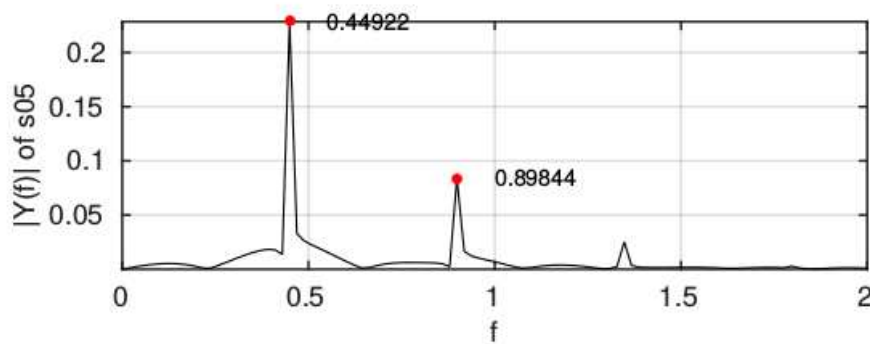
- ▶ 2D incompressible flow over a smooth ramp (FEM DNS, *UNS3 solver*)
- ▶ $Re_L = U_\infty L/\nu = 7700$,
 $Re_H = U_\infty H/\nu = 4620$
- ▶ Vortex shedding with characteristic frequency and occasional vortex pairing
- ▶ Importance of control:
Reduction of recirculation region due to adverse pressure gradient to benefit lift and drag force



Best open-loop periodic forcing

☰ Kaiser+ 2014 JFM, Kaiser+ 2017 TCFD

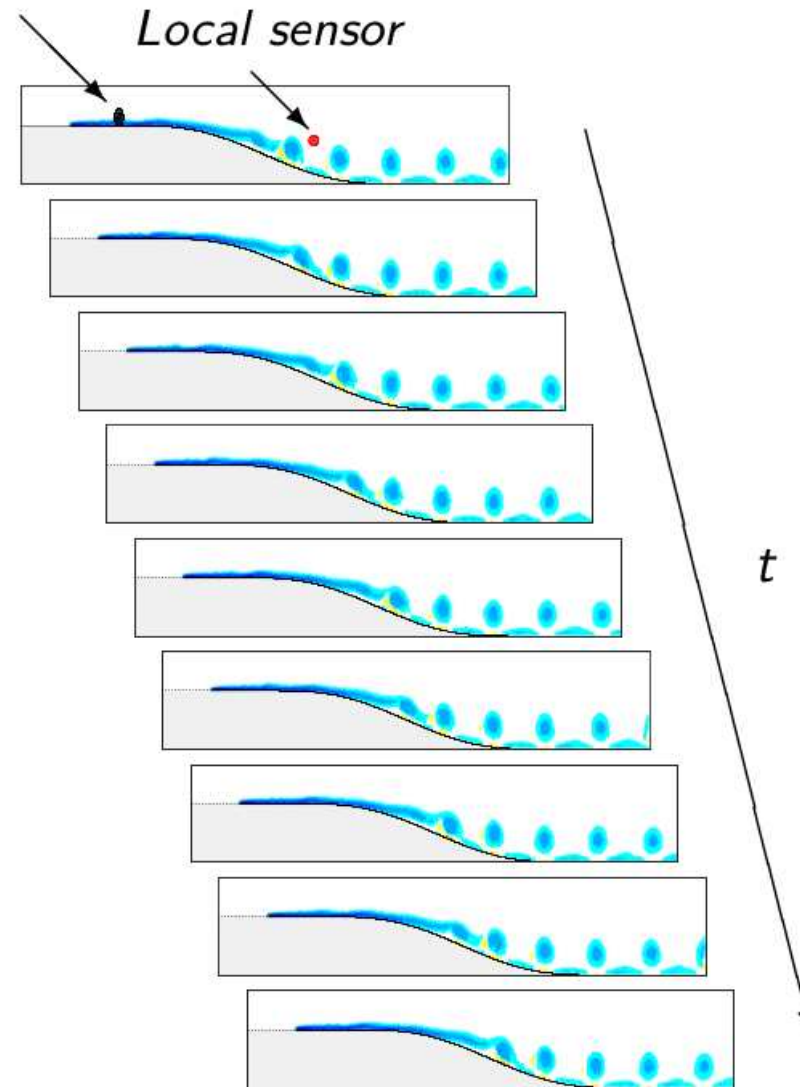
- ▶ Sinusoidal excitation with $f_p = 0.45 \approx 2 f_{nat}$
- ▶ Vortex pairing is suppressed
- ▶ Flow responds with excitation frequency and higher harmonics



- ▶ Can we improve open-loop results using a cluster-based feedback control?

(Turning open-loop control on or off dependent on the cluster)

Volume force



Feedback control using CROM—Theory

☰ Kaiser+ 2014 JFM, Kaiser+ 2017 TCFD

The transition matrix depends now also on the actuation input b :

$$\mathbf{P} := \text{Prob}(\mathbf{c}_j | \mathbf{c}_k) \quad \longrightarrow \quad \mathbf{P}^b := \text{Prob}(\mathbf{c}_j | \mathbf{c}_k, b)$$

Controlled Markov process defined by

- ▶ Finite set of states (*cluster affiliation*): $a \in A = \{1, \dots, K\}$ with $K = \#\text{clusters}$
- ▶ Finite set of possible actions: $b \in B = \{b_1, \dots, b_P\}$
- ▶ Cost function: $C(a, b) \stackrel{!}{=} \min$
- ▶ Transition matrix model $P_{aa'}^b$: action b applied in state a at time t will lead to state a' at time $t + 1$
- ▶ Discount parameter α : ensures convergence and trade-off between immediate and future costs

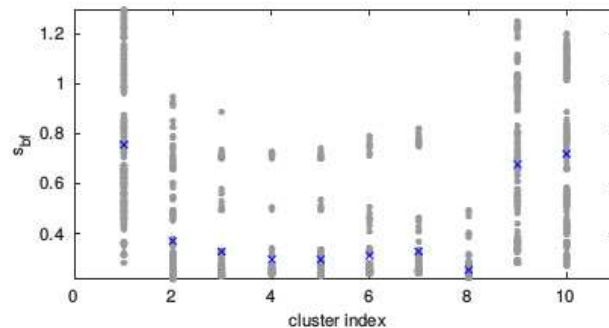
Goal is to find an optimal control law $\pi^*(a)$ that maximizes the expected total discounted costs

$$V^\pi(a, b) = \sum_{t=0}^T \alpha^t / C_t(a, b) \stackrel{!}{=} \max \quad \text{with} \quad b = \pi(a)$$

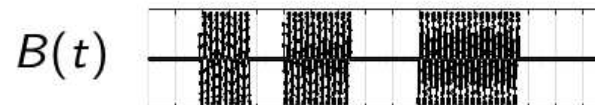
Feedback control using CROM—Practice I

☰ Kaiser+ 2014 JFM, Kaiser+ 2017 TCFD

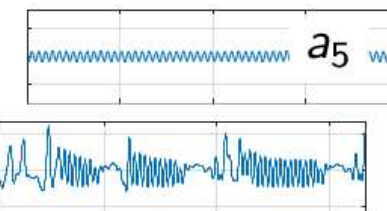
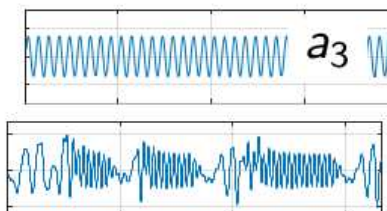
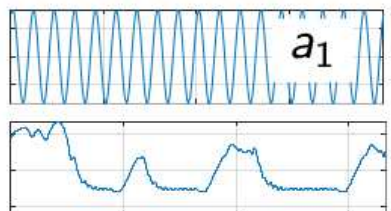
0. Define cluster-dependent cost function $C(a) = \int_{\Omega} H(-c_{x,k}) d\Omega$



1. Collect data for cluster and transition matrix identification
 - ▶ Shall include natural state, open-loop state with $f_p = 0.45$ and transients
 - ▶ E.g.: switching from 'on' to 'off' randomly



2. Projection of snapshots onto first $N = 10$ open-loop POD modes



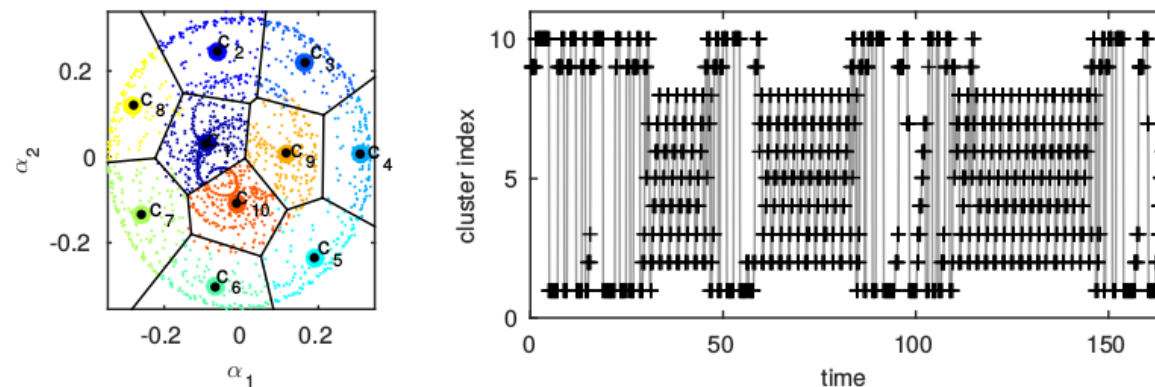
open-loop POD

projection from 1.

Feedback control using CROM—Practice II

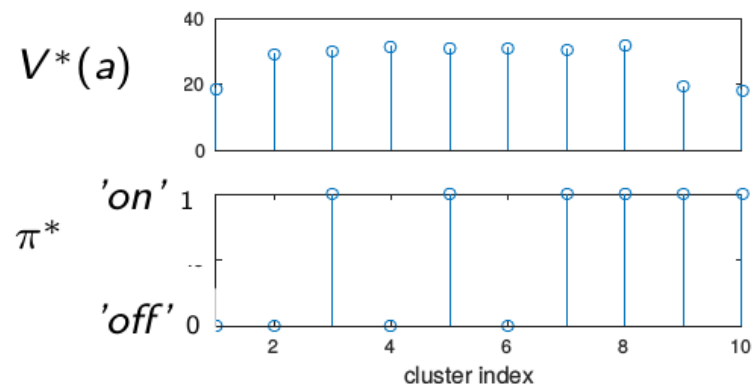
☰ Kaiser+ 2014 JFM, Kaiser+ 2017 TCFD

3. Application of k-means algorithm to determine clusters



4. Estimation of transition matrix P_{jk}^b with $b = 0, 1$ (either 'on' or 'off')

5. Offline control law determination using the identified model



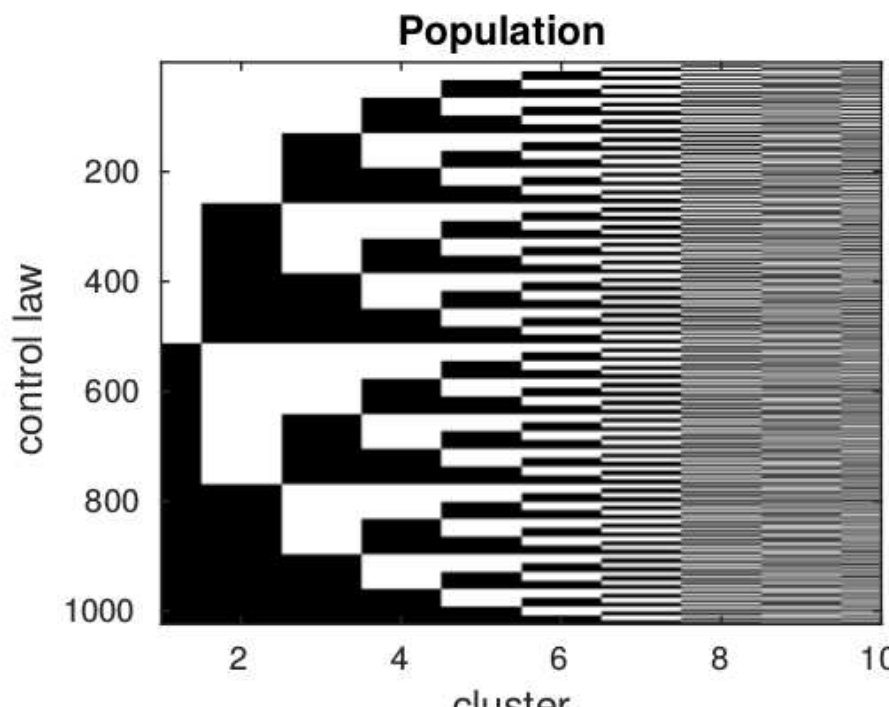
$V^*(a)$: Optimal value function
that maximizes the total
expected discounted costs when
starting in cluster a and
applying control law π^*

6. Finally: Application of control law

Search space

☰ Kaiser+ 2014 JFM, Kaiser+ 2017 TCFD

- ▶ Comparison of model-based control using CROM with all possible combinations.
- ▶ Having $K = 10$ clusters, $2^{10} = 1024$ possible control laws exist.



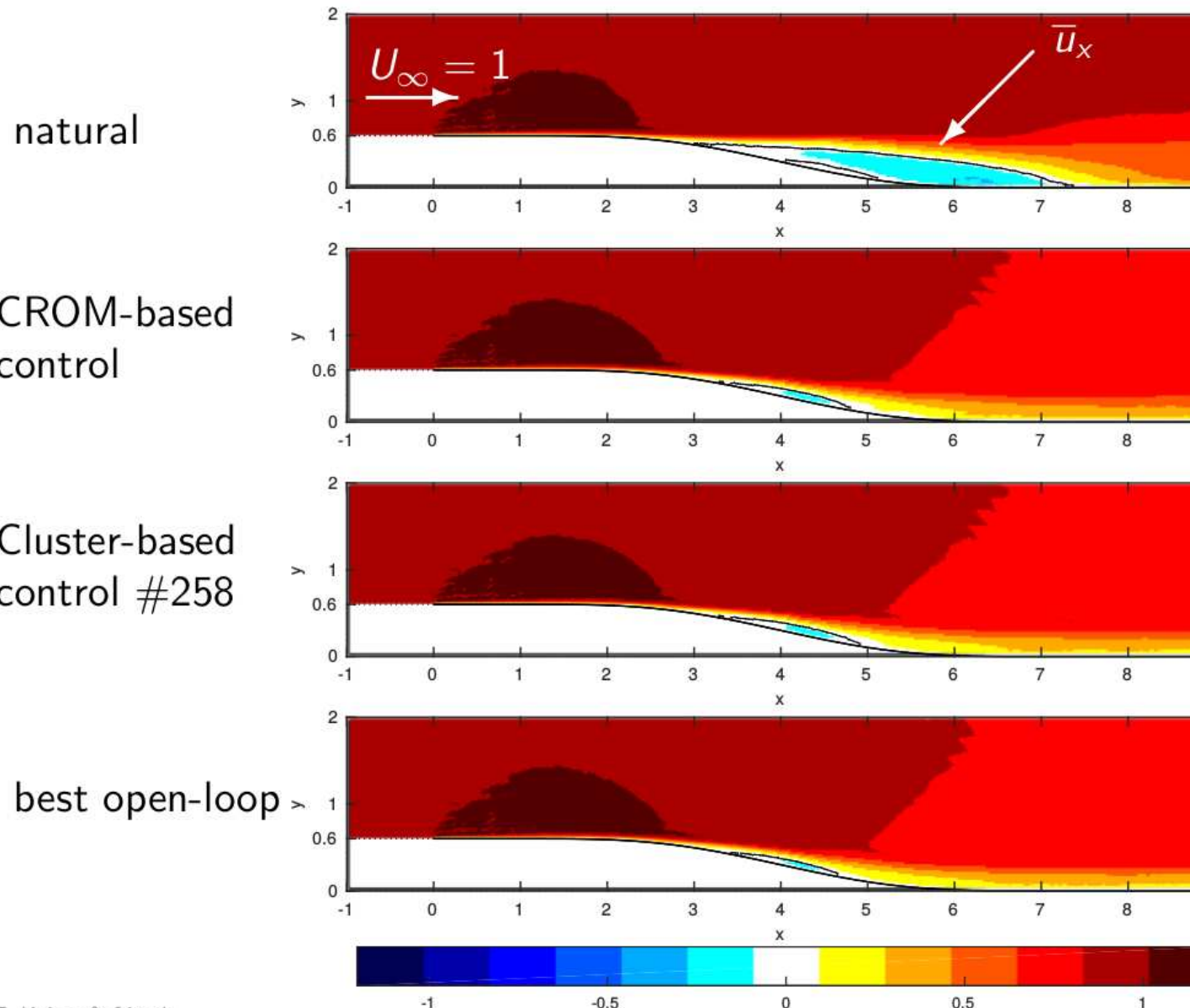
'on'



'off'

Comparison of controlled flows I

☰ Kaiser+ 2014 JFM, Kaiser+ 2017 TCFD



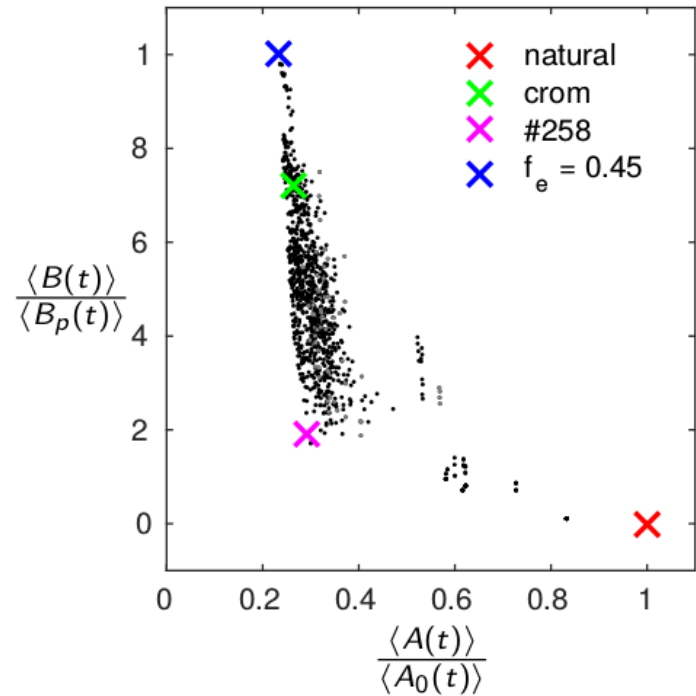
Comparison of controlled flows II

 Kaiser+ 2014 JFM, Kaiser+ 2017 TCFD

$$A(t) = \int_{\Omega} H(-u_x(\mathbf{x}, t)) d\mathbf{x}, \quad \langle A(t) \rangle = \frac{1}{T_2 - T_1} \int_{T_1}^{T_2} A(t) dt$$

$A_0(t)$: instantaneous recirculation area of natural flow

$B_p(t)$: instantaneous energy input for $f_p = 0.45$



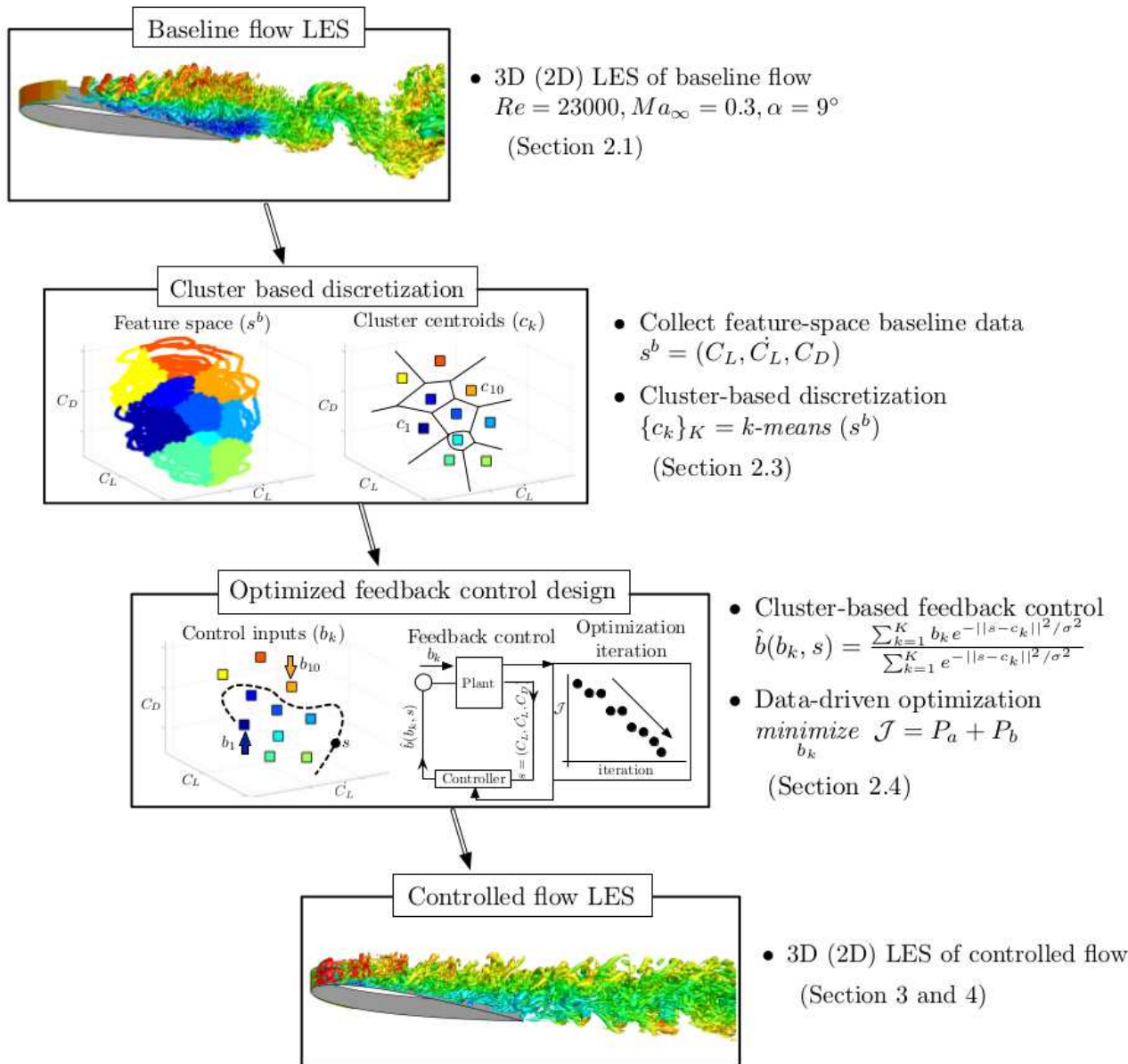
	$\frac{\langle A(t) \rangle}{\langle A_0(t) \rangle}$	$\frac{\langle B(t) \rangle}{\langle B_p(t) \rangle}$	q_k
natural '0000000000'	100%	0%	
CROM '0010101111'	26%	72%	
#258 '0100000010'	29%	19%	
$f_p = 0.45$, '1111111111'	23%	100%	

■ 'on' (1) ■ 'off' (0)



Cluster-based feedback control

A.G. Nair, C.-A. Yeh, E. Kaiser, B.R. Noack, S.L. Brunton & K. Taira 2018 JFM preprint



Cluster-based feedback control

A.G. Nair, C.-A. Yeh, E. Kaiser, B.R. Noack, S.L. Brunton & K. Taira 2018 JFM preprint

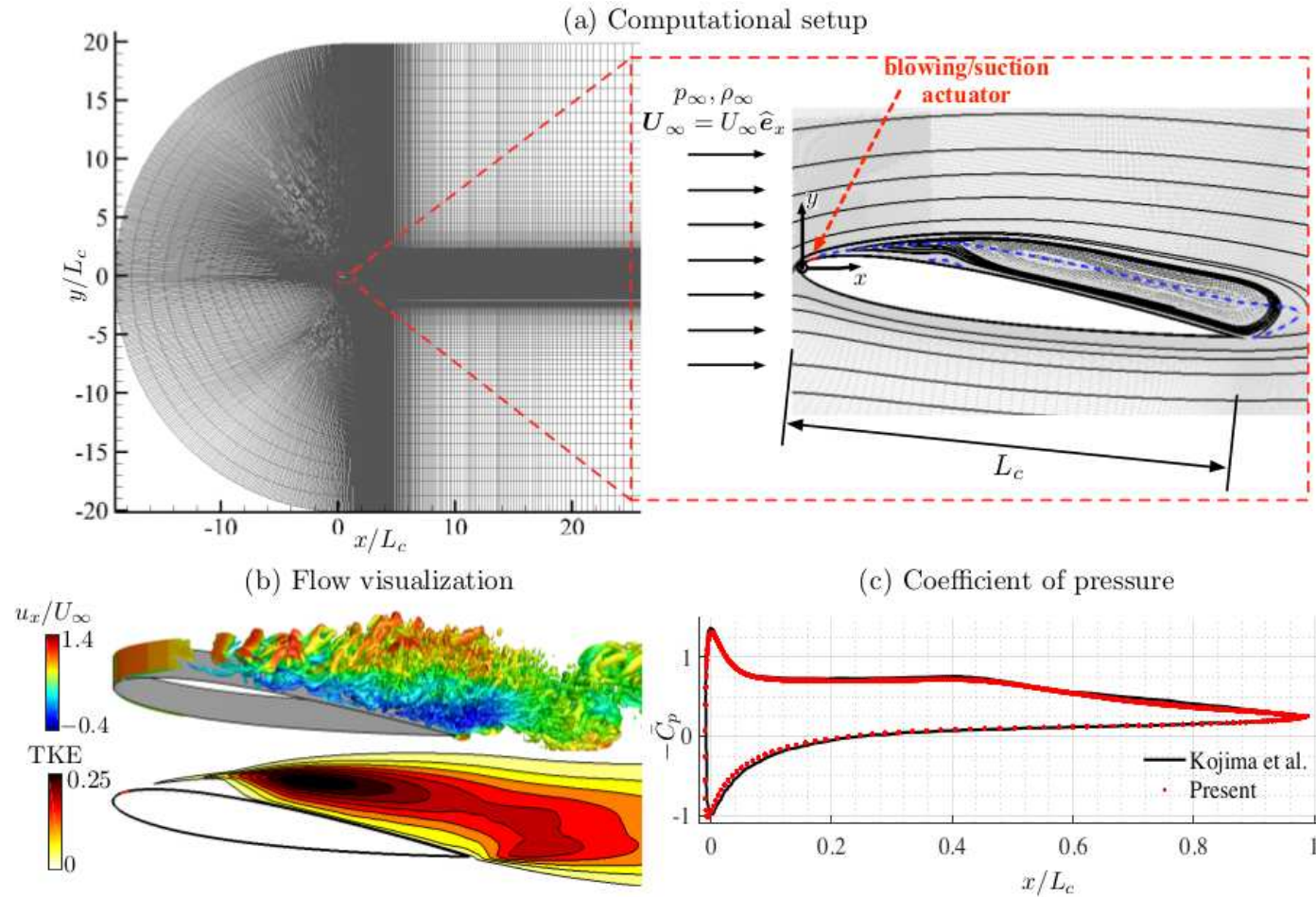


FIGURE 2. (a) Computational domain, $x - y$ plane (left) and near field of a NACA 0012 airfoil at an angle of attack of $\alpha = 9^\circ$ (right) indicating the streamlines for 3D spanwise-periodic baseline flow. The actuator surface is indicated in red. The blue dashed line indicates contour line corresponding to $\bar{u}_x/U_\infty = 0$. (b) Instantaneous flow field (highlighted by Q-criterion) colored by streamwise velocity and turbulent kinetic energy (TKE) and (c) time-averaged coefficient of pressure distribution on suction and pressure side of the airfoil for 3D baseline flow.

Cluster-based feedback control

A.G. Nair, C.-A. Yeh, E. Kaiser, B.R. Noack, S.L. Brunton & K. Taira 2018 JFM preprint

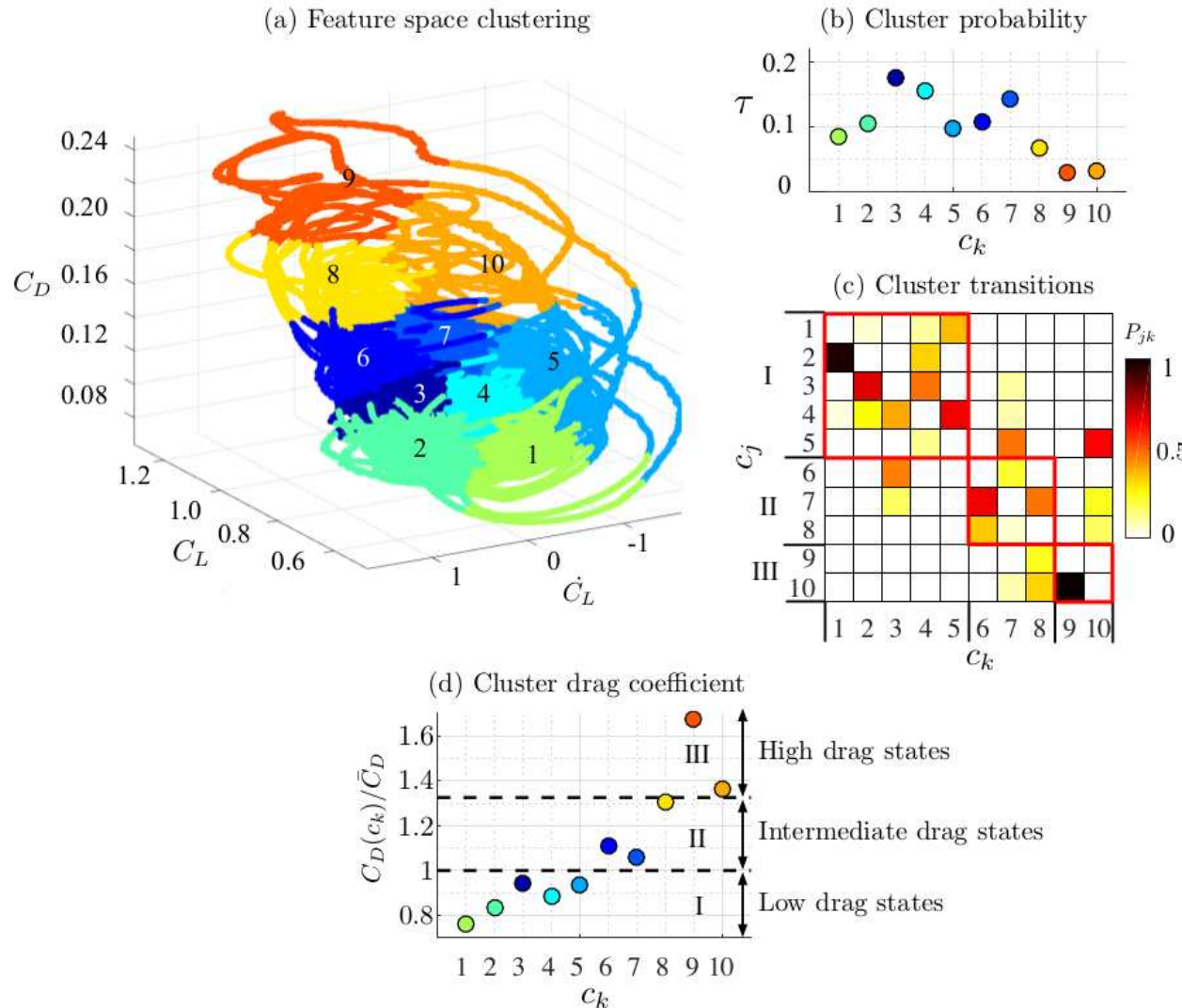


FIGURE 3. (a) Feature space clustering of the 2D baseline flow. (b) Cluster residence probabilities and (c) cluster transition probabilities. The red boxes indicate cluster subsets. (d) Normalized drag corresponding to cluster centroids.

Cluster-based feedback control

A.G. Nair, C.-A. Yeh, E. Kaiser, B.R. Noack, S.L. Brunton & K. Taira 2018 JFM preprint

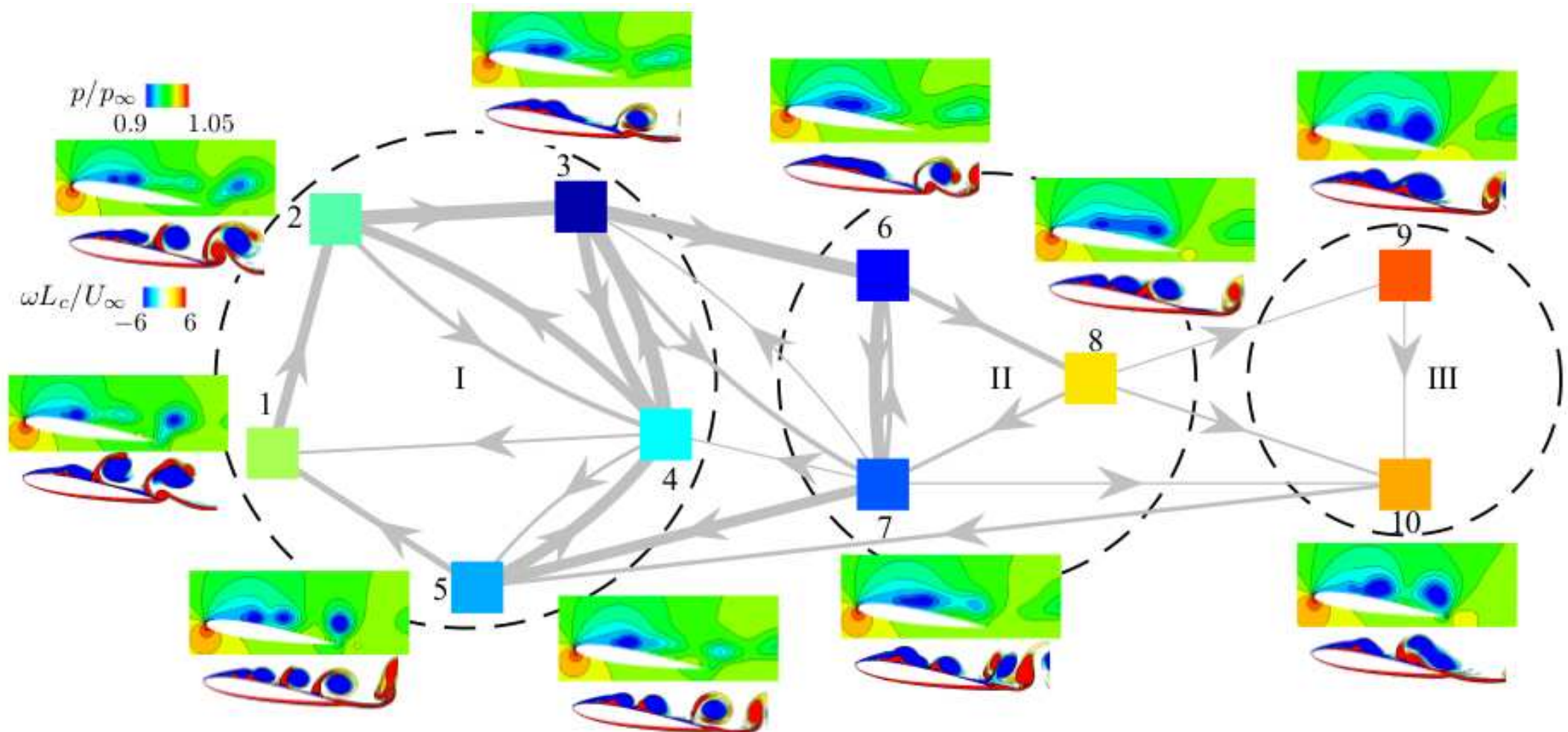


FIGURE 4. Graph of Markov chain highlighting transitions between clusters. 2D cluster-averaged pressure flow fields (p/p_∞) and instantaneous vorticity contours ($\omega L_c/U_\infty$) corresponding to each cluster are shown. The dashed circles indicate the cluster subsets.

Cluster-based feedback control

A.G. Nair, C.-A. Yeh, E. Kaiser, B.R. Noack, S.L. Brunton & K. Taira 2018 JFM preprint

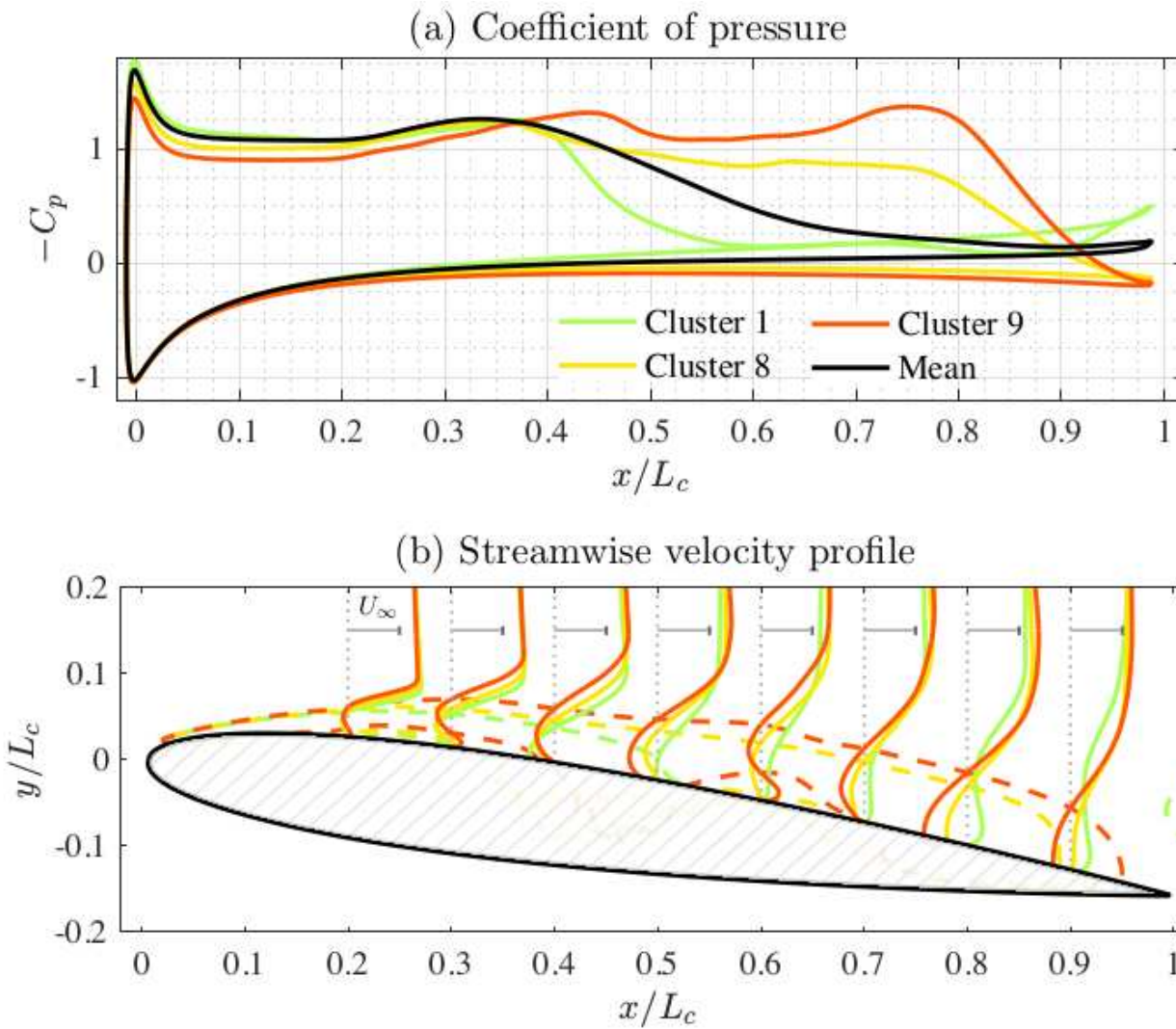


FIGURE 5. (a) Cluster-averaged pressure distribution over the suction and pressure surface of airfoil and (b) cluster-averaged streamwise velocity profiles for 2D baseline flow.

Cluster-based feedback control

A.G. Nair, C.-A. Yeh, E. Kaiser, B.R. Noack, S.L. Brunton & K. Taira 2018 JFM preprint

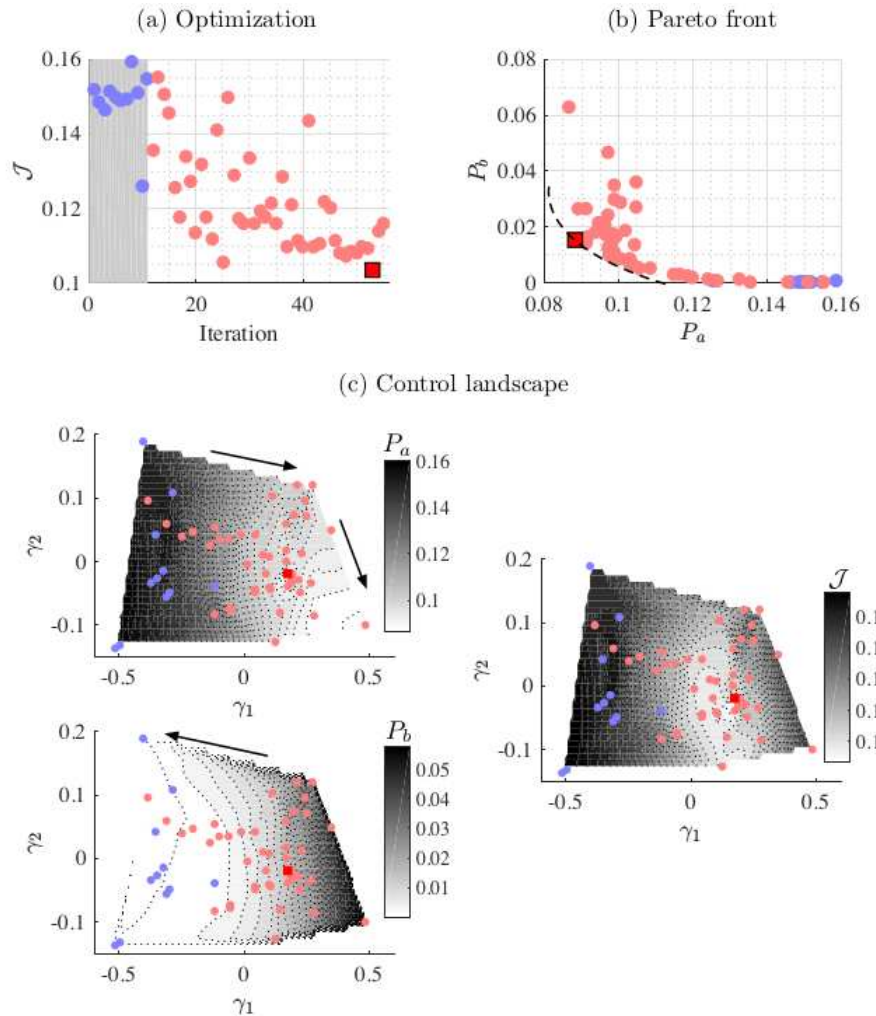


FIGURE 6. (a) Objective function minimization to determine the optimized control law and (b) Pareto front. The red square symbol denotes the optimized case. The dashed line in (b) indicates the Pareto front of control. (c) Control objective landscape, $P_{\text{drag}} = P_{\text{drag}}(\gamma_1, \gamma_2)$, $P_{\text{act}} = P_{\text{act}}(\gamma_1, \gamma_2)$, and $\mathcal{J} = \mathcal{J}(\gamma_1, \gamma_2)$ balancing P_{drag} and P_{act} , all three determined using multidimensional scaling. The transparent blue dots indicate initial simplex control cases. The arrows indicate directions of minimization.

Cluster-based feedback control

A.G. Nair, C.-A. Yeh, E. Kaiser, B.R. Noack, S.L. Brunton & K. Taira 2018 JFM preprint

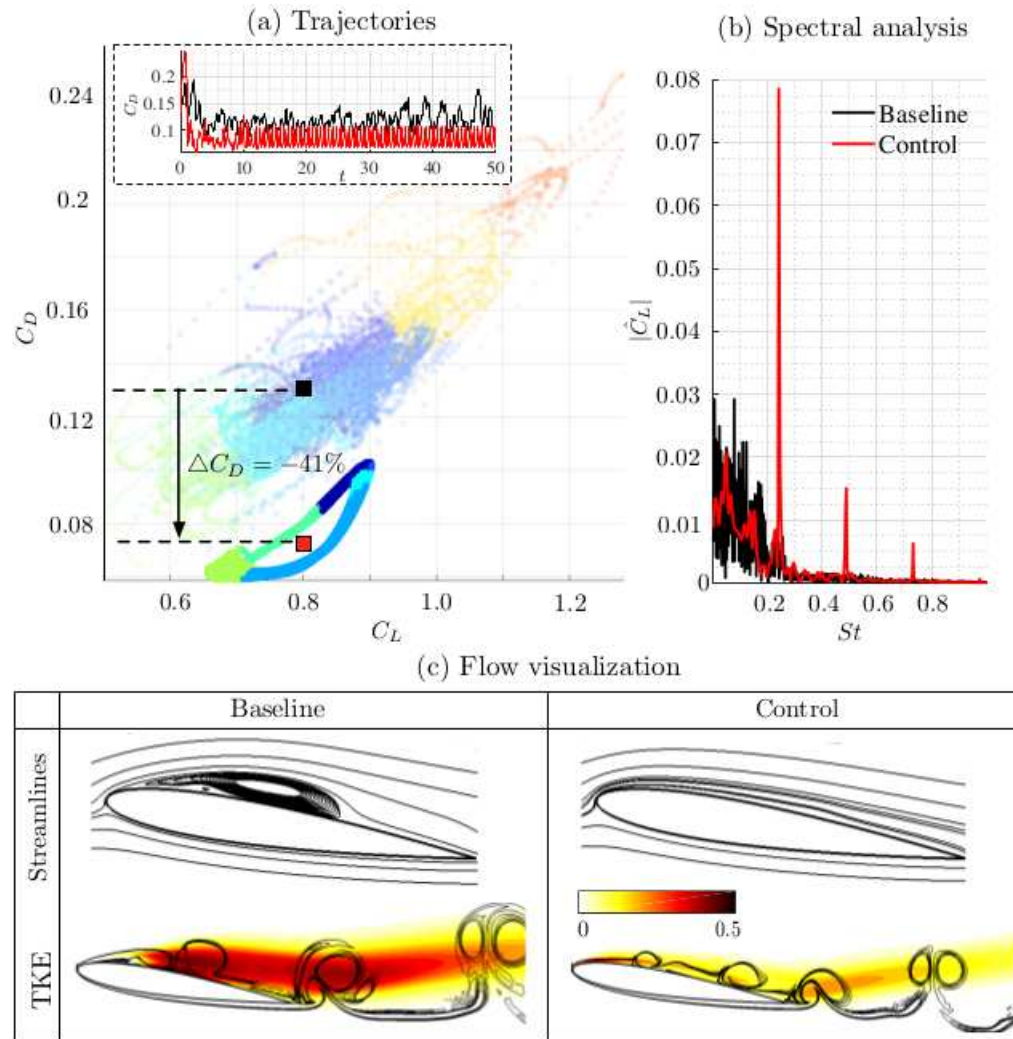


FIGURE 7. Comparison of baseline and optimized control case: (a) Trajectories, (b) spectral analysis of lift data, and (c) time-averaged streamlines and turbulent kinetic energy (TKE) fluctuations. Baseline trajectories are shown in transparent in (a). The contour lines in (c) (bottom) indicate instantaneous vorticity fields.

Cluster-based feedback control

A.G. Nair, C.-A. Yeh, E. Kaiser, B.R. Noack, S.L. Brunton & K. Taira 2018 JFM preprint

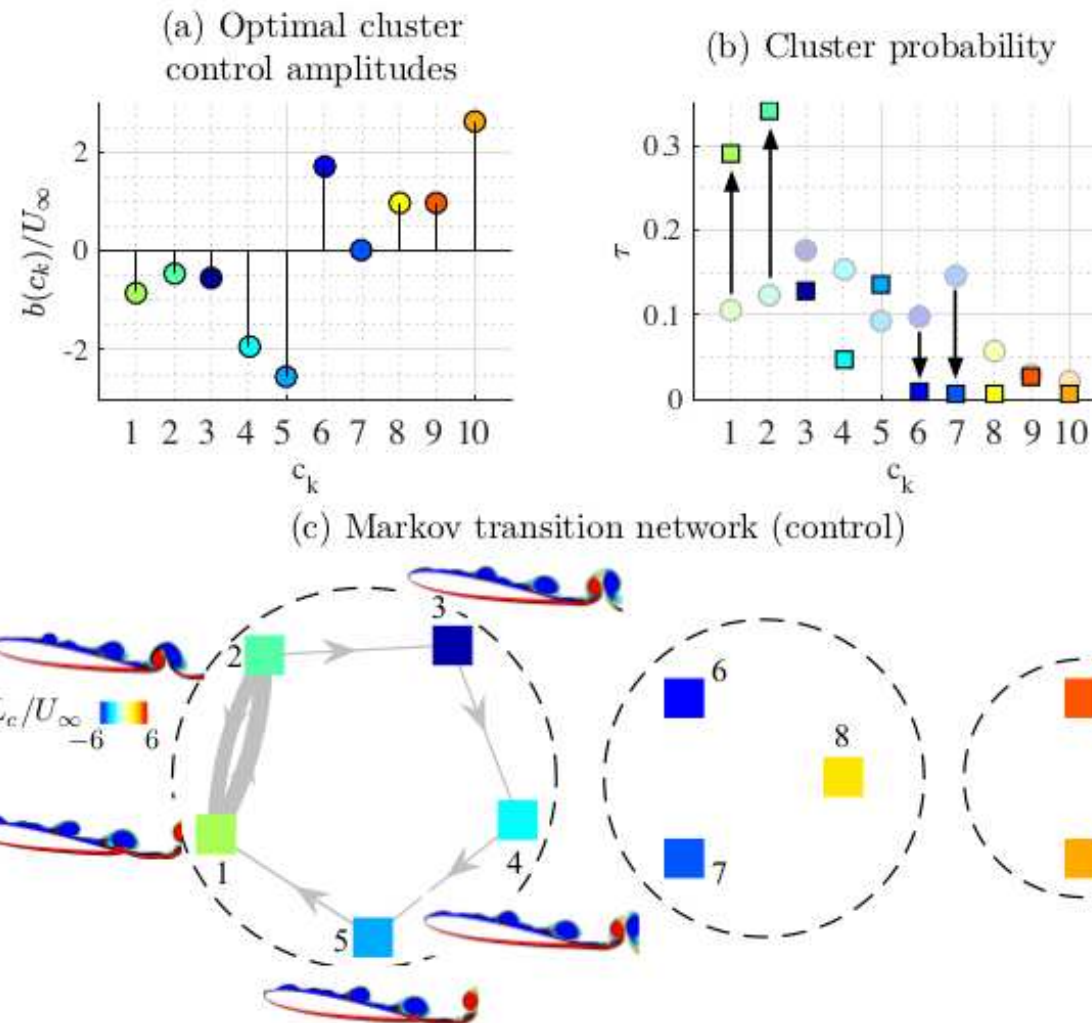


FIGURE 8. (a) Cluster jet velocity, (b) cluster residence probability for baseline (shown in transparent round symbols) and controlled flows (shown in bright square symbols) and (c) controlled Markov transition network with instantaneous vorticity contours ($\omega L_c/U_\infty$).

Cluster-based feedback control

A.G. Nair, C.-A. Yeh, E. Kaiser, B.R. Noack, S.L. Brunton & K. Taira 2018 JFM preprint

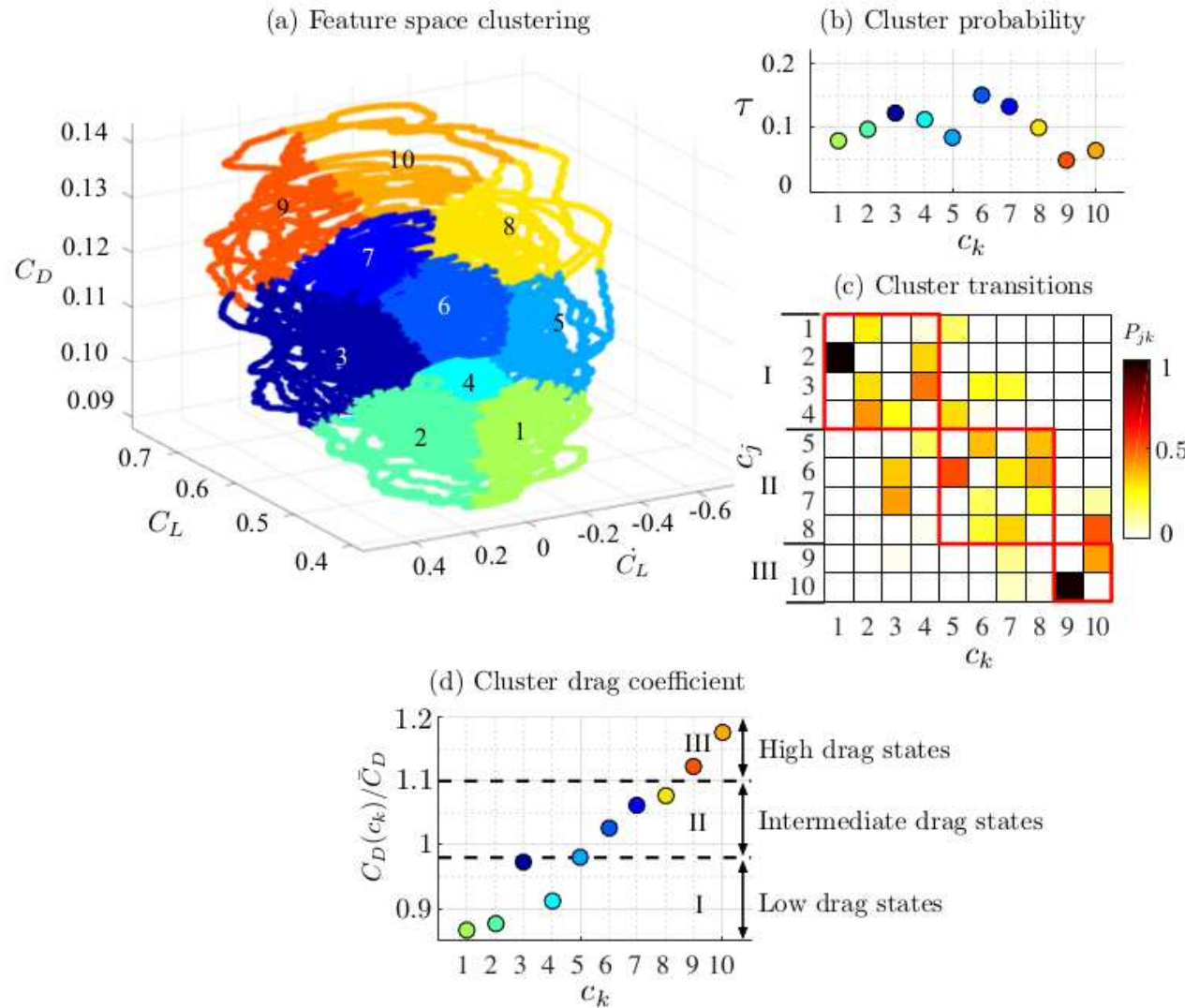


FIGURE 9. (a) Feature space clustering of 3D baseline flow data. (b) Cluster probabilities, (c) transitions probabilities and (d) normalized, average drag coefficient across clusters. The red boxes and the dashed circles indicate the cluster subsets.

Cluster-based feedback control

A.G. Nair, C.-A. Yeh, E. Kaiser, B.R. Noack, S.L. Brunton & K. Taira 2018 JFM preprint

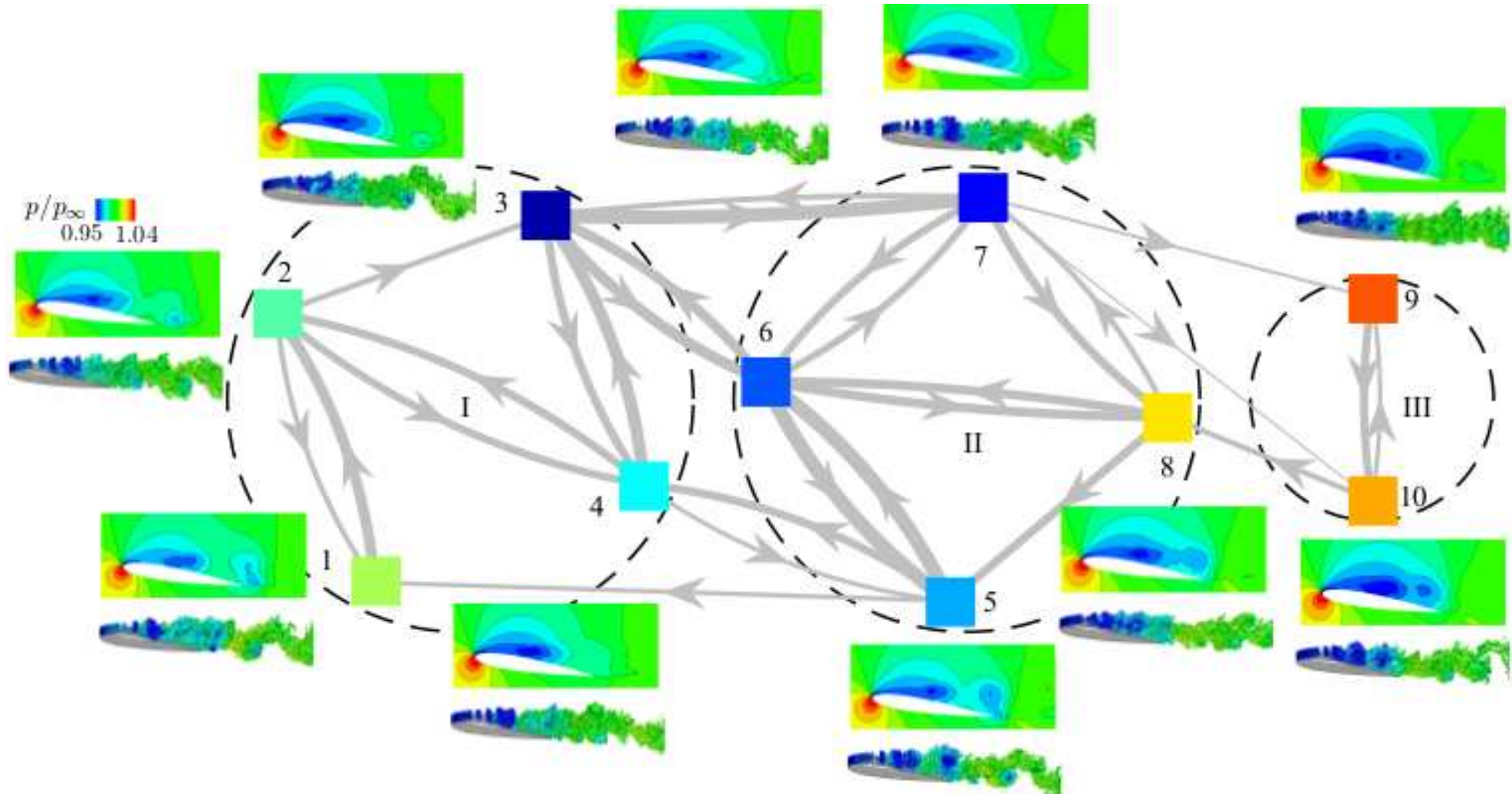


FIGURE 10. Graph of Markov chain highlighting transitions between clusters for the 3D baseline flow. The dashed circles indicate the cluster subsets.

Cluster-based feedback control

A.G. Nair, C.-A. Yeh, E. Kaiser, B.R. Noack, S.L. Brunton & K. Taira 2018 JFM preprint

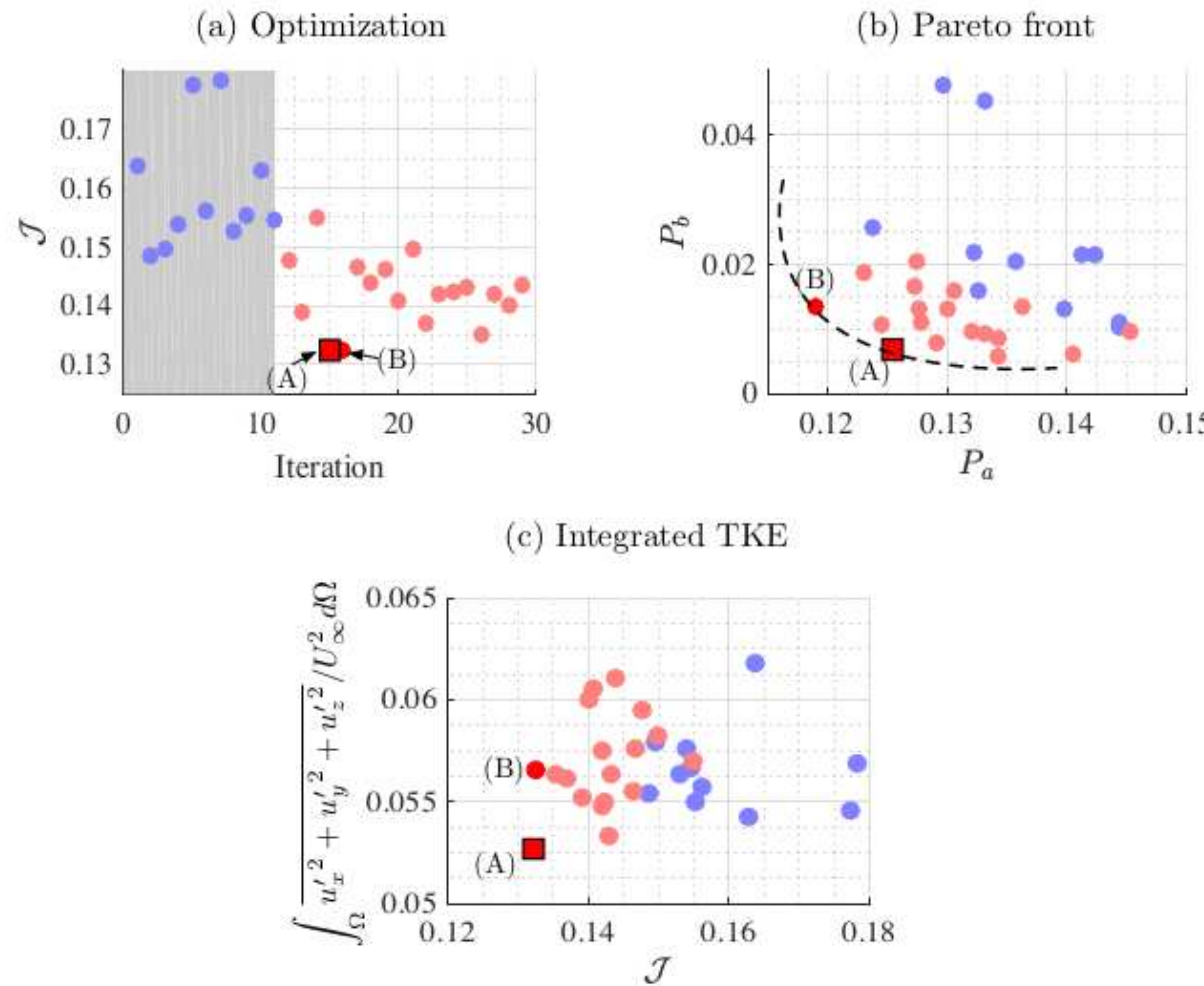


FIGURE 11. (a) Objective function \mathcal{J} minimization to determine the optimized control case, and (b) Pareto front (P_{drag} , P_{act}). The square symbol denotes the optimized case. (c) Integrated turbulent kinetic energy over the entire computational domain. The transparent blue dots indicate initial simplex control cases and the red square symbol denotes the optimized case.

Cluster-based feedback control

A.G. Nair, C.-A. Yeh, E. Kaiser, B.R. Noack, S.L. Brunton & K. Taira 2018 JFM preprint

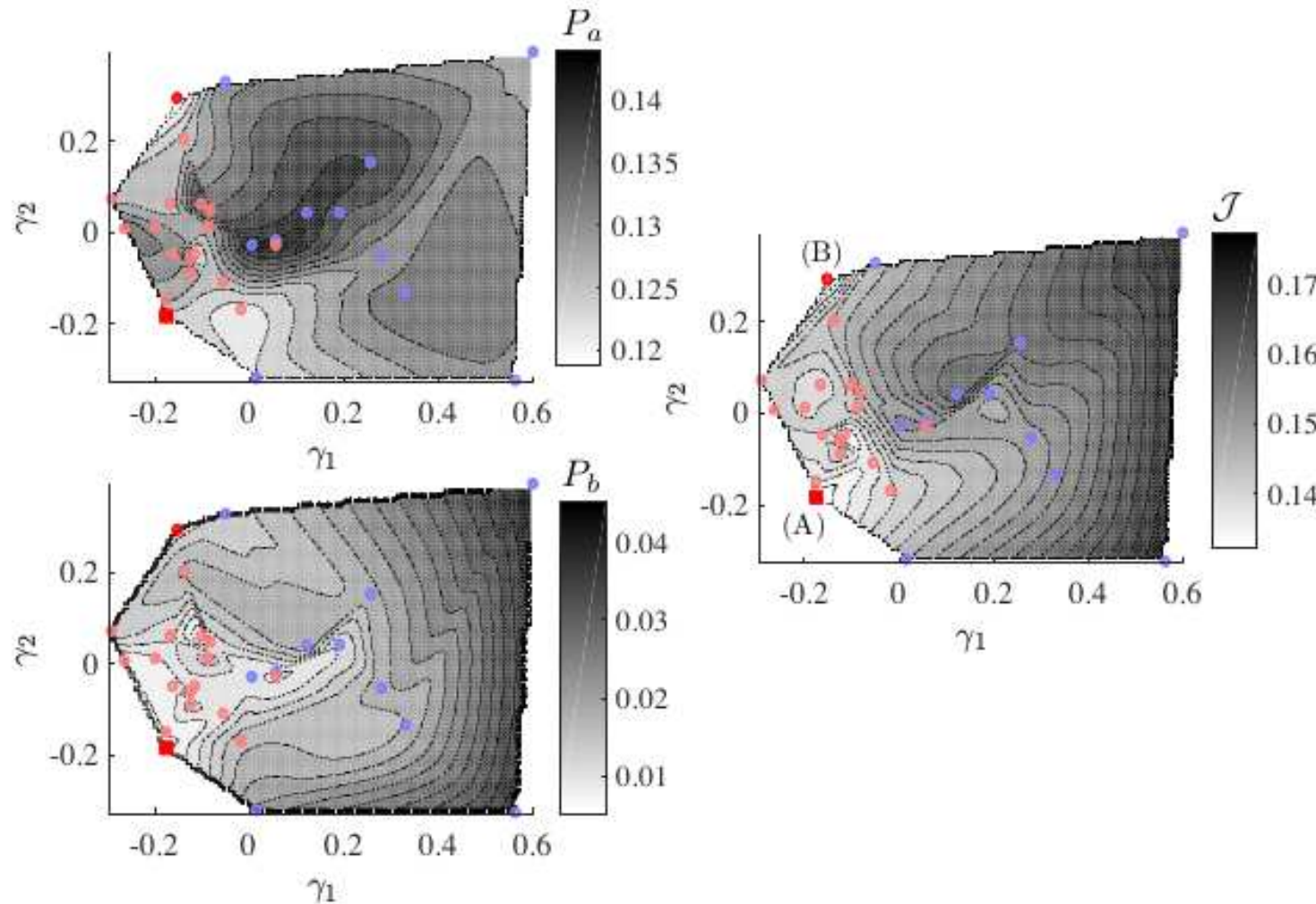


FIGURE 12. Control landscape, $P_{\text{drag}} = P_{\text{drag}}(\gamma_1, \gamma_2)$, $P_{\text{act}} = P_{\text{act}}(\gamma_1, \gamma_2)$, and $\mathcal{J} = \mathcal{J}(\gamma_1, \gamma_2)$, using multidimensional scaling. The transparent blue dots indicate initial simplex control cases and the red square symbol denotes the optimized case.

Cluster-based feedback control

A.G. Nair, C.-A. Yeh, E. Kaiser, B.R. Noack, S.L. Brunton & K. Taira 2018 JFM preprint

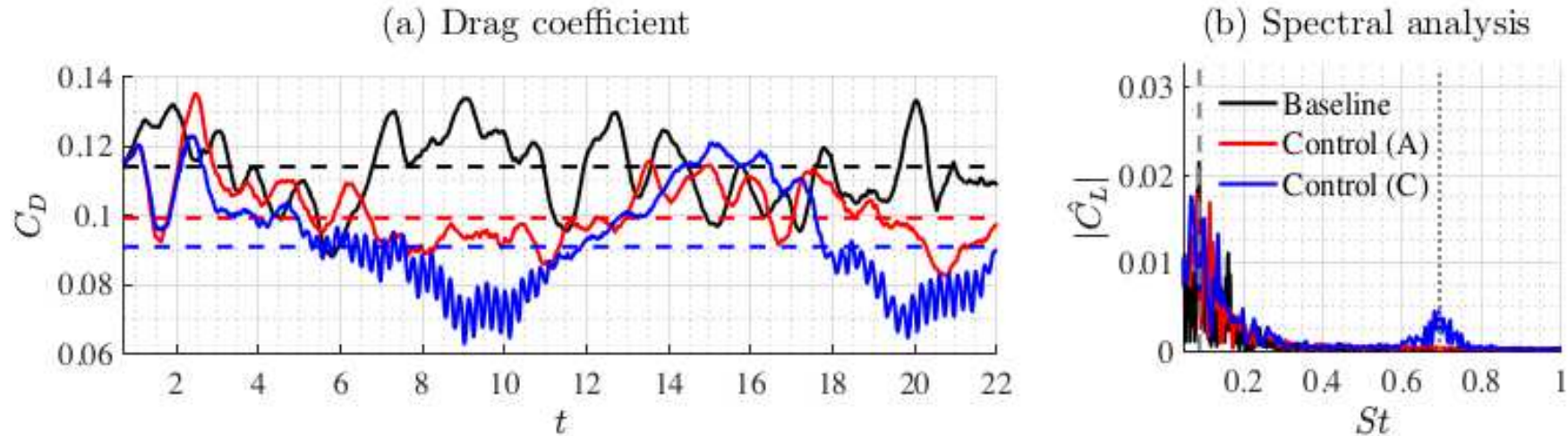


FIGURE 13. Comparison of baseline, optimized control case A ($\overline{C}_\mu = 0.0068$) and control case C with higher feedback gain ($\beta = 1.6, \overline{C}_\mu = 0.016$): (a) Drag coefficient, (b) spectral analysis of lift data. The dashed lines in (a) indicate the mean drag. The dashed line in (b) corresponds to the dominant shedding frequency and dotted line corresponds to the shear layer frequency.

Cluster-based feedback control

A.G. Nair, C.-A. Yeh, E. Kaiser, B.R. Noack, S.L. Brunton & K. Taira 2018 JFM preprint

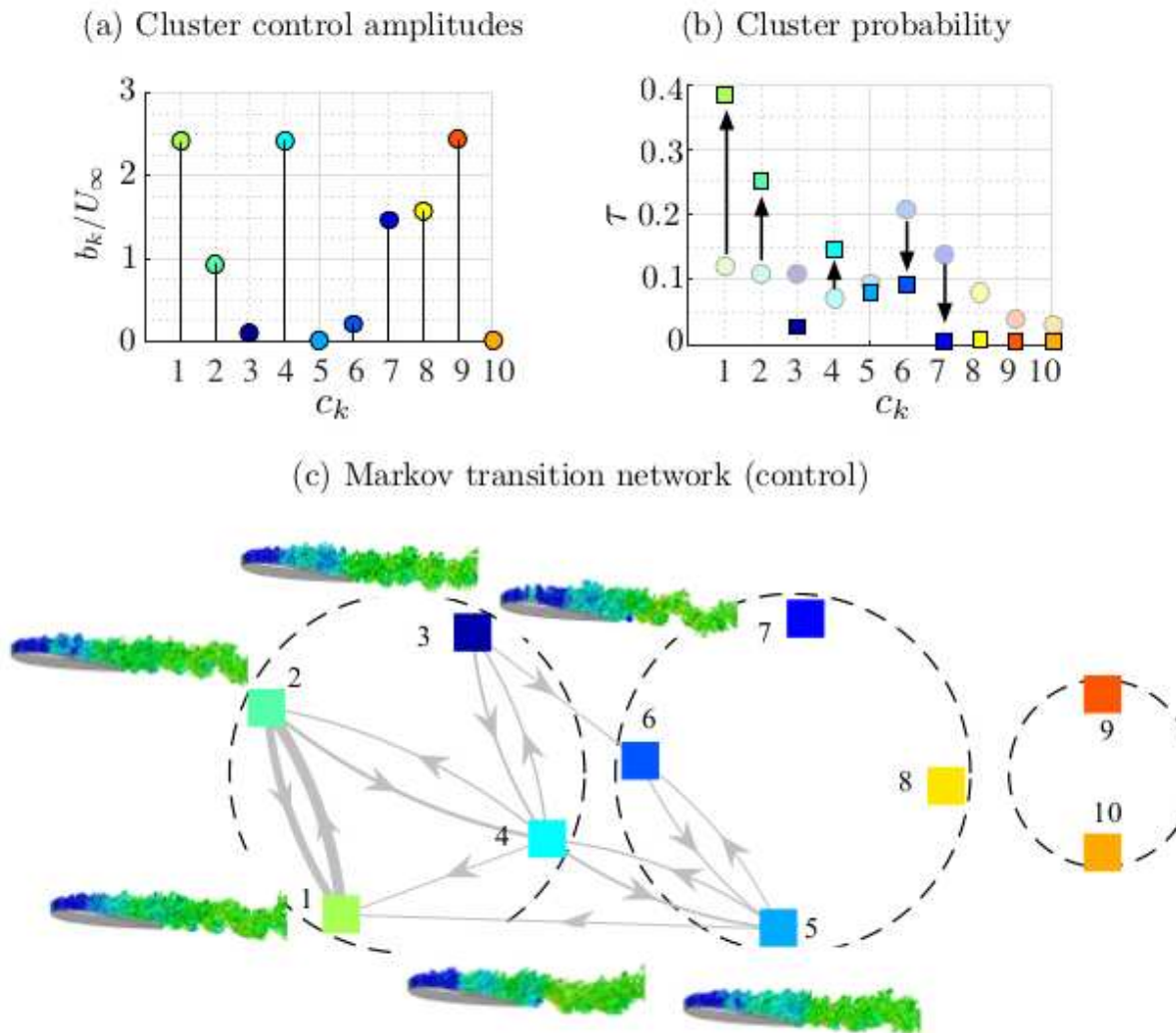


FIGURE 14. Comparison of optimized control case A with baseline: (a) Cluster jet velocities, (b) cluster probability for baseline (shown in transparent round symbols) and controlled flows (shown in square symbols) and (c) graph of optimally controlled Markov chain.

Cluster-based feedback control

A.G. Nair, C.-A. Yeh, E. Kaiser, B.R. Noack, S.L. Brunton & K. Taira 2018 JFM preprint

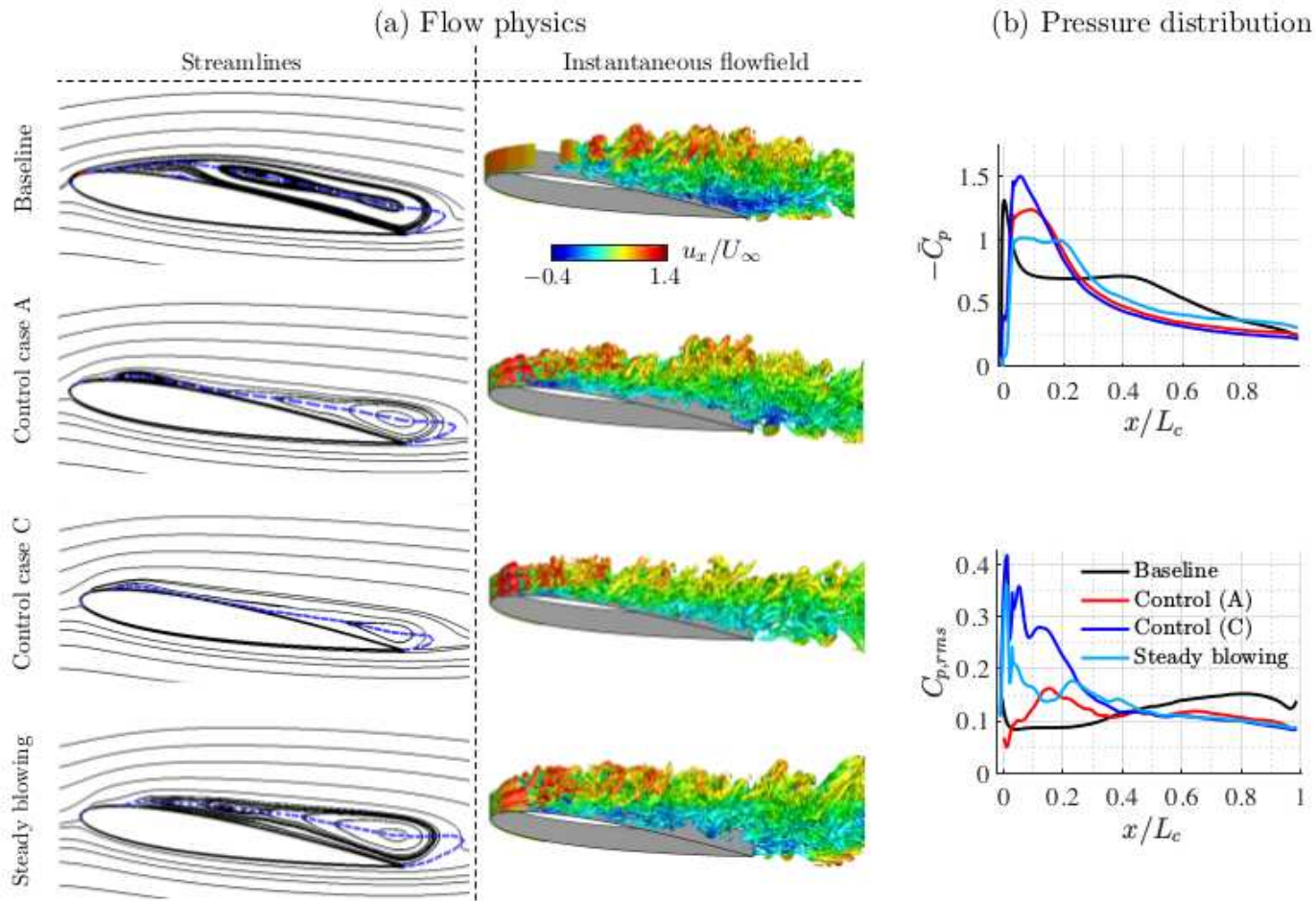


FIGURE 15. Comparison of baseline, optimized control case A ($\bar{C}_\mu = 0.0068$), control case C with higher feedback gain ($\beta = 1.6, \bar{C}_\mu = 0.016$) and steady blowing at $\bar{C}_\mu = 0.016$: (a) time-averaged streamlines and instantaneous flow field (highlighted by Q-criterion) colored by streamwise velocity, and (b) time-averaged and root-mean square fluctuation of coefficient of pressure distribution on suction side of the airfoil. The blue dashed line in (c) indicates the contour line of zero time- and spanwise-averaged streamwise velocity.